VOLUME 1, No. 4 (1956)

NUCLEAR PHYSICS

MONTHLY JOURNAL DEVOTED TO THE EXPERIMENTAL AND THEORETICAL STUDY OF ATOMIC NUCLEI, NUCLEAR FIELDS AND THE FUNDAMENTAL ASPECTS OF COSMIC RADIATION

EDITOR: L. ROSENFELD - MANCHESTER

M. H. Kalos, L. C. Biedenharn and J. M. Blatt, Numerical calculations for the neutron-proton system with tensor forces . 233

A. H. Wapstra and G. J. Nijgh, Indications for a strong influence of the nuclear size on magnetic dipole conversion coefficients 245

J. M. Araújo, Collective motions of a shell structure. 259

A. V. Cohen, S. B. Hyder and P. H. White, Limits to some (n, np) cross-sections at 14,5 MeV neutron energy 278

H. de Waard and T. R. Gerholm, Orbital momentum forbidden magnetic dipole transitions in some odd proton nuclei . . . 281

G. Racah, Remarques sur une formulation mathématique du modèle de Gell-Mann 302

H. Wergeland and H. Överaas, Curvature correction to the sagitta distribution of ionization tracks 304

Marie-Antoinette Tonnelat, Alexandre Proca 308

Book reviews. 311

NORTH-HOLLAND PUBLISHING COMPANY - AMSTERDAM

March 1956

EDITORIAL BOARD

AUSTRIA:	B. Karlik (Vienna), H. Thirring (Vienna)
BELGIUM:	M. de Hemptinne (Louvain), J. Verhaeghe (Ghent)
CANADA:	G. Volkoff (Vancouver)
DENMARK:	C. Møller (Copenhagen), S. Rozental (Copenhagen)
EGYPT & ARAB COUNTRIES:	F. El Bedewi (Alexandria), M. G. Nooh (Cairo)
FINLAND:	L. Simons (Helsinki)
FRANCE:	A. Berthelot (Saclay), S. Gorodetzky (Strasbourg), F. Joliot (Paris)
GERMANY:	W. Gentner (Freiburg i. B.), J. H. D. Jensen (Heidelberg)
GREAT BRITAIN:	S. Devons (Manchester)
HUNGARY:	L. Janossy (Budapest)
INDIA:	H. Bhabha (Bombay), B. Peters (Bombay), R. Ramanna (Trombay)
IRISH REPUBLIC:	J. McConnell (Maynooth)
ISRAEL:	G. Racah (Jerusalem)
ITALY:	E. Amaldi (Rome)
JAPAN:	S. Kikuchi (Tokyo), S. Tomonaga (Tokyo)
NETHERLANDS:	H. Brinkman (Groningen), S. R. de Groot (Leiden)
NORWAY:	E. Hylleraas (Oslo), A. Lundby (Oslo), H. Wergeland (Trondheim)
POLAND:	L. Infeld (Warsaw)
PORTUGAL:	J. M. Araújo (Porto), J. R. de Almeida Santos (Coimbra)
SOUTH AMERICA:	G. Beck (Saõ Paulo), J. Leite Lopes (Rio de Janeiro)
SPAIN:	J. M. Otero (Madrid), C. Sanchez del Rio (Madrid)
SWEDEN:	O. Klein (Stockholm), K. Siegbahn (Uppsala), I. Waller (Uppsala)
SWITZERLAND:	P. Huber (Basel), P. Scherrer (Zürich)
U.S.S.R.:	M. A. Markov (Moscow), I. S. Shapiro (Moscow), D. V. Skobeltzyn (Moscow)
YUGOSLAVIA:	I. Supek (Zagreb)
U.S.A. & MEXICO:	V. Weisskopf (Cambridge, Mass.)
AUSTRALIA & NEW ZEALAND:	H. Messel (Sydney), M. L. Oliphant (Canberra)

CONTRIBUTIONS may be sent to the Editor, Professor L. Rosenfeld, Dept. of Theoretical Physics, The University, Manchester, either directly, or preferably through the intermediary of one of the members of the Editorial Board of the country or region in which the author is working. They may be written in English, French or German.

BOOKS FOR REVIEW should be sent to Professor Rosenfeld.

NUCLEAR PHYSICS is published in monthly issues. The subscription price of a volume of 700 pages is fl 57.00; 114s; $ 15.00. Postfree.

SUBSCRIPTIONS should be sent to the publishers, NORTH-HOLLAND PUBLISHING COMPANY, P.O.Box 103, Amsterdam or to any subscription-agent. Subscriptions for U.S.A. are to be sent exclusively to INTERSCIENCE PUBLISHERS, INC., 250 Fifth Avenue, New York 1, N.Y.

Printed in the Netherlands.

Nuclear Physics, North-Holland Publishing Co., Amsterdam, **1 (1956)**

NUMERICAL CALCULATIONS FOR THE NEUTRON-PROTON SYSTEM WITH TENSOR FORCES†

M. H. KALOS ††
Laboratory of Nuclear Studies,
Cornell University, Ithaca, New York

L. C. BIEDENHARN
Physics Department, The Rice Institute, Houston, Texas

and J. M. BLATT
Physics Department, University of Sydney, Sydney, Australia

Received 27 August 1955

Abstract: Low-energy properties of the neutron-proton system are tabulated for a variety of central and tensor potentials.

This report is devoted to a study of some purely phenomenological combinations of central and tensor potentials of varying ranges and strengths. In general, the emphasis is on a survey of the effects of the introduction of tensor forces so that for the most part no attempt has been made to fit the experimentally known parameters of the system. (Such fits have been interpolated from our results, but will not be included here.) The square well calculations are those of Biedenharn [1]), while the rest were obtained with the University of Illinois electronic digital computer.

The method of calculation used for the square wells differs from that employed with the automatic computer, but in both cases a ground state wave function is obtained with the correct deuteron binding energy. Let

$$R = \hbar/(2MB)^{\frac{1}{2}} = (4.317 \pm 0.003)10^{-13}\ \text{cm}$$

be the 'radius of the deuteron'. Here

M = reduced mass of the N−P system,
B = binding energy = 2.225 ± 0.002 MeV. [2])

† Assisted in part by the joint program of the Office of Naval Research and the U.S. Atomic Energy Commission.

†† Present address: Nuclear Development Corporation of America, White Plains, N.Y.

Results are computed and tabulated with R as the unit of length and B the unit of energy. To change the value of the binding energy, it is necessary simply to change the value of R in relating our numbers to the experiments.

Both the central and tensor potentials are parametrized in terms of the intrinsic range, b, and the well depth, s, introduced by Blatt and Jackson [3] †.

The quantities tabulated together with the experimental values (in units of R) are as follows:

b_c = central range;
s_c = depth parameter of central well;
b_t = tensor range;
s_t = depth parameter of tensor potential;
p_D = percent D state; it is usually estimated that $0.02 \leqq p_D \leqq 0.06$;
Q = quadrupole moment = $(0.01469 \pm 0.0001)R^2$ [4];
ϱ = $\varrho_t(-B, -B)$ = deuteron effective range [5];
a_t = triplet scattering length = $(1.245 \pm 0.006)R$ [6];
r_{ot} = $\varrho_t(0,0)$ = triplet effective range [5];
a_s = singlet scattering length = $(-5.487 \pm 0.006)R$ [6];
r_{os} = $\varrho_s(0,0)$ = singlet effective range = $(0.58 \pm 0.06)R$ [7]; ††
P = shape dependent parameter in triplet state [3].

In computing singlet state results, it is assumed that the singlet potential is the same as the central potential in the triplet state; that is, the possibility of spin dependent central forces is ignored.

The values listed for b_c, s_c, and b_t usually do not contain insignificant zeros. These numbers can be assumed correct through the fourth decimal place. Otherwise, most of the results have an error no worse than about two in the last digit quoted (and usually better). One important exception occurs for the Yukawa potentials of very short range. The computer does not treat the x^{-1} singularity at the origin of the potential correctly and the resulting error becomes important when the range is short. A measure of this error can be deduced from the value of a_s^{-1} for $s = 1$. This number should be zero for all values of b_c. We see that for $b_c = 0.1$, it is about 0.03. The accuracy of other numbers derived from the same potential is

† Note that when the range, b, becomes zero, this parametrization is degenerate in the sense that $s = 1$ identically. For this special case, a better measure of the strength is the scattering length itself.

†† This work gives the best singlet range deduced from low energy N—P scattering. The analysis of P—P scattering [8]) gives a range which depends somewhat on the potential shape but whose average value is $(0.62 \pm 0.03)\ R$.

TABLE I

No central force

b_e	s_e	b_t	s_t	p_D	Q	ϱ	a_t	r_{ot}	a_s	r_{os}	P
Exponential tensor force											
...	0	0.2	1.4695	2.843	0.00297	0.1453	1.0783	0.1451	0	...	0.027
		0.6	1.7023	7.102	0.01709	0.3820	1.2375	0.3861	0	...	−0.020
		1.0	1.9537	10.00	0.03386	0.5565	1.3911	0.5697	0	...	−0.020
Yukawa tensor force											
...	0	0.2	1.5588	2.669	0.00323	0.1361	1.0751	0.1340	0	...	1.183
		0.5	1.7097	5.585	0.01268	0.3033	1.1782	0.3015	0	...	0.019
		0.8	1.8617	7.614	0.02265	0.4336	1.2730	0.4252	0	...	0.024
		1.1	2.0140	9.096	0.03194	0.5353	1.3522	0.5083	0	...	0.048
Gauss tensor force											
...	0	0.2	1.4025	2.965	0.00275	0.1554	1.0843	0.1558	0	...	−0.026
		0.5	1.5924	6.659	0.01340	0.3544	1.2172	0.3599	0	...	−0.031
		0.8	1.8016	9.534	0.02790	0.5144	1.3557	0.5359	0	...	−0.036
		1.1	2.0297	11.786	0.04434	0.6396	1.4957	0.6885	0	...	−0.039
Morse tensor force											
...	0	0.5	0.9307	4.048	0.00839	0.2549	1.1464	0.2547	0	...	0.023
		0.8	0.9764	5.350	0.01578	0.3608	1.2184	0.3570	0	...	0.016

TABLE II

Square – Square

b_e	s_e	b_t	s_t	$\hat{p}_D$	Q	a_t	r_{ot}	a_s	r_{os}	P
0	1	0.6583	0.8812	3.18	0.01079	1.1430	0.2430		0	0.263
0	1	0.7455	0.9715	3.82	0.01378	1.1774	0.2914		0	0.209
0	1	0.8365	1.0662	4.51	0.01722	1.2162	0.3422		0	0.170
0	1	0.6023	0.8812	3.14	0.00974	1.1369	0.2358	4.864	0	0.207
0	1	0.6583	0.8812	3.18	0.01079	1.1430	0.2430		0	0.263
0	1	0.7240	0.8812	3.19	0.01194	1.1486	0.2482	−5.342	0	0.353
0	1	1.0074	0.8812	2.94	0.01530	1.1549	0.2305	−1.594	0	1.555
0	1	0.7063	1.0663	4.53	0.01456	1.2019	0.3304	1.921	0	0.080
0	1	0.7860	1.0663	4.53	0.01626	1.2117	0.3396	5.875	0	0.127
0	1	0.8364	1.0663	4.51	0.01722	1.2162	0.3422		0	0.169
0	1	0.8970	1.0663	4.46	0.01824	1.2203	0.3421	−6.090	0	0.239
0.2939	0.8812	0.6068	0.9388	4.09	0.01205	1.2184	0.3612	−1.770	0.3137	−0.026
0.3160	0.8812	0.6725	0.9980	4.64	0.01459	1.2452	0.3975	−1.902	0.3372	−0.027
0.3397	0.8812	0.7473	1.0662	5.25	0.01772	1.2767	0.4384	−2.045	0.3625	−0.028
0.2666	0.8103	0.5332	0.9532	3.97	0.01014	1.1972	0.3316	−0.925	0.2976	−0.029
0.3074	0.8103	0.6456	1.0509	4.94	0.01444	1.2440	0.3962	−1.067	0.3432	−0.029
0.3457	0.8103	0.7606	1.1534	5.93	0.01941	1.2942	0.4610	−1.200	0.3859	−0.031
0.3923	1.0125	0.5492	0.7249	2.91	0.00924	1.2194	0.3637	25.7	0.3899	−0.037
0.4471	1.0125	0.6706	0.8322	3.74	0.01354	1.2644	0.4241	29.2	0.4443	−0.038
0.4987	1.0125	0.7979	0.9468	4.88	0.01882	1.3135	0.4860	32.6	0.4956	−0.038
0.3733	1.0128	0.3733	0.6044	1.73	0.00462	1.1859	0.3160	23.9	0.3709	−0.036
0.4781	1.0128	0.5259	0.7313	2.96	0.00931	1.2458	0.3999	30.6	0.4751	−0.039
0.5776	1.0128	0.6931	0.8704	4.39	0.01586	1.3120	0.4851	37.0	0.5740	−0.041
0.5433	1.4269	0.5433	0.2980	0.69	0.00503	1.2181	0.4462	1.461	0.4638	−0.040
0.5975	1.4269	0.7170	0.4291	1.51	0.00988	1.3149	0.4889	1.607	0.5100	−0.041
0.6507	1.4269	0.9110	0.5841	2.57	0.01642	1.3583	0.5411	1.750	0.5555	−0.042
0.4645	0.8200	0.4180	0.8514	3.00	0.00721	1.2190	0.3629	−1.720	0.5151	−0.035
0.5742	0.8200	0.5455	0.9487	4.23	0.01202	1.2772	0.4407	−2.126	0.6368	−0.038
0.6786	0.8200	0.6786	1.0511	5.53	0.01807	1.3381	0.5168	−2.513	0.7525	−0.040
0.6427	1.0643	0.6427	0.8249	3.94	0.01441	1.3228	0.4989	8.612	0.6233	−0.040

TABLE III

Gauss – Gauss

b_e	s_e	b_t	s_t	p_D	Q	ϱ	a_t	r_{ot}	a_e	r_{oe}	P
0.1	0.6	0.5	1.3086	5.23	0.01128	0.3087	1.1830	0.3101	−0.1202	0.1412	−0.013
		0.65	1.4568	6.78	0.01763	0.3966	1.2491	0.4016	−0.1202	0.1412	−0.021
		0.8	1.5961	8.18	0.02471	0.4768	1.3176	0.4879	−0.1202	0.1412	−0.026
	0.9	0.5	0.9228	3.13	0.00814	0.2314	1.1301	0.2290	−0.7067	0.1071	0.054
		0.8	1.2344	5.57	0.01872	0.3886	1.2384	0.3818	−0.7067	0.1071	0.029
		1.1	1.5330	7.80	0.03163	0.5344	1.3609	0.5259	−0.7067	0.1071	0.015
	1.0	0.5	0.6460	1.73	0.00581	0.1730	1.0940	0.1704	-9×10^{2}	0.1000	0.140
		0.8	0.9095	3.33	0.01347	0.2909	1.1647	0.2751	-9×10^{2}	0.1000	0.186
		1.1	1.1795	4.94	0.02280	0.4238	1.2518	0.3799	-9×10^{2}	0.1000	0.204
0.5	0.6	0.5	1.1476	4.48	0.01119	0.3679	1.2269	0.3723	−0.6007	0.7060	−0.023
		0.8	1.3430	6.93	0.02272	0.4755	1.3177	0.4894	−0.6007	0.7060	−0.031
		1.1	1.5896	8.98	0.03590	0.5847	1.4248	0.6093	−0.6007	0.7060	−0.029
	0.9	0.5	0.8875	3.13	0.00948	0.3757	1.2328	0.3799	−3.532	0.5353	−0.020
		0.8	1.0563	5.08	0.01902	0.4506	1.2948	0.4607	−3.532	0.5353	−0.027
		1.1	1.2835	6.78	0.02974	0.5398	1.3747	0.5514	−3.532	0.5353	−0.019
	0.938	0.67	0.9341	4.03	0.01429	0.4144			−5.919	0.5211	
		0.71	0.9578	4.28	0.01555	0.4243			−5.919	0.5211	
		0.748	0.9814	4.50	0.01677	0.4340			−5.919	0.5211	
		0.79	1.0087	4.75	0.01813	0.4450			−5.919	0.5211	
		0.83	1.0356	4.98	0.01945	0.4559			−5.919	0.5211	
		0.87	1.0635	5.21	0.02079	0.4670			−5.919	0.5211	
	1.0	0.5	0.7898	2.64	0.00874	0.3785	1.2350	0.3827	-3×10^{3}	0.5000	−0.020
		0.8	0.9454	4.34	0.01747	0.4412	1.2866	0.4502	-3×10^{3}	0.5000	−0.026
		1.1	1.1589	5.86	0.02719	0.5206	1.3550	0.5282	-3×10^{3}	0.5000	−0.014
0.7	0.6	0.5	1.2135	4.59	0.01199	0.4131	1.2604	0.4135	−0.8411	0.9884	−0.002
		.65	1.2783	5.91	0.01784	0.4601	1.3024	0.4690	−0.8411	0.9884	−0.022
		.8	1.3637	7.08	0.02404	0.5083	1.3483	0.5255	−0.8411	0.9884	−0.031
	0.9	0.5	0.9963	3.43	0.01077	0.4403	1.2826	0.4412	−4.946	0.7495	−0.003
		0.65	1.0439	4.53	0.01593	0.4713	1.3118	0.4795	−4.946	0.7495	−0.019
		0.8	1.1156	5.53	0.02131	0.5056	1.3450	0.5207	−4.946	0.7495	−0.027
	1.0	0.5	0.9171	3.02	0.01023	0.4491	1.2902	0.4506	-5×10^{3}	0.7000	−0.004
		0.65	0.9592	4.03	0.01513	0.4752	1.3151	0.4832	-5×10^{3}	0.7000	−0.018
		0.8	1.0256	4.95	0.02019	0.5048	1.3440	0.5191	-5×10^{3}	0.7000	−0.026

TABLE IV

Gauss – Yukawa

b_e	s_e	b_t	s_t	p_D	Q	ϱ	a_t	r_{ot}	a_s	r_{os}	P
0.1	0.6	0.5	1.2056	3.60	0.00915	0.2279	1.1274	0.2237	−0.1202	0.1412	0.101
		0.8	1.4115	5.37	0.01701	0.3454	1.2019	0.3274	−0.1202	0.1412	0.123
		1.1	1.5998	6.79	0.02465	0.4486	1.2690	0.4012	−0.1202	0.1412	0.175
	0.9	0.5	0.7473	1.73	0.00584	0.1573	1.0845	0.1538	−0.7067	0.1071	0.281
		0.8	0.9134	2.77	0.01091	0.2305	1.1244	0.2129	−0.7067	0.1071	0.434
		1.1	1.0713	3.68	0.01582	0.3073	1.1630	0.2561	−0.7067	0.1071	0.717
	1.0	0.5	0.4964	0.85	0.00397	0.1251	1.0663	0.1233	-10^3	0.1000	0.275
		0.8	0.6152	1.41	0.00740	0.1650	1.0865	0.1538	-10^3	0.1000	0.742
		1.1	0.7301	1.91	0.01065	0.2112	1.1063	0.1757	-10^3	0.1000	1.527
0.5	0.6	0.5	1.2640	3.64	0.01084	0.3433	1.2073	0.3432	−0.6007	0.7060	0.003
		0.8	1.3521	5.17	0.01833	0.4140	1.2596	0.4113	−0.6007	0.7060	0.006
		1.1	1.4675	6.30	0.02498	0.4805	1.3063	0.4597	−0.6007	0.7060	0.048
	0.9	0.5	0.9899	2.50	0.00923	0.3615	1.2212	0.3630	−3.532	0.5353	−0.008
		0.8	1.0499	3.64	0.01529	0.4051	1.2538	0.4051	−3.532	0.5353	−0.002
		1.1	1.1411	4.49	0.02051	0.4502	1.2840	0.4364	−3.532	0.5353	0.036
	1.0	0.5	0.8847	2.09	0.00851	0.3674	1.2258	0.3694	-3×10^3	0.5000	−0.010
		0.8	0.9358	3.06	0.01402	0.4024	1.2520	0.4034	-3×10^3	0.5000	−0.006
		1.1	1.0175	3.79	0.01872	0.4398	1.2767	0.4289	-3×10^3	0.5000	0.029
0.7	0.6	0.5	1.3578	3.84	0.01192	0.3924	1.2420	0.3868	−0.8411	0.9884	0.025
		0.8	1.4299	5.48	0.02017	0.4597	1.2976	0.4583	−0.8411	0.9884	0.002
		1.1	1.5312	6.66	0.02730	0.5210	1.3461	0.5089	−0.8411	0.9884	0.020
	0.9	0.5	1.1383	2.86	0.01091	0.4290	1.2719	0.4258	−4.946	0.7495	0.011
		0.8	1.1781	4.19	0.01808	0.4720	1.3095	0.4738	−4.946	0.7495	−0.005
		1.1	1.2555	5.15	0.02408	0.5144	1.3434	0.5094	−4.946	0.7495	−0.007
	1.0	0.5	1.0551	2.52	0.01043	0.4402	1.2815	0.4382	-5×10^3	0.7000	0.007
		0.8	1.0857	3.72	0.01718	0.4760	1.3134	0.4788	-5×10^3	0.7000	−0.007
		1.1	1.1551	4.59	0.02277	0.5123	1.3426	0.5095	-5×10^3	0.7000	0.003

TABLE V

Yukawa – Gauss

b_e	s_e	b_t	s_t	p_D	Q	ϱ	a_t	r_{ot}	a_s	r_{os}	P
0.1	0.6	0.5	1.3364	5.39	0.01152	0.3149	1.1876	0.3171	−0.1058	0.1845	−0.018
		0.8	1.6160	8.33	0.02506	0.4814	1.3221	0.4938	−0.1058	0.1845	−0.027
		1.1	1.8827	10.70	0.04076	0.6149	1.4609	0.6487	−0.1058	0.1845	−0.033
	0.9	0.5	0.9660	3.37	0.00852	0.2420	1.1370	0.2397	−0.5794	0.1154	0.046
		0.8	1.2770	5.89	0.01946	0.4011	1.2489	0.3959	−0.5794	0.1154	0.022
		1.1	1.5747	8.16	0.03275	0.5460	1.3742	0.5427	−0.5794	0.1154	0.006
	1.0	0.5	0.6588	1.79	0.00592	0.1756	1.0954	0.1722	−29.4	0.1005	0.193
		0.8	0.9229	3.42	0.01368	0.2953	1.1677	0.2788	−29.4	0.1005	0.193
		1.1	1.1940	5.06	0.02315	0.4290	1.2562	0.3863	−29.4	0.1005	0.188
0.5	0.6	0.5	1.1586	4.48	0.01099	0.3579	1.2160	0.3533	−0.5303	0.9204	0.023
		0.8	1.3859	7.06	0.02302	0.4780	1.3175	0.4867	−0.5303	0.9204	−0.020
		1.1	1.6388	9.22	0.03680	0.5925	1.4325	0.6163	−0.5303	0.9204	−0.027
	0.9	0.5	0.8733	3.00	0.00897	0.3564	1.2127	0.3460	−2.948	0.5748	0.057
		0.8	1.0823	5.05	0.01886	0.4443	1.2849	0.4432	−2.948	0.5748	0.001
		1.1	1.3230	6.87	0.03011	0.5427	1.3737	0.5458	−2.948	0.5748	−0.005
	1.0	0.5	0.7565	2.40	0.00803	0.3551	1.2109	0.3425	-3×10^{3}	0.5002	0.073
		0.8	0.9500	4.16	0.01691	0.4284	1.2702	0.4231	-3×10^{3}	0.5002	0.015
		1.1	1.1765	5.76	0.02692	0.5163	1.3455	0.5112	-3×10^{3}	0.5002	0.009
0.7	0.6	0.5	1.1778	4.49	0.01136	0.3901	1.2336	0.3708	−0.7424	1.2886	0.077
		0.8	1.3808	7.05	0.02357	0.4990	1.3324	0.5011	−0.7424	1.2886	−0.009
		1.1	1.6163	9.17	0.03731	0.6038	1.4434	0.6269	−0.7424	1.2886	−0.025
	0.9	0.5	0.9243	3.16	0.00969	0.4066	1.2416	0.3766	−4.128	0.8046	0.118
		0.8	1.1077	5.27	0.02013	0.4848	1.3138	0.4738	−4.128	0.8046	0.018
		1.1	1.3283	7.10	0.03172	0.5716	1.4009	0.5752	−4.128	0.8046	−0.007
	1.0	0.5	0.8269	2.67	0.00895	0.4119	1.2442	0.3784	-10^{4}	0.7003	0.131
		0.8	0.9988	4.55	0.01861	0.4784	1.3059	0.4622	-10^{4}	0.7003	0.032
		1.1	1.2087	6.21	0.02926	0.5566	1.3825	0.5523	-10^{4}	0.7003	0.003

TABLE VI

Yukawa – Yukawa

b_c	s_c	b_t	s_t	p_D	Q	ϱ	a_t	r_{ot}	a_s	r_{os}	P
0.1	0.6	0.5	1.2482	3.77	0.00947	0.2361	1.1325	0.2321	−0.1058	0.1845	0.074
		0.8	1.4548	5.60	0.01758	0.3559	1.2098	0.3388	−0.1058	0.1845	0.104
		1.1	1.6420	7.04	0.02542	0.4593	1.2785	0.4141	−0.1058	0.1845	0.152
	0.9	0.5	0.7823	1.85	0.00610	0.1629	1.0876	0.1592	−0.5794	0.1154	0.218
		0.8	0.9584	2.99	0.01146	0.2418	1.1313	0.2236	−0.5794	0.1154	0.383
		1.1	1.1229	3.97	0.01666	0.3229	1.1733	0.2708	−0.5794	0.1154	0.620
	1.0	0.5	0.4981	0.85	0.00398	0.1242	1.0656	0.1218	−29.4	0.1005	0.355
		0.8	0.6215	1.43	0.00747	0.1656	1.0866	0.1535	−29.4	0.1005	0.804
		1.1	0.7392	1.95	0.01077	0.2132	1.1072	0.1768	−29.4	0.1005	1.528
0.5	0.6	0.5	1.2013	3.44	0.01010	0.3221	1.1877	0.3111	−0.5303	0.9204	0.085
		0.8	1.3273	5.01	0.01762	0.4000	1.2444	0.3869	−0.5303	0.9204	0.051
		1.1	1.4633	6.20	0.02447	0.4726	1.2953	0.4412	−0.5303	0.9204	0.086
	0.9	0.5	0.8871	2.16	0.00807	0.3323	1.1934	0.3169	−2.948	0.5748	0.114
		0.8	0.9876	3.27	0.01396	0.3799	1.2280	0.3640	−2.948	0.5748	0.076
		1.1	1.0996	4.14	0.01920	0.4295	1.2606	0.3994	−2.948	0.5748	0.110
	1.0	0.5	0.7629	1.69	0.00716	0.3359	1.1955	0.3192	-3×10^3	0.5002	0.119
		0.8	0.8515	2.59	0.01236	0.3727	1.2222	0.3557	-3×10^3	0.5002	0.087
		1.1	0.9512	3.32	0.01695	0.4125	1.2477	0.3836	-3×10^3	0.5002	0.119
0.6634	0.6891	0.6783	1.2218	4.12	0.01468	0.4000	1.2399	0.3771	−1.018	1.048	0.092
0.7	0.6	0.5	1.2477	3.54	0.01071	0.3600	1.2076	0.3319	−0.7424	1.289	0.163
		0.8	1.3604	5.14	0.01861	0.4329	1.2655	0.4097	−0.7424	1.289	0.072
		1.1	1.4866	6.34	0.02570	0.5003	1.3171	0.4659	−0.7424	1.289	0.077
	0.9	0.5	0.9718	2.39	0.00907	0.3871	1.2238	0.3497	−4.128	0.8046	0.188
		0.8	1.0605	3.60	0.01563	0.4328	1.2617	0.4015	−4.128	0.8046	0.103
		1.1	1.1650	4.54	0.02136	0.4793	1.2970	0.4407	−4.128	0.8046	0.101
	1.0	0.5	0.8671	1.98	0.00835	0.3959	1.2294	0.3561	-10^4	0.7003	0.189
		0.8	0.9465	3.03	0.01435	0.4328	1.2605	0.3986	-10^4	0.7003	0.116
		1.1	1.0416	3.85	0.01957	0.4717	1.2898	0.4316	-10^4	0.7003	0.111

TABLE VII

Yukawa – Exponential

b_s	s_s	b_t	s_t	p_D	Q	ϱ	a_t	r_{ot}	a_s	r_{os}	P
0.1	0.6	0.5	1.3058	4.70	0.01068	0.2787	1.1616	0.2777	−0.1058	0.1845	0.013
		0.8	1.5635	7.18	0.02171	0.4279	1.2713	0.4264	−0.1058	0.1845	0.002
		1.1	1.8005	9.17	0.03355	0.5517	1.3790	0.5488	−0.1058	0.1845	0.002
	0.9	0.5	0.8874	2.67	0.00743	0.2029	1.1120	0.1999	−0.5794	0.1154	0.091
		0.8	1.1515	4.60	0.01573	0.3296	1.1923	0.3157	−0.5794	0.1154	0.109
		1.1	1.4025	6.34	0.02501	0.4540	1.2793	0.4196	−0.5794	0.1154	0.116
	1.0	0.5	0.5855	1.33	0.00502	0.1484	1.0794	0.1452	−29.4	0.1005	0.298
		0.8	0.7920	2.47	0.01068	0.2303	1.1251	0.2153	−29.4	0.1005	0.361
		1.1	0.9996	3.58	0.01695	0.3273	1.1785	0.2797	−29.4	0.1005	0.530
0.5	0.6	0.5	1.1700	3.99	0.01055	0.3391	1.2011	0.3314	−0.5303	0.9204	0.047
		0.8	1.3505	6.10	0.02031	0.4390	1.2801	0.4371	−0.5303	0.9204	0.003
		1.1	1.5501	7.81	0.03043	0.5352	1.3630	0.5312	−0.5303	0.9204	0.005
	0.9	0.5	0.8707	2.58	0.00851	0.3432	1.2021	0.3302	−2.948	0.5748	0.084
		0.8	1.0275	4,18	0.01634	0.4104	1.2544	0.4017	−2.948	0.5748	0.030
		1.1	1.2065	5.55	0.02436	0.4851	1.3132	0.4701	−2.948	0.5748	0.034
	1.0	0.5	0.7507	2.04	0.00757	0.3444	1.2023	0.3296	-3×10^{3}	0.5002	0.097
		0.8	0.8930	3.38	0.01455	0.3984	1.2440	0.3871	-3×10^{3}	0.5002	0.044
		1.1	1.0574	4.55	0.02164	0.4620	1.2921	0.4435	-3×10^{3}	0.5002	0.050
0.7	0.6	0.5	1.2016	4.05	0.01104	0.3742	1.2199	0.3506	−0.7424	1.289	0.114
		0.8	1.3620	6.15	0.02107	0.4656	1.2980	0.4557	−0.7424	1.289	0.018
		1.1	1.5459	7.84	0.03129	0.5535	1.3791	0.5483	−0.7424	1.289	0.005
	0.9	0.5	0.9372	2.78	0.00936	0.3958	1.2318	0.3620	−4.128	0.8046	0.151
		0.8	1.0744	4.46	0.01781	0.4573	1.2860	0.4361	−4.128	0.8046	0.052
		1.1	1.2381	5.86	0.02626	0.5243	1.3457	0.5061	−4.128	0.8046	0.029
	1.0	0.5	0.8365	2.33	0.00863	0.4030	1.2360	0.3661	-10^{4}	0.7003	0.160
		0.8	0.9629	3.80	0.01640	0.4539	1.2812	0.4285	-10^{4}	0.7003	0.067
		1.1	1.1157	5.05	0.02413	0.5121	1.3324	0.4890	-10^{4}	0.7003	0.042

TABLE VIII

Exponential – Yukawa

b_e	s_e	b_t	s_t	$\hat{p}_D$	Q	ϱ	a_t	r_{ot}	a_s	r_{os}	P
0.1	0.6	0.5	1.2208	3.66	0.00926	0.2309	1.1294	0.2264	−0.1147	0.1565	0.117
		0.8	1.4274	5.46	0.01722	0.3494	1.2050	0.3319	−0.1147	0.1565	0.113
		1.1	1.6155	6.88	0.02494	0.4527	1.2726	0.4060	−0.1147	0.1565	0.167
	0.9	0.5	0.7575	1.76	0.00591	0.1589	1.0855	0.1556	−0.6618	0.1098	0.262
		0.8	0.9274	2.84	0.01108	0.2340	1.1267	0.2163	−0.6618	0.1098	0.427
		1.1	1.0877	3.77	0.01608	0.3123	1.1663	0.2608	−0.6618	0.1098	0.689
	1.0	0.5	0.4932	0.84	0.00395	0.1242	1.0659	0.1223	$+10^4$	0.1000	0.351
		0.8	0.6133	1.40	0.00738	0.1643	1.0861	0.1528	$+10^4$	0.1000	0.808
		1.1	0.7287	1.90	0.01062	0.2106	1.1061	0.1750	$+10^4$	0.1000	1.563
0.5	0.6	0.5	1.2287	3.53	0.01045	0.3332	1.1982	0.3284	−0.5737	0.7822	0.034
		0.8	1.3343	5.07	0.01792	0.4066	1.2520	0.3993	−0.5737	0.7822	0.026
		1.1	1.4595	6.22	0.02464	0.4757	1.3004	0.4502	−0.5737	0.7822	0.065
	0.9	0.5	0.9377	2.33	0.00865	0.3483	1.2088	0.3426	−3.309	0.5491	0.035
		0.8	1.0170	3.45	0.01462	0.3934	1.2420	0.3866	−3.309	0.5491	0.027
		1.1	1.1181	4.30	0.01984	0.4403	1.2732	0.4196	−3.309	0.5491	0.064
	1.0	0.5	0.8258	1.90	0.00786	0.3534	1.2124	0.3475	-9×10^5	0.5000	0.035
		0.8	0.8953	2.84	0.01323	0.3891	1.2388	0.3825	-9×10^5	0.5000	0.027
		1.1	0.9858	3.57	0.01788	0.4275	1.2639	0.4091	-9×10^5	0.5000	0.062
0.7	0.6	0.5	1.3021	3.70	0.01133	0.3776	1.2265	0.3617	−0.8032	1.095	0.081
		0.8	1.3912	5.30	0.01935	0.4467	1.2824	0.4353	−0.8032	1.095	0.031
		1.1	1.5038	6.48	0.02643	0.5105	1.3319	0.4880	−0.8032	1.095	0.045
	0.9	0.5	1.0573	2.65	0.01003	0.4103	1.2505	0.3919	−4.632	0.7688	0.073
		0.8	1.1190	3.90	0.01687	0.4541	1.2878	0.4410	−4.632	0.7688	0.035
		1.1	1.2091	4.85	0.02272	0.4981	1.3221	0.4781	−4.632	0.7688	0.042
	1.0	0.5	0.9655	2.28	0.00944	0.4206	1.2585	0.4020	-10^6	0.7000	0.068
		0.8	1.0185	3.39	0.01582	0.4567	1.2898	0.4431	-10^6	0.7000	0.036
		1.1	1.1004	4.24	0.02123	0.4940	1.3190	0.4747	-10^6	0.7000	0.042

TABLE IX

Exponential – Exponential

b_c	s_c	b_t	s_t	p_D	Q	ϱ	a_t	r_{ot}	a_s	r_{os}	P
0.1	0.6	0.5	1.2819	4.59	0.01048	0.2738	1.1582	0.2727	−0.1147	0.1565	0.013
		0.8	1.5449	7.07	0.02143	0.4235	1.2675	0.4215	−0.1147	0.1565	00.04
		1.1	1.7851	9.06	0.03320	0.5482	1.3750	0.5438	−0.1147	0.1565	0.005
	0.9	0.8	1.1184	4.39	0.01524	0.3201	1.1854	0.3057	−0.6618	0.1098	0.126
		1.1	1.3686	6.09	0.02428	0.4438	1.2701	0.4075	−0.6618	0.1098	0.123
	1.0	0.5	0.5737	1.29	0.00492	0.1467	1.0786	0.1443	1.3×10^{4}	0.1000	0.232
		0.8	0.7782	2.39	0.01049	0.2266	1.1230	0.2114	1.3×10^{4}	0.1000	0.403
		1.1	0.9842	3.49	0.01666	0.3221	1.1750	0.2748	1.3×10^{4}	0.1000	0.558
0.5	0.7798	0.679	1.0918	4.34	0.01473	0.3958					
	0.9	0.5	0.8917	2.69	0.00887	0.3560	1.2150	0.3520	−3.309	0.5491	0.022
		0.8	1.0257	4.24	0.01660	0.4177	1.2634	0.4168	−3.309	0.5491	0.001
		1.1	1.1935	5.55	0.02443	0.4876	1.3185	0.4798	−3.309	0.5491	0.015
	1.0563	0.829	0.8450	3.21	0.01470	0.4097					
0.7	1.1865	1.0009	0.7119	2.50	0.01472	0.4163					
	0.7996	0.6369	1.1195	4.25	0.01472	0.4365					
	1.0949	0.74	0.8759	3.23	0.01471	0.4641					
	1.2378	0.8425	0.7427	2.65	0.01472	0.4767					

therefore on the order of a few percent. (Here the actual error will depend upon the importance of the central potential in the triplet state.) Except for the depth of the exponential well, the parameters for the range and depth of the potentials are taken from Blatt and Jackson [3]).

Most values of P are computed from the relation

$$P = \frac{(1 - a_t^{-1} - \frac{1}{2}r_{0t})}{r_{0t}^3}$$

and may suffer from inaccuracies in a_t and r_{0t}. For the most part, we estimate an error in P of about 0.005. For the shortest ranges, the error may be as large as 0.1. The square well results for P were computed from an integral expression [1]) and are accurate to the figures given.

In tables I-IX, the notation 'Yukawa-exponential' means that the central potential is of the Yukawa shape and the tensor potential has an exponential shape. Wave functions are not available for most of the cases shown in the tables. For the 'Yukawa-Gauss', 'Yukawa-exponential', 'Yukawa-Yukawa', and 'Exponential-Yukawa' combinations, short tables of wave functions which permit a sketch of the shape have been printed.

Results on the Yukawa-Yukawa combination have already been published by Feshbach and Schwinger [9]). Because our calculations are usually more accurate and include the scattering state at zero energy, we have included the new results. Interpolation shows that they are in agreement with the earlier work.

We wish to acknowledge the excellent work of Miss Patricia Boland in the square well computations and the helpful cooperation of the staff of the ILLIAC digital computer.

References

1) L. C. Biedenharn, Thesis submitted to the Massachusetts Institute of Technology, 1949 (unpublished)
2) C. W. Li *et al.*, Phys. Rev. **83** (1951) 512
3) J. M. Blatt and J. D. Jackson, Phys. Rev. **76** (1949) 18
4) G. F. Newell, Phys. Rev. **77** (1950) 141; H. G. Kolsky *et al.*, Phys. Rev. **81** (1951) 1061
5) H. A. Bethe, Phys. Rev. **76** (1949) 38; N. Austern, Phys. Rev. **92** (1953) 670; L. C. Biedenharn and J. M. Blatt, Phys. Rev. **93** (1954) 1387
6) Burgy, Ringo and Hughes, Phys. Rev. **84** (1951) 1160; E. Melkonian, Phys. Rev. **76** (1949) 1766
7) Fields, Becker and Adair, Phys. Rev. **94** (1954) 389
8) J. D. Jackson and J. M. Blatt, Rev. Mod. Phys. **22** (1950) 77
9) H. Feshbach and J. Schwinger, Phys. Rev. **84** (1951) 194

Nuclear Physics, North-Holland Publishing Co., Amsterdam, **1 (1956)**

INDICATIONS FOR A STRONG INFLUENCE OF THE NUCLEAR SIZE ON MAGNETIC DIPOLE CONVERSION COEFFICIENTS

A. H. WAPSTRA and G. J. NIJGH

Instituut voor Kernphysisch Onderzoek, Amsterdam, Nederland

Received 21 September 1955

Abstract: An analysis of the conversion coefficients of the 279 keV transition in ^{203}Tl indicates that the theoretical conversion coefficients as computed by Rose *et al.* disagree with the experimental data. In this case as well as in those of other transitions in heavy nuclei a better agreement is obtained if the theoretical K and L_I shell conversion coefficients for M1 transitions are lowered by about 40 %. Probably this is due to the fact that the finite size of the nucleus was not taken into account in the theoretical calculations. The data about L_{II} conversion are controversial.

1. Introduction

At the Glasgow conference on Nuclear Physics, July 1954, one of us [1]) reported that the measured K and L_I shell conversion coefficients of the mixed M1 — E2 279.17 keV transition in ^{203}Tl showed a disagreement with the theoretical values [2, 3]). A similar discrepancy was noted by Feather [4]) for the case of the Th F line and by Sunyar [5]) for that of the 209 keV transition in ^{199}Au. A theoretical prediction of such a deviation was made by Sliv and Listengarten [6]) who estimated that due to the finite size of the nucleus the K and L_I shell conversion coefficients for M1 transitions at $Z = 83$ should be lowered by a factor of 2/3.

2. The 279 keV Transition in ^{203}Tl

This transition was reinvestigated at this Institute[13]). The preliminary result of this work is $\alpha_K = 0.164 \pm 0.005$ and $K/L = 3.35 \pm 0.05$. Table 2.1 gives the theoretical M1 and E2 conversion coefficients. The K shell conversion values were obtained from the tables of Rose, Goertzel and Perry [2]) but corrected for screening by a factor 0.98 which was obtained by comparing their values with those given recently by Rose, Goertzel and Swift [3]). The L_I and L_{II}

shell conversion coefficients were obtained from ref. [3]) by graphical interpolation of log α against the charge number and the logarithm of the energy; the L_{III} shell coefficients were derived by doing the same thing with log L_{III}/L_{II} (this because at the moment of writing L_{III} shell conversion coefficients were only reported for $Z = 55$ and $Z = 85$ and because it may be expected that L_{III}/L_{II} is only a slowly varying function of Z).

TABLE 2.1

Theoretical M1 and E2 conversion coefficients for a 279 keV transition in Tl

	K	L_I	L_{II}	L_{III}
$100\beta_1$	52	8.1	0.72	0.045
$100\alpha_2$	7.6	1.14	2.45	1.24

According to very fundamental points of the theory (involving only the statement that the angular momentum description is appropriate [7])) the conversion coefficients of mixed M1 − E2 transitions are represented by the formula

$$\alpha_X = a\beta_{1X} + (1 - a)\alpha_{2X}. \tag{2.1}$$

The coefficient a represents the fraction of the gamma rays that are of M1 character and therefore is the same for all subshells X = K, L_I, L_{II} etc. Eliminating a we easily find a relation between α_K and K/L:

$$\alpha_K = \frac{(\beta_{1K}\alpha_{2L} - \alpha_{2K}\beta_{1L})\,K/L}{(\beta_{1K} - \alpha_{2K}) - (\beta_{1L} - \alpha_{2L})\,K/L}. \tag{2.2}$$

This function is shown in fig. 1 together with the experimental results; it is seen that the latter disagree definitely with the theoretical curve.

In view of the explanation to be given in section 8 we have also plotted a curve computed as above but with the theoretical M1 conversion coefficients in the K and L_I shells decreased by a factor $f = 0.6$. It is seen that even this large correction does not quite account for this discrepancy.

With an eye on the following section it may be remarked that the fraction a of M1 gamma rays is found to be 0.196 ± 0.007 and 0.278 ± 0.010 from the experimental values of α_K and K/L respectively, combined with the Rose *et al.* theoretical values given in table 2.1. If a correction factor f is applied to β_{1K} and β_{1LI} it is pos-

sible to plot α_K as a function of K/L not using a but f as a variable parameter (fig. 1, thin dotted curves); these curves together with the

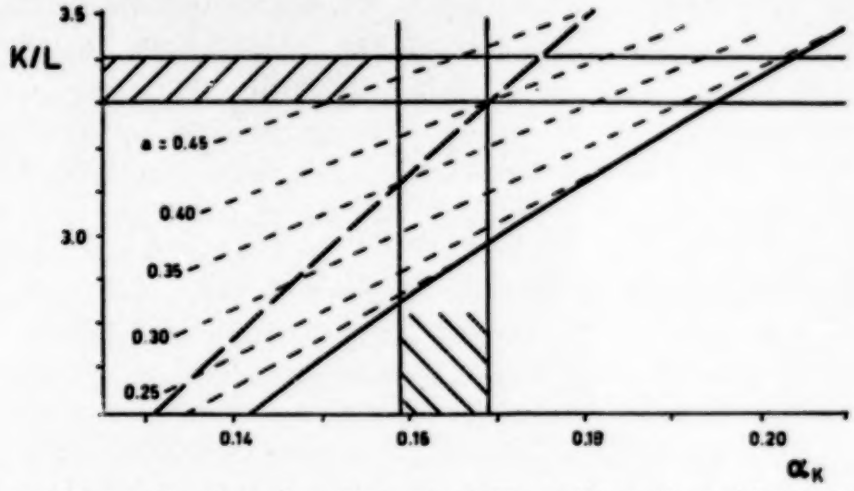

Fig. 1. K/L as a function of α_K for a mixed M1 – E2 transition of 279 keV in Tl according to Rose *et al.* (drawn curve). The dashed curve is obtained by decreasing β_{1K} and β_{1LI} by 40 %. Shaded: experimental values. The meaning of the dotted curves is explained in the text.

experimental results point to $a = 0.44$. It will be clear that more light can be thrown upon this discrepancy by discussing the L subshell ratios. This will be done in a paper describing a measurement of these ratios [8]); it may only be mentioned here that the absolute values of the L_{II} and L_{III} conversion coefficients computed from this measurement yielded an average value 0.41 for a, agreeing reasonably well with the highest value 0.44 mentioned above.

A preliminary discussion of this state of affairs was given elsewhere [9]). It might be added that neither in this case nor in those discussed below a mixture of E1 and M2 radiations would give a better agreement with the theoretical values.

3. The 400 keV Transition in ^{203}Tl

Following the decay of ^{203}Pb a 400 keV transition [10,11]) is found to occur between 679 and 279 keV states in ^{203}Tl. We [11]) found a value 0.120 ± 0.015 for its K shell conversion coefficient by comparing its gamma and e_K^- line intensities with those of the 279 keV transition, using a scintillation spectrometer and an iron free lens beta ray spectrometer. This conversion coefficient does not depend on that found by us for the 279 keV transition due to the fact that the scintillation spectrometer had been calibrated for intensity

measurements at 279 keV by comparing the K X-ray peak and the 279 keV photopeak of ^{203}Hg [12]) (and at 411 keV using the same procedure with ^{198}Au). Therefore the reported [11]) intensity ratio $279\gamma/400\gamma = 21.7$ does contain the 279 keV conversion coefficient (with the better value for α_K 0.164 ± 0.005 [13]) this ratio becomes 20.1), but the K shell conversion coefficient of the 400 keV transition does not. In view of the fact that both Varma's and our measurements can scarcely be expected to be better than about 10 % precise, the difference with Varma's value $279\gamma/400\gamma = 23.5$ is not significant. It is therefore somewhat surprising that Varma's value 0.076 ± 0.012 for the 400 keV K shell conversion coefficient is so much lower than ours. It should be mentioned that the $K/(L + M)$ ratio of the 400 keV conversion lines shows a similar discrepancy: Varma finds 3.7 while our value is 4.9 ± 0.4. This could be explained by assuming that due to some contamination our 400 keV K line was double. We have repeated our measurements with line halfwidths beter than 1 %; these measurements did not give any indication for such a contamination. We are therefore inclined to assume that our values are more dependable than Varma's.

Varma also measured the angular correlation between the 279 and 400 keV γ-rays; his results have recently been confirmed at Utrecht [34]). The ground state of ^{203}Tl has [35]) a spin of $\frac{1}{2}$; the mixed M1 — E2 character of the 279 keV transition allows only a spin 3/2 for the 279 keV state. The E2 character of the 679 keV cross-over transition [11]) indicates a spin 5/2 for the 679 keV state (though 3/2 cannot be excluded). The relation between the multipole mixtures for a $5/2(M1 + E2)3/2(M1 + E2)\frac{1}{2}$ transition [14]) following from Varma's results has been plotted in fig. 2. It is now seen that our value for a_{400} (defined by eq. (2.1)) does not agree with any value of a_{279} obtained in the preceding section. This deviation could again be explained by multiplying Rose *et al.*'s theoretical β_{1K} by 0.6: $0.6\beta_{1K} = 0.12$ (and $\alpha_{2K} = 0.034$) would yield that the 400 keV transition is practically pure M1 ($a > 0.8$), agreeing with the two upper parts of the curve of fig. 2 for all discussed values of a_{279}. In the case of a spin 3/2 for the 679 keV state Varma's angular correlation would yield either $a_{400} < 0.1$ or $a_{400} > 0.9$, which again would lead to the same conclusion (which makes it impossible to determine the spin of the upper state from the angular correlation experiment). We think therefore that this case points again strongly to a correction to β_{1K} of the same magnitude as that found for the 279 keV transition.

It may be added that according to the nuclear shell model the 279 keV transition occurs between $d_{3/2}$ and $s_{1/2}$ states. In a strict

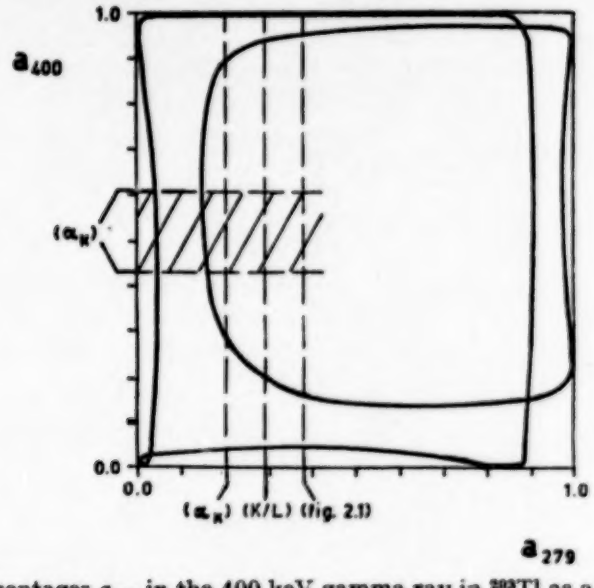

Fig. 2. M1-percentages a_{400} in the 400 keV gamma ray in ^{203}Tl as a function of a_{279} following from Varma's angular correlation experiment for a 5/2(M1 + E2)3/2(M1 + E2)½ cascade. The values of a derived from both experimental conversion coefficients and K/L ratios are indicated.

single-particle model such a transition should be forbidden for M1 transitions ($\Delta l = 2$). This might be the reason that the M1 fraction in this transition is so much delayed that E2 can compete with it ($\tau = (1 \pm 0.4) \times 10^{-9}$ sec [15]); theoretical half-life for E2 4×10^{-9} sec, for M1 2×10^{-12} sec [16])). On the other hand the 400 keV transition should occur between $d_{5/2}$ and $d_{3/2}$ states, so that M1 is allowed. The theoretical half-life ratio E2/M1 being [16]) $\approx 10^{-3}$ it should be expected that the E2 admixture is low.

The $\Delta l = 2$ selection rule for M1 does not check in many investigated cases, e.g. in the second $d_{3/2} - s_{1/2}$ step of the two-step isomeric transitions in Sn, Te and Xe [17]); it might, however, be expected that it would still be fairly strong in a nearly double magic nucleus like ^{203}Tl ($Z = 81, N = 122$).

4. The 242, 295 and 352 keV Transitions in ^{214}Bi (RaB → RaC)

The absolute intensities of the conversion lines in RaB have been measured by Ellis and Aston [18, 19]); their results agree within reasonable errors with those of Gurney [20]). Recently the relative intensities were remeasured with care by Mladjenović and Slätis [21]); their

results agree with those of Ellis and Aston. The values given in Table 4.1 are averages from the results of Ellis and Aston and

TABLE 4.1

Intensities of conversion electrons and gamma rays of the F, G and H transitions per 100 decays of RaB

Designation	Energy	$\bar{e}_K$	$\bar{e}_{LI}$	$\bar{e}_{LII}$	$\bar{e}_{LIII}$	$\bar{e}_{M+N}$	$\bar{e}_{tot}$	γ
F	242	4.25	0.78	0.17	0.008	0.31	5.5	10
G	295	5.00	0.79	0.13	< 0.008	0.33	6.3	25
H	352	5.40	0.92	0.17	< 0.010	0.44	6.9	45

Mladjenović and Slätis. The absolute γ-intensities have been measured by Ellis and Aston [18]); they agree with the more recent relative intensities measured by Muller *et al.* [22]). On the other hand Gray [23]) found from a total absorption curve that the ratio of high energy to low energy γ-radiation in the Ra deposit had been significantly underestimated by Ellis and Aston, which might indicate that the three γ-ray intensities in table 4.1 are all somewhat high. Measurements of the continuous β-spectrum, however, yield only two β-branches of 650 and 590 keV [24]) which should then be followed mainly by the F, G and H lines in parallel. This checks with the fact that the total intensity of Ellis and Aston's γ-rays and conversion lines (sum of the last two columns in table 4.1) is nearly 100 per 100 decays; this means that the error can scarcely be very large. We have therefore only corrected the γ-intensities by 15 %

TABLE 4.2

Experimental conversion coefficients for the F, G and H transitions in RaC compared with the theoretical M1 and E2 conversion coefficients

energy	conversion	K	L_I	L_{II}	L_{III}
242	$100\beta_1$ (theor.)	94	14.8	1.36	0.079
	100α (exp.)	50	9.2	2.0	< 0.09
	$100\alpha_2$ (theor.)	10.8	1.70	5.4	2.85
295	$100\beta_1$ (theor.)	57	8.6	0.79	0.044
	100α (exp.)	23.5	3.7	0.61	< 0.04
	$100\alpha_2$ (theor.)	7.0	1.09	2.46	1.14
352	$100\beta_1$ (theor.)	35	5.3	0.49	0.025
	100α (exp.)	14.1	2.40	0.45	< 0.026
	$100\alpha_2$ (theor.)	4.7	0.73	1.17	0.51

(also in order to allow for some other weak γ-rays known to be present in the decay of RaB); if anything, this correction is expected

to be somewhat large; then the computed conversion coefficients should be somewhat large too. The conversion coefficients computed in this way are compared in table 4.2 with the theoretical values.

It appears from the L_{II}/L_{III} ratios that, unless a very large correction should have to be made to the theoretical conversion coefficients, all three γ-rays should be more than 90% pure M1 transitions. But this means that the theoretical M1 conversion coefficients for these energies should be multiplied with a factor 0.45 for the K and 0.50 for the L_I shell conversion (1.05 for the L_{II} shell).

These cases have also been discussed by Sliv and Listengarten [6]). They find that all three transitions should be mixed M1 + E2. A discussion of this result will be given in section 8.

5. The 238 keV Transition in ^{212}Bi (ThB → ThC)

The 238 keV level in ThC is excited in (83 ± 3) % of the decays of ThC [25]); its K conversion line, the well-known Th F line, is emitted in (30.3 ± 1) %, its L and (M + N) lines in (5.5 ± 0.3) % and 1.7 % of the decays [25, 26, 27, 28]); therefore in 45.5 % a gamma ray is emitted. The conversion coefficients following from these data together with the photographically measured $L_I : L_{II} : L_{III}$ ratios [29]) 22 : 1.4 : 0.1 are compared in table 5.1 with the theoretical values.

TABLE 5.1

Conversion coefficients for the Th F transition				
	K	L_I	L_{II}	L_{III}
$100\beta_1$ (theor.)	102	15.5	1.43	0.082
100α (exp.)	66	11.3	0.72	0.05
$100\alpha_s$ (theor.)	11.2	1.77	5.8	3.1

The L_{II}/L_{III} ratio again does not allow more than 10 % of E2-admixture; we then find correction factors 0.65, 0.73 and 0.50 for K, L_I and L_{II} respectively. It is thought that the large deviation for L_{II} may be due to the difficulty of estimating photographically the relative intensity of this part of the narrow $L_I - L_{II}$ doublet. This explanation cannot hold for the K and L_I lines, which have been determined more than once by counting [25, 26, 27, 28]). Therefore this case again offers evidence for lower M1 K and L_I shell conversion coefficients.

In a very recent private communication Sokolovski, Edvarson

and Siegbahn have informed us that they find in their ironfree double focusing β ray spectrometer that the $K/L_I/L_{II}$ conversion ratios for this transition agree with Rose *et al.*'s theoretical values, indicating that the L_{II} conversion coefficients may be low too.

It should be added that this case has been mentioned earlier by Feather [4]).

6. ^{182}W and ^{183}W

Undoubtedly the most extensive set of reasonably dependable conversion coefficients was recently published by Murray *et al.* [30]) in their study of the decay of ^{182}Ta and ^{183}Ta. The relative intensities of the γ-rays were measured with a curved-crystal spectrometer, those of the conversion electrons with an iron free thick lens beta ray spectrometer. Division of these two sets of data yields relative values for the conversion coefficients. Murray *et al.* converted these relative values to absolute ones by assigning the theoretical M1 K conversion coefficient to a selected transition that was (on the basis of L subshell conversion ratios) known to be a relatively pure M1 transition. The result is that many conversion coefficients agree with the theoretical M1 values, but only very few with the theoretical E2 ones; on the other hand many conversion coefficients are about 30 % higher than the theoretical E2 values (see ref. 30, fig. 4). For this reason, combined with the considerations above, we think it probable that the latter transitions are pure or almost pure E2 transitions, but that the theoretical M1 conversion coefficients (and therefore Murray *et al.*'s calibration) are high. The most suspect case is the 100.09 keV transition ascribed to the de-excitation of the first excited state in ^{182}W. On the basis of systematics of first excited states in even nuclei this transition should be pure E2 radiation; its experimental conversion coefficient $\alpha_K = 1.5$ is, however, significantly higher than the theoretical value $\alpha_2 = 1.05$.

We therefore changed the calibration in such a way that the supposedly pure E2 transitions agreed in the average with the theoretical E2 conversion coefficients. (Fig. 3, upper part). The lower part of fig. 3 shows the resulting correction factors α (exp.)/β_1(theor.) for the transitions assigned as M1.

It appears that average correction factors $f = 0.69$ and 0.86 should be applied to the theoretical K and L_I shell conversion coefficients in this case, rather independent of energy. This conclusion might be influenced by the presence of E2 admixtures in some of

these transitions, causing the experimental value to be somewhat low. We think, however, that the occurrence of more than 10 % E2 admixture should be considered as statistically rather improbable in view of the large difference between the theoretical lifetimes. Therefore this case again offers evidence for large corrections to M1 K and L_I shell conversion coefficients.

The fact that in this case the difference between the correction factors for K and L_I conversion is much larger than in the cases discussed above remains unexplained. E2 admixtures in the tungsten case cannot explain the difference because the K/L_I ratio for E2 radiation is even larger than that for M1: this would therefore tend to lower the L_I shell correction factor with respect to the K shell one. It might be due to the different nuclear mass or charge;

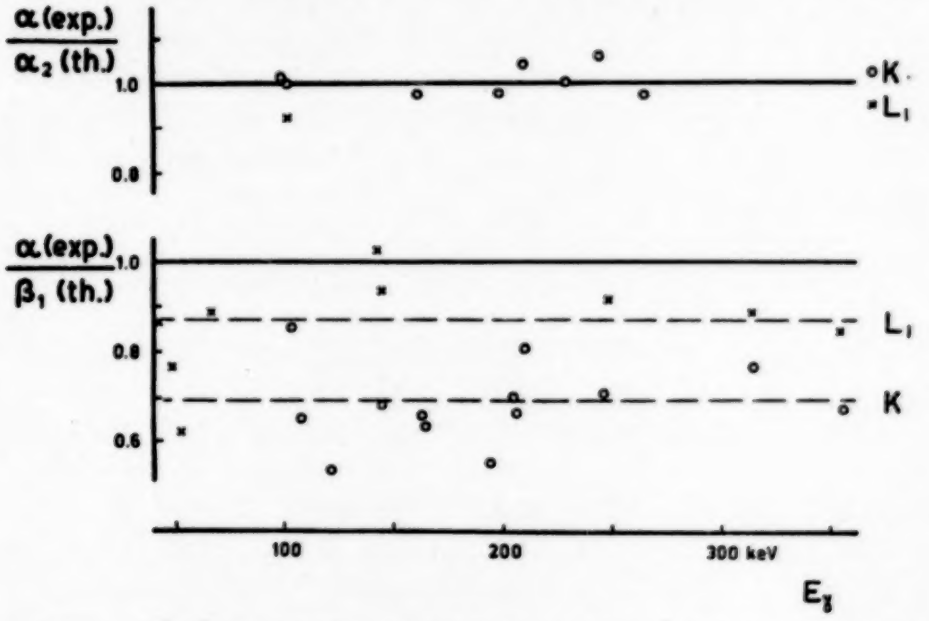

Fig. 3. Ratio of experimental and theoretical conversion coefficients for transitions in ^{182}W and ^{183}W. The upper part shows E2, the lower part M1 radiations; circles and crosses indicate K and L_I shell conversion coefficients respectively.

if this cannot explain this difference we are inclined to consider the relative magnitudes of the K and L_I shell correction factors obtained in sections 4 and 5 as slightly more dependable than those found here in view of the fact that a larger difference would mean an even larger correction factor in the case of the 279 keV transition in ^{203}Tl (section 2).

Murray *et al.* report data about three E1 and one M2 transitions. The correction factors for the E1 transitions come out $f_K(152) =$

0.46, $f_K(222) = 1.01$, $f_{LI}(67) = 1.44$, $f_{LI}(222) = 1.49$ (the values between parentheses are the respective gamma ray energies). For the 102.5 keV M2 transition $f_K = 0.79$ and $f_{LI} = 0.56$. It is thought that in these cases the deviation from unity should be studied better before allowing any conclusions about the deviations for these multipolarities.

Murray *et al.* also report data about some high energy transitions. We will not discuss these values as in some of these cases we are inclined to question the multipole assignment.

It is hoped that in other cases too the proposed corrections to the M1 conversion coefficients may drastically reduce the number of cases in which large E2 admixtures had to be assumed. We may only mention here the beautiful investigation of ^{206}Bi by Alburger and Pryce [31]) in which they had to assume 20—50 % E2 admixture to M1 transitions in order to get consistent intensity values, and the 209 keV $p_{3/2} - p_{1/2}$ transition in ^{199}Hg, in which the L-conversion ratios indicate a M1 transition, but the K- and L_I-conversion coefficients are factors 0.57 and 0.63 low (this case has been mentioned before by Sunyar [5])).

7. Low Energy Transitions

Because of the possibility that the correction factor might deviate even more from 1 if the conversion lines have very low energies we will here discuss two low energy transitions, though the results will appear to be less clear cut than those discussed before.

The lines A1, E, Ea, Eb, and Eb1 in the active Th-deposit should probably be explained as the K, L_I, L_{II}, M and N conversion lines of a 115 keV γ-ray E following the decay of Th B. The conversion line intensities are computed from Flammersfeld's [28]) measurements

TABLE 7.1

Intensity ratios for the Th E-line				
	K	L_I	L_{II}	L_{III}
β_1 (theor.)	620	100	8.6	0.6
α (exper.)	90	100	6	weak
α_2 (theor.)	650	100	1300	900

for the complex A—A1—Aa and E—Ea lines together with photographically measured intensity ratios [29]) for the separate components in each multiplet. The results are compared with the theore-

tical conversion coefficients in table 7.1. The L subshell ratios indicate a pure M1 transition. But in that case a very large correction should be applied to the K conversion coefficient. This effect might be connected with the low energy of the K conversion line (27.1 keV) †.

The total conversion coefficient of the 39.8 keV transition following the α-decay of ThC was recently determined by Weale [32]), the separate L conversion coefficients were computed from this value together with photographic intensity ratios [29]), and are compared in table 7.2 with theoretical values. It appears from the L_{II} and L_{III} conversion line intensity values that this transition can scarcely contain more than a few tenth of a percent E2. In this case the correction factors for L_I and L_{II} are 0.45 and 0.50 respectively. It might be significant that in this case as well as in that of the Th E

TABLE 7.2

Conversion coefficients for the Th A line			
	L_I	L_{II}	L_{III}
β_1 (theor.)	31	2.8	0.2
α (exper.)	14 ± 2	1.4	0.3
α_2 (theor.)	7.8	280	280

line discussed above the ratio L_I/L_{II} comes out about in agreement with the theoretical M1 value; it can, however, scarcely be excluded that this is due to the difficulties in the photographic intensity measurements. On the other hand it should be somewhat unexpected that the deviation for the 27.1 keV K-line of the E transition should be so large while that for the 26.7 keV L_I line of the A transition should be almost normal. In this respect it should be mentioned that older measurements [33]) gave much lower values for the A line conversion coefficients. It can therefore not be excluded from the present discussion that for low energy lines the corrections to the theoretical M1 conversion coefficients are even larger than those found in the preceding sections.

8. Discussion

The preceding sections indicate that large differences exist between the theoretical M1 conversion coefficients as computed by Rose *et al.* and the actual values. It might be asked why such a large

† We are indebted to Dr O. B. Nielsen for drawing our attention to this case.

effect has so far escaped detection. The answer may be that it is known that M1 transitions may contain E2 admixtures. This means that in order to detect a deviation at least two measurements are necessary out of α_K, K/L, L sub-shell ratios and angular correlations. Measurements of α_K are in most cases difficult and rather poor (this might be one of the reasons that we have so far not been able to find sufficiently accurate cases for determining the dependence of the deviation on nuclear charge or mass). The evaluation of L sub-shell ratios asks for higher resolving power and better source conditions than are mostly available. Also the measurement and interpretation of angular correlations is no simple task. Nevertheless we think that the cases discussed above together present a strong indication that the K and L_I conversion coefficients for 100—400 keV M1 transitions in nuclei with mass number around 200 are about 40 % lower than the values computed by Rose *et al.* The discussion of the three γ lines on the Ra deposit indicates that the L_{II} conversion coefficients are affected less; the other cases (sections 5 and 7), however, indicate the L_I/L_{II} ratios to be approximately in agreement with Rose *et al.*'s theoretical values.

Sliv and Listengarten [6]) have investigated the effect on the conversion coefficient due to the influence of the finite nuclear size on the electron wave functions. They find that both K and L_I conversion coefficients of M1 transitions computed without finite size corrections should be about a factor 1.5 high. The large magnitude of this effect cannot be considered unreasonable in view of the 18% discrepancy between the nuclear magnetic moment values for ^{203}Tl and ^{205}Tl as derived from atomic beam resonance experiments and from optical hyperfine structure measurements that has been explained in terms of the influence of the finite size of the nucleus on the wave functions of the valency electrons. This influence on the inner electrons could thus easily account for even larger effects. We therefore assume that the neglect of the finite nuclear size in Rose *et al.*'s computations explains the deviation found above.

This would also explain why the deviations for K conversion are always slightly larger than for L_I conversion. This effect tends to decrease K/L_I. This is at variance with the fact that the value 8.5 found by Sliv and Listengarten for the RaB line is higher than the value 6.6 derived from Rose *et al.*'s tables, in which the finite size effects were not taken into account. In view of the fact that Rose *et al.*'s values allow an almost pure M1 assignment to the F, G and H

lines in RaB while Sliv and Listengarten had to assume a strong E2 admixture (which would disagree with the L_{II}/L_{III} ratio) we are inclined to have more confidence in Rose *et al.*'s values in this respect.

According to Sliv and Listengarten [6]) the correction factor for K shell conversion should be 0.95, 0.65, and 0.50 for $Z=49$, 83 and 92 respectively. Comparison with the experimental results above points to even larger deviations. Sliv and Listengarten [6]) report that the correction factor for L_I should be about 4 % higher than that for K conversion, in approximate agreement with most cases discussed above. The deviation in the ^{182}W and ^{183}W cases (section 6) might be due to experimental errors. It can, however, not be excluded that this deviation is due to the charge and current distributions in the W nuclei differing somewhat from those in the other cases investigated above, which are all near to magic numbers $Z = 82$ and $N = 126$. If the effect really depends so much on current and charge distributions it might be possible that the correction will appear to be different not only for different isotopes of one element, but perhaps even for different transitions in the same nucleid. According to Sliv and Listengarten [6]), however, the model of the nucleus should not have an appreciable effect on the calculated correction factors.

Concerning the energy dependence Sliv and Listengarten predict only a small decrease of the correction factor (0.71 to 0.66 for $Z = 83$) if the energy increases from 250 keV to 1.5 MeV. Indeed the still rather scarce experimental material indicates at most a small energy dependence (see fig. 3), apart from the uncertain case of the Th A1-line.

We wish to thank Dr M. E. Rose for various useful remarks and suggestions made in the course of our work. We also wish to acknowledge helpful comments and the communication of results prior to publication from Professor K. Siegbahn, Fil. Lic. K. Edvarson and Miss E. Sokolovski. This work is part of a program of the Foundation for Fundamental Research of Matter F.O.M. of the Organisation for Pure Scientific Research Z.W.O.

References

1) A. H. Wapstra *et al.*, Proc. Conf. Nucl. Phys., Glasgow, 1954, p. 210
2) M. E. Rose, G. H. Goertzel and C. L. Perry, Oak Ridge National Laboratory Report ORNL-1023
3) M. E. Rose, G. H. Goertzel and C. Swift, privately circulated results (see also ref. [36]), pp. 908, 910)

4) N. Feather, see ref. [36]), pp. 745—746
5) A. W. Sunyar, Phys. Rev. **98** (1955) 653
6) L. A. Sliv, Zh. eksper. teor. Fiz. **21** (1951) 770
L. A. Sliv and M. A. Listengarten, Zh. eksper. teor. Fiz. **22** (1952) 29
7) M. E. Rose, private communication.
8) K. Edvarson, K. Siegbahn and A. H. Wapstra, to be published (see also ref. [36]), pp. 92—93)
9) G. J. Nijgh, thesis, Amsterdam 1955
10) J. Varma, Phys. Rev. **94** (1954) 1688
11) A. H. Wapstra, D. Maeder, G. J. Nijgh and L. Th. M. Ornstein, Physica **20** (1954) 169
12) B. Åstrom, A. H. Wapstra, S. Thulin and I. Bergström, Ark. Fys. **7** (1954) 247
13) G. J. Nijgh, A. H. Wapstra, N. Grobben, L. Th. M. Ornstein, O. Almén and J. R. Huizenga, to be published
14) M. E. Rose, Phys. Rev. **93** (1954) 477
15) F. R. Metzger and W. B. Todd, Phys. Rev. **95** (1954) 627 (A)
16) R. Montalbetti, Canad. J. Phys. **30** (1952) 660
17) M. Goldhaber and R. D. Hill, Rev. Mod. Phys. **24** (1952) 179
18) C. D. Ellis and G. H. Aston, Proc. Roy. Soc. **129** (1930) 180
19) C. D. Ellis, Proc. Roy. Soc. **143** (1933) 350
20) R. W. Gurney, Proc. Roy. Soc. **109** (1925) 540
21) M. Mladjenović and H. Slätis, Ark. Fys. **8** (1954) 65
22) D. E. Muller, H. C. Hoyt, D. J. Klein and J. W. M. DuMond, Phys. Rev. **88** (1952) 775
23) L. H. Gray, Proc. Roy. Soc. **159** (1937) 263
24) S. Kageyama, J. Phys. Soc. Japan **8** (1953) 689
25) D. G. E. Martin and H. O. W. Richardson, Proc. Roy. Soc. A **195** (1948) 287
26) A. Flammersfeld, Z. Phys. **114** (1939) 227
27) N. Feather, J. Kyles and R. W. Pringle, Proc. Phys. Soc. A **61** (1948) 466
28) O. B. Nielsen, private communication.
29) See ref. [36]), pp. 922—923
30) J. J. Murray, F. Boehm, P. Marmier and J. W. M. DuMond, Phys. Rev. **97** (1955) 1007
31) D. E. Alburger and M. H. L. Pryce, Phys. Rev. **95** (1954) 1482
32) J. W. Weale, Proc. Phys. Soc. **68** (1955) 35
33) B. B. Kinsey, Canad. J. Res. **26A** (1948) 426
34) H. J. van den Bold, private communication
35) D. A. Jackson, Z. Phys. **75** (1932) 223
36) Beta and Gamma Ray Spectroscopy, edited by K. Siegbahn, North-Holland Publishing Company, Amsterdam, 1955

Nuclear Physics, North-Holland Publishing Co., Amsterdam, **1 (1956)**

COLLECTIVE MOTIONS OF A SHELL STRUCTURE†

J. M. ARAÚJO

Dept. of theoretical physics, The University, Manchester††

Received 28 October 1955

Abstract: Collective motions in atomic nuclei are studied using a generalised independent particle model (time dependent well potential). After calculating nucleon wave functions in a time dependent infinitely deep well, the expectation values of the energy and angular momentum are evaluated. These are shown to be formally identical with the liquid drop quantities. By imposing on the expectation value of the energy the condition of time independence, an eigenfrequency equation is obtained. The calculated frequencies and static deformabilities show considerable fluctuations. Some experimental evidence for these fluctuations is discussed.

1 Introduction

The model of Bohr and Mottelson [1, 2, 3]) has had considerable success, the idea of collective excitation proving to be a most fruitful one for the understanding of nuclear level schemes and many other nuclear properties. However, there are some unsatisfactory points in the very basis of their description of nuclear structure. One difficulty concerns the number of nuclear degrees of freedom; the introduction of collective coordinates, treated as independent variables, makes the number of coordinates greater than $3A$. As the number of collective coordinates (describing "deformations" of the nuclear field), which can be legitimately introduced, may not exceed $\sim A^{\frac{1}{2}}$, the number of extra degrees of freedom will, for a heavy nucleus, be only a small fraction of the total number of true degrees of freedom. Still, although it may be a good approximation, in the case of reasonably heavy nuclei, to treat the coordinates of all the nucleons and the collective coordinates as independent variables, such procedure leads, at least formally, to some difficulties. Another difficulty in the foundations of Bohr-Mottelson's model consists in using the liquid drop idealisation for the description of the collective aspects of nuclear structure. In fact the idea of irrotational flow of a classical incompressible fluid seems rather hard to reconcile with the assumptions of an independent particle model.

† This paper forms part of work submitted to the University of Manchester as a thesis for the degree of Ph. D. (May 1955).

†† On leave of absence from Universidade do Porto, Portugal.

These difficulties were already dealt with by Bohr [3]) and, more recently, Süssman [4]), Tolhoek [5]) and Coester [6]) considered, in greater detail, coordinate transformations which introduce collective coordinates into the quantal description of the nucleus. By an appropriate choice of the definition of collective coordinates one can reproduce Bohr's result for the effective mass parameters (B_λ); but, as pointed out before, namely by Coester, there is little to recommend one particular choice for the definition of collective coordinates. And it appears that the restoring force parameters (C_λ) depend on the number of collective coordinates one chooses to introduce.

In this paper we investigate the consequences of assuming the validity of an independent particle model for the low-lying nuclear excited states of the collective type. Then we may expect that, when a collective motion of the nuclear matter sets in, the associated nuclear field will vary in time accordingly. So that we must deal not with a static spherically symmetric nuclear field but with an oscillating one which will, in general, deviate from spherical symmetry.

Inglis [7, 8]) has recently put forward an essentially similar idea. Comparison of his work with our method and results will be made in a later section.

2. The Nucleon Wave Functions in an Oscillating Well Potential

For the sake of simplicity we shall consider an infinitely deep square well potential and neglect spin-orbit coupling. The boundary $S(t)$ of the well will be described in the usual way:

$$R(\theta,\varphi,t) = R_0\left[1 + \sum_{\lambda\mu} \alpha_{\lambda\mu}(t) Y_{\lambda\mu}(\theta,\varphi)\right]. \tag{1}$$

We make the additional assumption that $|\alpha_{\lambda\mu}(t)| \ll 1$. To begin with, the deformation parameters $\alpha_{\lambda\mu}(t)$ will be treated as classical observables and their time dependence will be quite arbitrary.

The nucleon wave functions must then satisfy the time dependent Schrödinger equation

$$-\frac{\hbar^2}{2M}\Delta\psi = i\hbar\frac{\partial\psi}{\partial t} \tag{2}$$

together with the boundary condition

$$\psi = 0 \text{ on } S(t). \tag{3}$$

Since $|\alpha_{\lambda\mu}(t)| \ll 1$, the problem is one of a time dependent perturba-

tion of boundary conditions. Several methods have been proposed for dealing with the problem of boundary perturbations, namely by Brillouin [9]), Feshbach [10]) and Wasserman [11]). But none of these methods, originally devised to treat time independent perturbations of boundary conditions, seems suitable for the present problem. However, there are two simple methods of tackling the problem. In fact, one has only to find complete sets of functions satisfying individually either (i) the time dependent Schrödinger equation, or (ii) the time dependent boundary condition (3).

For case (i) one may take the set of functions

$$\Phi_{lm\omega}(\mathbf{r}, t) = Y_{lm}(\theta, \varphi) j_l(\varkappa(\omega) r) e^{-i\omega t}, \tag{4}$$

where the j's are spherical Bessel functions, Y_{lm} the spherical harmonics (for which we shall use Condon and Shortley's definition) and

$$\omega = \frac{\hbar}{2M} \varkappa(\omega)^2 . \tag{5}$$

In order to specify uniquely a particular solution of (2) and (3) we need some subsidiary condition. We shall use the limiting condition

$$\psi \to \Phi_{l_0 m_0 \omega_0} \text{ when } \alpha_{\lambda\mu}(t) \to 0. \tag{6}$$

Therefore we may write

$$\psi_{l_0 m_0 \omega_0}(\mathbf{r}, t) = \sum_{lm} Y_{lm}(\theta, \varphi) \int d\omega e^{-i\omega t} j_l(\varkappa(\omega) r) g_{lm}(l_0 m_0 \omega_0; \omega) \tag{7}$$

where

$$g_{lm}(l_0 m_0 \omega_0; \omega) = \delta_{l l_0} \delta_{m m_0} \delta(\omega - \omega_0) + g^{(1)}_{lm}(l_0 m_0 \omega_0; \omega) + g^{(2)}_{lm}(l_0 m_0 \omega_0; \omega) + \ldots \tag{8}$$

and $j_{l_0}(\varkappa(\omega_0) R_0) = 0$. The superscripts (1), (2), ... of the g's denote orders with respect to $\alpha_{\lambda\mu}$. For the sake of simplicity we shall, in the following, drop the indices l_0, m_0, ω_0 (corresponding to the predominant state in the wave function $\psi_{l_0 m_0 \omega_0}$) in g_{lm}, $g^{(1)}_{lm}$, $g^{(2)}_{lm}$, etc.

The boundary condition (3) now gives, in first order,

$$\sum_{lm} Y_{lm}(\theta, \varphi) \int d\omega\, e^{-i\omega t} j_l(\varkappa(\omega) R_0) g^{(1)}_{lm}(\omega) + \varkappa(\omega_0) R_0 j'_{l_0}(\varkappa(\omega_0) R_0) \cdot \cdot e^{-i\omega_0 t} \sum_{\lambda\mu} \alpha_{\lambda\mu}(t)\, Y_{l_0 m_0}(\theta, \varphi)\, Y_{\lambda\mu}(\theta, \varphi) = 0. \tag{9}$$

The product of any number of spherical harmonics can always be expanded in spherical harmonics; for instance, we may write

$$Y_{l_0 m_0}(\theta,\varphi)\, Y_{\lambda\mu}(\theta,\varphi) = \sum_{lm} c(l_0 m_0;\lambda\mu;lm)\, Y_{lm}(\theta,\varphi)$$

where the quantities

$$c(l_0 m_0;\lambda\mu;lm) = \int Y_{l_0 m_0}(\theta,\varphi)\, Y_{\lambda\mu}(\theta,\varphi)\, Y^*_{lm}(\theta,\varphi)\, d\Omega$$

($d\Omega = \sin\theta\, d\theta\, d\varphi$) are given by Gaunt's formula. Let us, for a closed-shell nucleus, express the deformation $\alpha_{\lambda\mu}(t)$ as a superposition of deformations corresponding to oscillations with frequencies $\omega_{\lambda\mu}$: $\alpha_{\lambda\mu}(t) = \Sigma_{\omega_{\lambda\mu}} \alpha_{\lambda\mu\omega_{\lambda\mu}} e^{i\omega_{\lambda\mu}t}$ ($\omega_{\lambda\mu}$ formally taking negative as well as positive values). Since (9) is an identity in θ, φ, t, we can then derive

$$j_l(\varkappa(\omega)R_0)\, g^{(1)}_{lm}(\omega) = -\varkappa(\omega_0)\, R_0 j'_{l_0}(\varkappa(\omega_0)\, R_0) \sum_{\lambda\mu\omega_{\lambda\mu}} c(l_0 m_0;\lambda\mu;lm)\cdot$$
$$\cdot\, \alpha_{\lambda\mu\omega_{\lambda\mu}} \delta(\omega - \omega_0 + \omega_{\lambda\mu}). \quad (10)$$

In a similar way we get for $g^{(2)}_{lm}(\omega)$

$$j_l(\varkappa(\omega)R_0)\, g^{(2)}_{lm}(\omega) =$$
$$\varkappa(\omega_0) R_0 j'_{l_0}(\varkappa(\omega_0)R_0) \sum_{\lambda\mu\omega_{\lambda\mu}\lambda'\mu'\omega_{\lambda'\mu'}\alpha\beta} c(l_0 m_0;\lambda\mu;\alpha\beta)\cdot \quad (11)$$
$$\cdot\, c(\alpha\beta;\lambda'\mu';lm)\alpha_{\lambda\mu\omega_{\lambda\mu}}\alpha_{\lambda'\mu'\omega_{\lambda'\mu'}}[-\alpha + f_\alpha(\omega_0-\omega_{\lambda\mu})]\,\delta(\omega-\omega_0+\omega_{\lambda\mu}+\omega_{\lambda'\mu'})$$

where

$$f_\alpha(\omega) = \varkappa(\omega) R_0 \frac{j_{\alpha-1}(\varkappa(\omega)R_0)}{j_\alpha(\varkappa(\omega)R_0)}. \quad (12)$$

Since $R(\theta,\varphi,t)$ is necessarily real, we may also write

$$j_l(\varkappa(\omega)R_0) g^{(1)}_{lm}(\omega) =$$
$$-\varkappa(\omega_0)R_0 j'_{l_0}(\varkappa(\omega_0)R_0) \sum_{\lambda\mu\omega_{\lambda\mu}} c(lm;\lambda\mu;l_0 m_0)\alpha^*_{\lambda\mu\omega_{\lambda\mu}}\delta(\omega-\omega_0-\omega_{\lambda\mu}) \quad (10')$$
$$j_l(\varkappa(\omega)R_0) g^{(2)}_{lm}(\omega) =$$
$$+\varkappa(\omega_0)R_0 j'_{l_0}(\varkappa(\omega_0)R_0) \sum_{\lambda\mu\omega_{\lambda\mu}\lambda'\mu'\omega_{\lambda'\mu'}\alpha\beta} c(lm;\lambda\mu;\alpha\beta)\, c(\alpha\beta;\lambda'\mu';l_0 m_0)\cdot$$
$$\cdot\, \alpha^*_{\lambda\mu\omega_{\lambda\mu}}\alpha^*_{\lambda'\mu'\omega_{\lambda'\mu'}}[-\alpha + f_\alpha(\omega_0+\omega_{\lambda'\mu'})]\,\delta(\omega-\omega_0-\omega_{\lambda\mu}-\omega_{\lambda'\mu'}); \quad (11')$$

these alternative expressions for $g^{(1)}_{lm}(\omega)$, $g^{(2)}_{lm}(\omega)$ will be useful in a later section.

We shall now sketch method (ii). Let us consider the set of eigenfunctions, for the boundary condition (3), of some linear operator O; the eigenvalues will be time dependent but the time is to be regarded as a parameter. The wave functions ψ satisfying equations (2) and (3) can be expanded in terms of this complete set.

The obovius choice for the operator O is the time independent hamiltonian of equation (2). Let us suppose that the wave functions $v_\varkappa(\mathbf{r}, \alpha(t))$ which satisfy

$$-(\hbar^2/2M)\,\Delta v_\varkappa(\mathbf{r}, \alpha(t)) = E_\varkappa(\alpha(t)) v_\varkappa(\mathbf{r}, \alpha(t)) \tag{13}$$

and

$$v_\varkappa(\mathbf{R}, \alpha(t)) = 0 \tag{14}$$

have been determined and were chosen to be orthogonal and normalised. We can then write

$$\psi = \sum_\varkappa a_\varkappa(t)\, v_\varkappa(\mathbf{r}, \alpha(t)) \exp\left\{-i/\hbar \int E_\varkappa(\alpha(t))\, dt\right\} \tag{15}$$

and it can be easily shown that

$$\dot{a}_n = \sum_\varkappa a_\varkappa \exp\left\{i/\hbar \int [E_n(\alpha(t)) - E_\varkappa(\alpha(t))]\, dt\right\} \cdot \frac{\hbar^2}{2M} \cdot$$

$$\cdot \frac{R_0}{E_\varkappa(\alpha(t)) - E_n(\alpha(t))} \cdot \sum \dot{\alpha}_{\lambda\mu} \int_{S(t)} \frac{\partial v_\varkappa}{\partial r} \cdot \frac{\partial}{\partial \nu} v_n^* \cdot Y_{\lambda\mu}(\theta, \varphi)\, d\sigma. \tag{16}$$

Naturally, method (ii) is very similar to the so called adiabatic perturbation method (e.g. Schiff [12])).

The time independent problem represented by (13) and (14) can be solved by a method essentially due to Cabrera[13]). We shall write for the wave function $v^{(i)}_{l\omega_i}$

$$v^{(i)}_{l\omega_i} = \sum_{\alpha\beta} Y_{\alpha\beta}(\theta, \varphi) j_\alpha(\varkappa^{(i)}_{l\omega_i} r)\, g_{\alpha\beta} \tag{17}$$

where

$$g_{\alpha\beta} = \delta_{\alpha l} a^{(i)}_\beta + \varepsilon_{\alpha l}(g^{(1)}_{\alpha\beta} + g^{(2)}_{\alpha\beta} + \ldots), \quad \varepsilon_{\alpha l} = 1 - \delta_{\alpha l} \tag{18}$$

and

$$\varkappa^{(i)}_{l\omega_i} = \varkappa_{l\omega_i(0)} + \varkappa^{(i)}_{l\omega_i(1)} + \varkappa^{(i)}_{l\omega_i(2)} + \ldots, \quad j_l(\varkappa_{l\omega_i(0)} R_0) = 0. \tag{19}$$

For the energy we shall have

$$2M/\hbar^2 E^{(i)}_{l\omega_i} = \varkappa^2_{l\omega_i(0)} + 2\varkappa_{l\omega_i(0)} \varkappa^{(i)}_{l\omega_i(1)} +$$

$$+ [2\varkappa_{l\omega_i(0)} \varkappa^{(i)}_{l\omega_i(2)} + (\varkappa^{(i)}_{l\omega_i(1)})^2] + \ldots \tag{20}$$

Exactly as in method (i) we can derive

$$\sum_m a^{(i)}_m \{\varkappa^{(i)}_{l\omega_i(1)} \delta_{m\beta} + \varkappa_{l\omega_i(0)} \sum_{\lambda\mu} \alpha_{\lambda\mu} c(lm; \lambda\mu; l\beta)\} = 0, \tag{21}$$

$$\sum_m a^{(i)}_m \{\varkappa^{(i)}_{l\omega_i(2)} \delta_{m\beta} - \varkappa_{l\omega_i(0)} \sum_{\lambda\mu\lambda'\mu'\gamma\delta} \alpha_{\lambda\mu} \alpha_{\lambda'\mu'} c(lm; \lambda\mu; \gamma\delta)\, c(\gamma\delta; \lambda'\mu'; l\beta) \cdot$$

$$\cdot [\delta_{\gamma l} + \varepsilon_{\gamma l}(-\gamma + f_\gamma(\omega_i))]\} = 0, \tag{22}$$

(for $-l \leqq \beta \leqq +l$ and the same range of the superscript (i)) as well as equations giving $g^{(1)}_{\alpha\beta}$, $g^{(2)}_{\alpha\beta}$, etc.

It follows from (21) and (22) that $\varkappa^{(i)}_{l\omega_i(1)}$ and $\varkappa^{(i)}_{l\omega_i(2)}$ are the eigenvalues of the commuting hermitian matrices

$$M^{[1]}_{\beta m} = -\varkappa_{l\omega_i(0)} \sum_{\lambda\mu} \alpha_{\lambda\mu}\, c(lm;\lambda\mu;l\beta), \tag{23}$$

$$M^{[2]}_{\beta m} = +\varkappa_{l\omega_i(0)} \sum_{\lambda\mu\lambda'\mu'\gamma\delta} \alpha_{\lambda\mu}\alpha_{\lambda'\mu'}\, c(lm;\lambda\mu;\gamma\delta)\, c(\gamma\delta;\lambda'\mu';l\beta) \cdot \cdot [\delta_{\gamma l} + \varepsilon_{\gamma l}(-\gamma + f_\gamma(\omega_i))]; \tag{24}$$

$\mathbf{a}^{(i)}$ are the corresponding eigenvectors. Except for some particular cases (e.g. deformations preserving cylindrical symmetry) the determination of these eigenvalues and eigenvectors is not possible. Still, as we shall see in the next section, one can, for the case of closed-shell nuclei, calculate the interesting quantities without having the explicit knowledge of those eigenvalues and eigenvectors.

We shall mostly use method (i) and only occasionally refer to method (ii). In fact, method (i) is analytically simpler and more powerful than method (ii). On the other hand, in method (ii), the states one mixes to the "predominant" state in order to satisfy the time dependent Schrödinger equation are eigenstates of the hamiltonian, satisfying the boundary condition on $S(t)$. Therefore method (ii) is closely connected with the familiar picture of energy hypersurfaces and transitions between them. In case of method (i), the states one has to mix to the "predominant" state in order to satisfy the time dependent boundary condition do not satisfy any simple relation on $S(t)$. As a result, intermediary steps of the calculations may have a clearer physical meaning in method (ii) than in (i).

3. The Energy and Angular Momentum

We shall now use the wave functions given by (7), (8), (10), (11) and (12) to calculate the expectation value of the energy. The nuclear hamiltonian is

$$H = -(\hbar^2/2M) \sum_{i=1}^{A} \Delta_i + V_n + V_c;$$

for the sake of simplicity we shall leave out the Coulomb term V_c although this is certainly not justifiable for heavy nuclei. Concerning the nuclear interaction term V_n we shall assume that its expectation value does not change when the deformation (defined

by the set of values of $\alpha_{\lambda\mu}$) keeps the volume constant. That is, we shall assume that

$$\delta \langle \Psi | V_n | \Psi \rangle = 0 \tag{25}$$

where δ signifies a difference between the expectation values calculated with the "oscillating well" wave functions and the static spherically symmetric well wave functions (the volume being the same in both cases). Since the change in volume is

$$\delta V = R_0^3 \{ \sqrt{4\pi}\, \alpha_{00} + \sum_{\lambda\mu} |\alpha_{\lambda\mu}|^2 + \ldots \},$$

assumption (25) is valid if

$$\sqrt{4\pi}\, \alpha_{00} = - \sum_{\lambda\mu} |\alpha_{\lambda\mu}|^2 \tag{26}$$

(to second order in the α's).

Since the wave functions are orthogonal, the expectation value of the kinetic energy is simply a sum of one-particle terms. For the wave function (7) we have

$$\frac{\langle \psi | K | \psi \rangle}{\langle \psi | \psi \rangle} = \alpha_{l_0\omega_0} \sum_{lm l'm'} \iint d\omega\, d\omega'\, e^{i(\omega'-\omega)t} \hbar\omega g^*_{l'm'}(\omega') g_{lm}(\omega) J(lm\omega; l'm'\omega') \tag{27}$$

where

$$\alpha^{-1}_{l_0\omega_0} = \int_0^{R_0} j_{l_0}(\varkappa(\omega_0) r)^2 r^2\, dr = \tfrac{1}{2} R_0^3 [j_{l_0+1}(\varkappa(\omega_0) R_0)]^2, \tag{28}$$

$$J(lm\omega; l'm'\omega') = \int_{V(t)} Y^*_{l'm'}(\theta, \varphi)\, Y_{lm}(\theta, \varphi)\, j_{l'}(\varkappa(\omega')^* r)\, j_l(\varkappa(\omega) r)\, d\tau. \tag{29}$$

The integral (29) can be written

$$J(lm\omega; l'm'\omega') = I^{(0)}(l\omega; l'\omega')\, \delta_{ll'} \delta_{mm'} + \\ + J^{(1)}(lm\omega; l'm'\omega') + J^{(2)}(lm\omega; l'm'\omega') + \ldots$$

where

$$I^{(0)}(l\omega; l'\omega') = \int_0^{R_0} j_{l'}(\varkappa(\omega')^* r)\, j_l(\varkappa(\omega) r)\, r^2\, dr,$$

$$J^{(1)}(lm\omega; l'm'\omega') = \\ = R_0^3 j_{l'}(\varkappa(\omega')^* R_0)\, j_l(\varkappa(\omega)\, R_0) \sum_{\lambda\mu} c(lm; \lambda\mu; l'm') \alpha_{\lambda\mu}(t),$$

$$J^{(2)}(lm\omega; l'm'\omega') = \tfrac{1}{2} R_0^2 \left[\frac{\partial}{\partial r} r^2 j_{l'}(\varkappa(\omega')^* r)\, j_l(\varkappa(\omega) r) \right]_{r=R_0} \cdot \\ \cdot \sum_{\lambda\mu\lambda'\mu'\alpha\beta} c(lm; \lambda\mu; \alpha\beta)\, c(\alpha\beta; \lambda'\mu'; l'm')\, \alpha_{\lambda\mu}(t)\, \alpha_{\lambda'\mu'}(t).$$

Equation (27) can then simply be rewritten as

$$\frac{\langle\psi|K|\psi\rangle}{\langle\psi|\psi\rangle}=\hbar\omega_0\Big\{1+\frac{\alpha_{l_0\omega_0}}{\omega_0}\int d\omega\, e^{i(\omega_0-\omega)t}(\omega-\omega_0)\,g^{(1)}_{l_0m_0}(\omega)\,I^{(0)}(l_0\omega;l_0\omega_0)$$

$$+\frac{\alpha_{l_0\omega_0}}{\omega_0}\int d\omega\, e^{i(\omega_0-\omega)t}(\omega-\omega_0)\,g^{(2)}_{l_0m_0}(\omega)\,I^{(0)}(l_0\omega;l_0\omega_0) \tag{30}$$

$$+\frac{\alpha_{l_0\omega_0}}{\omega_0}\sum_{lm}\iint d\omega d\omega'\, e^{i(\omega'-\omega)t}(\omega-\omega_0)\,g^{(1)*}_{lm}(\omega')\,g^{(1)}_{lm}(\omega)\,I^{(0)}(l\omega;l\omega')+\ldots\Big\}.$$

The radial integrals can easily be evaluated; one obtains

$$(\omega-\omega_0)\,I^{(0)}(l_0\omega;l_0\omega_0)=(\hbar/2M)\,\varkappa(\omega_0)\,R_0^2\,j'_{l_0}(\varkappa(\omega_0)R_0)\,j_{l_0}(\varkappa(\omega)R_0), \tag{31}$$

$$I^{(0)}(l\omega;l\omega')=\underline{(-1)^l}\,\frac{R_0^2}{\varkappa(\omega)^2-\varkappa(\omega')^2}\big[\varkappa(\omega')j_l(\varkappa(\omega)R_0)j_{l-1}(\varkappa(\omega')R_0)- \tag{32}$$

$$-\varkappa(\omega)\,j_{l-1}(\varkappa(\omega)R_0)\,j_l(\varkappa(\omega')R_0)\big],$$

where the underlined factor $(-1)^l$ is present only if $\omega'<0$. If one now makes use of equations (10), (10′), (11), (31) and (32), equation (30) becomes

$$\frac{\langle\psi|K|\psi\rangle}{\langle\psi|\psi\rangle}=$$

$$\hbar\omega_0\Big\{1-2\sum_{\lambda\mu}c(l_0m_0;\lambda\mu;l_0m_0)\,\alpha_{\lambda\mu}(t)+\sum_{\substack{\lambda\mu\omega_{\lambda\mu}\\ \lambda'\mu'\omega_{\lambda'\mu'}\alpha\beta}}c(l_0m_0;\lambda\mu;\alpha\beta)\cdot$$

$$\cdot\,c(\alpha\beta;\lambda'\mu';l_0m_0)\,\alpha_{\lambda\mu\omega_{\lambda\mu}}\alpha_{\lambda'\mu'\omega_{\lambda'\mu'}}\,e^{i(\omega_{\lambda\mu}+\omega_{\lambda'\mu'})t} \tag{33}$$

$$\cdot\Big[-\alpha+f_\alpha(\omega_0-\omega_{\lambda\mu})+\frac{\omega_{\lambda\mu}}{\omega_{\lambda\mu}+\omega_{\lambda'\mu'}}\big(f_\alpha(\omega_0+\omega_{\lambda'\mu'})-f_\alpha(\omega_0-\omega_{\lambda\mu})\big)\Big]\Big\}$$

to second order in the α's. If we sum (33) over a complete shell (in the sense of our model which ignores spin-orbit coupling), several simplifications result. The spherical harmonics addition theorem allows one to write

$$\sum_{m_0}c(l_0m_0;\lambda\mu;l_0m_0)=[(2l_0+1)/4\pi]\int d\Omega Y_{\lambda\mu}(\theta,\varphi)$$

$$=[(2l_0+1)/4\pi]\cdot\sqrt{4\pi}\,\delta_{\lambda0}\,\delta_{\mu0}\,; \tag{34}$$

therefore the first order term of (33) becomes, if one uses (26),

$$2\hbar\omega_0\,\frac{2l_0+1}{4\pi}\sum_{\lambda\mu}|\alpha_{\lambda\mu}|^2. \tag{35}$$

As to the second order term, we have

$$\sum_{m_0\beta} c(l_0 m_0; \lambda\mu; \alpha\beta)\, c(\alpha\beta; \lambda'\mu'; l_0 m_0) = \frac{(2l_0+1)\,(2\alpha+1)}{(4\pi)^2} \cdot$$
$$\cdot \iint d\Omega_1\, d\Omega_2\, P_{l_0}(\cos w)\, P_\alpha(\cos w)\, Y_{\lambda\mu}(\theta_1, \varphi_1)\, Y_{\lambda'\mu'}(\theta_2, \varphi_2)$$

where w denotes the angle between the directions (θ_1, φ_1) and (θ_2, φ_2). Since

$$P_{l_0}(\cos w)\, P_\alpha(\cos w) = 2\pi \sum_{\rho\sigma} C_{l_0\alpha\rho}\, Y^*_{\rho\sigma}(\theta_1, \varphi_1)\, Y_{\rho\sigma}(\theta_2, \varphi_2)$$

we may finally write

$$\sum_{m_0\beta} c(l_0 m_0; \lambda\mu; \alpha\beta)\, c(\alpha\beta; \lambda'\mu'; l_0 m_0) =$$
$$= \frac{1}{8\pi}(2l_0+1)\,(2\alpha+1)\, C_{l_0\lambda\alpha}(-1)^\mu \delta_{\lambda\lambda'}\, \delta_{\mu,-\mu'}. \quad (36)$$

In this equation $C_{l_0\lambda\alpha}$ denotes the integral

$$C_{l_0\lambda\alpha} = \int_{-1}^{+1} P_{l_0}(z) P_\lambda(z) P_\alpha(z)\, dz;$$

this corresponds to one of the special cases when the sum in Gaunt's formula can be evaluated (e.g. Condon and Shortley [14]):

$$C_{l_0\lambda\alpha} = \frac{2(g!)^2\,(l_0+\lambda-\alpha)!\,(\lambda+\alpha-l_0)!\,(\alpha+l_0-\lambda)!}{(2g+1)!\,(g-l_0)!^2\,(g-\lambda)!^2\,(g-\alpha)!^2} \quad (37)$$

where $2g = l_0 + \lambda + \alpha$.

If one denotes the occupied shells by (l, ω_{ln}) and takes into account equations (33), (35), (36) and assumption (25), one can write

$$\delta\langle\Psi|H|\Psi\rangle = +2 \sum_{\text{occ. shells}} \hbar\omega_{ln} \frac{2l+1}{8\pi} \sum_{\lambda\mu\omega_{\lambda\mu}\bar{\omega}_{\lambda\mu}} \alpha_{\lambda\mu\omega_{\lambda\mu}} \alpha^*_{\lambda\mu\bar{\omega}_{\lambda\mu}}\, e^{i(\omega_{\lambda\mu}-\bar{\omega}_{\lambda\mu})t} \cdot$$
$$\cdot \Big\{2 + \sum_\alpha (2\alpha+1) C_{l\lambda\alpha}\Big[-\alpha + f_\alpha(\omega_{ln}-\omega_{\lambda\mu}) + \quad (38)$$
$$+ \frac{\omega_{\lambda\mu}}{\omega_{\lambda\mu}-\bar{\omega}_{\lambda\mu}}\left(f_\alpha(\omega_{ln}-\bar{\omega}_{\lambda\mu}) - f_\alpha(\omega_{ln}-\omega_{\lambda\mu})\right)\Big]\Big\}$$

where $f_\alpha(\omega)$ and $C_{l\lambda\alpha}$ are given by (12) and (37) respectively.

So far the time dependence of the $\alpha_{\lambda\mu}$ has been taken to be quite arbitrary. If one now imposes on $\delta\langle\Psi|H|\Psi\rangle$ the condition of being time independent, one gets the eigenfrequency equation

$$F_\lambda(\omega_\lambda) = \sum_{\text{occ. } (l,\omega_{ln})} (2l+1)\omega_{ln}\{4 + \sum_\alpha (2\alpha+1) C_{l\lambda\alpha} [-2\alpha + f_\alpha(\omega_{ln} - \omega_\lambda) + f_\alpha(\omega_{ln} + \omega_\lambda)]\} = 0; \quad (39)$$

here we have dropped the suffix μ of $\omega_{\lambda\mu}$ because, as the structure of the function $F_\lambda(\omega)$ shows, the frequencies of collective motions depend on λ but not on μ.

Equation (38) can be further simplified; indeed it can easily be seen that, with the notation $\alpha_{\lambda\mu\omega_\lambda}(t) \equiv \alpha_{\lambda\mu\omega_\lambda} \exp(i\omega_\lambda t) + \alpha_{\lambda\mu(-\omega_\lambda)} \exp(-i\omega_\lambda t)$, one is allowed to rewrite it in the form

$$\delta\langle\Psi|H|\Psi\rangle = \tfrac{1}{2} \sum_{\lambda\mu\omega_\lambda} \{C_\lambda(\omega_\lambda)|\alpha_{\lambda\mu\omega_\lambda}(t)|^2 + B_\lambda(\omega_\lambda)|\dot{\alpha}_{\lambda\mu\omega_\lambda}(t)|^2\} \quad (40)$$

where

$$C_\lambda(\omega_\lambda) = \sum_{\text{occ. } (l\omega_{ln})} \hbar\omega_{ln} \frac{2l+1}{8\pi} \{8 + \sum_\alpha (2\alpha+1) C_{l\lambda\alpha} [2(-2\alpha + f_\alpha(\omega_{ln} - \omega_\lambda) + f_\alpha(\omega_{ln} + \omega_\lambda)) + g_\alpha(\omega_{ln} - \omega_\lambda) + g_\alpha(\omega_{ln} + \omega_\lambda)]\} \quad (41)$$

and

$$B_\lambda(\omega_\lambda)\omega_\lambda^2 = \sum_{\text{occ. } (l\omega_{ln})} \hbar\omega_{ln} \frac{2l+1}{8\pi} \sum_\alpha (2\alpha+1) C_{l\lambda\alpha} [g_\alpha(\omega_{ln} - \omega_\lambda) + g_\alpha(\omega_{ln} + \omega_\lambda)]. \quad (42)$$

In these equations $g_\alpha(\omega_{ln} - \omega)$ is given by

$$g_\alpha(\omega_{ln} - \omega) = \lim_{\omega' \to \omega} \frac{\omega}{\omega - \omega'} [f_\alpha(\omega_{ln} - \omega') - f_\alpha(\omega_{ln} - \omega)] = \frac{MR_0^2}{\hbar} \omega \left\{ \frac{j_{\alpha-1}(\varkappa(\omega_{ln} - \omega) R_0)\, j_{\alpha+1}(\varkappa(\omega_{ln} - \omega) R_0)}{j_\alpha(\varkappa(\omega_{ln} - \omega) R_0)^2} - 1 \right\}. \quad (43)$$

Of course the equality $C_\lambda(\omega_\lambda) = B_\lambda(\omega_\lambda)\omega_\lambda^2$ gives, again, the eigenfrequency condition (39). As a check on our result (40) we may consider the limiting case $\omega \to 0$; one should get the result corresponding to a static deformed boundary. It can easily be seen that

$$\lim_{\omega \to 0} [g_\alpha(\omega_{ln} - \omega) + g_\alpha(\omega_{ln} + \omega)] = 0$$

and

$$\lim_{\omega \to 0} [f_l(\omega_{ln} - \omega) + f_l(\omega_{ln} + \omega)] = 2l + 3,$$

and therefore that

$$C_\lambda(0) = 2 \sum_{\text{occ. } (l\omega_{ln})} \hbar\omega_{ln} \frac{2l+1}{8\pi} \{4 + \sum_\alpha (2\alpha+1) C_{l\lambda\alpha} [2\varepsilon_{\alpha l}(-\alpha + f_\alpha(\omega_{ln})) + 3\delta_{\alpha l}]\}. \quad (44)$$

On the other hand, the static deformation energy can be calculated from equations (20), (21) and (22). For the case of a closed-shell nucleus we do not need to know $\varkappa^{(i)}_{l\omega_i(1)}$ and $\varkappa^{(i)}_{l\omega_i(2)}$. The interesting quantities can be calculated from the matrices (23) and (24):

$$\sum_i \varkappa^{(i)}_{l\omega_i(1)} = \operatorname{tr} M^{[1]} = -\varkappa_{l\omega_i(0)} \sum_{m\lambda\mu} \alpha_{\lambda\mu} c(lm;\lambda\mu;lm),$$

$$\sum_i \varkappa^{(1)}_{l\omega_i(2)} = \operatorname{tr} M^{[2]} = +\varkappa_{l\omega_i(0)} \sum_{m\lambda\mu\lambda'\mu'\alpha\beta} \alpha_{\lambda\mu}\alpha_{\lambda'\mu'} c(lm;\lambda\mu;\alpha\beta)\, c(\alpha\beta;\lambda'\mu';lm) \cdot \cdot [\delta_{\alpha l} + \varepsilon_{\alpha l}(-\alpha + f_\alpha(\omega_i))],$$

$$\sum_i [\varkappa^{(i)}_{l\omega_i(1)}]^2 = \operatorname{tr}(M^{[1]})^2 = \varkappa^2_{l\omega_i(0)} \sum_{m\lambda\mu\lambda'\mu'\alpha\beta} \alpha_{\lambda\mu}\alpha_{\lambda'\mu'} c(lm;\lambda\mu;\alpha\beta)\, c(\alpha\beta;\lambda'\mu';lm)\delta_{\alpha l}.$$

The equivalence with (44) can be easily seen if use is made of (20), (34) and (36).

One could also use method (ii) of the previous section to calculate the expectation value of the energy. However, if one does not make the "adiabatic assumption" (and there are no a priori reasons to believe it valid), the calculations are rather more involved. Putting

$$a_n(t) = \delta_{mn} + a^{(1)}_n(t) + a^{(2)}_n(t) + \ldots,$$

one gets for the expectation value of the energy

$$E_m(\alpha(t)) + \sum_n [E_n(\alpha(t)) - E_m(\alpha(t))] |a^{(1)}_n(t)|^2$$

to second order in the α's. One can evaluate $a^{(1)}_n(t)$ by substituting, in (16), $\dot{\alpha}_{\lambda\mu}$ by its Fourier expansion and integrating with respect to the time. The summation over all states n can be carried out by means of Euler's expansion of the Bessel functions and the result shown to be the same as (40).

Although the solutions of (39) will be considered in some detail in section 4, we shall now derive an upper limit for the smallest frequency of collective motion of order λ. We shall make use of an expansion of the Bessel functions

$$J_l(z) = \frac{(\frac{1}{2}z)^l}{\Gamma(l+1)} \cdot \prod_{n=1}^{\infty} \left\{ 1 - \frac{z^2}{j^2_{l,n}} \right\} \tag{45}$$

due to Euler (e.g. Watson [15]); here $j_{l,n}$ denote the zeros of $J_l(z)$. Equation (45) allows one to rewrite (39) as

$$F_\lambda(\omega_\lambda) = F_\lambda(0) - 4\omega^2_\lambda \sum_{\text{occ.}(l\omega_{ln}),\,\alpha\nu} (2l+1)(2\alpha+1) C_{l\lambda\alpha} \frac{\omega_{ln}\,\omega_{\alpha\nu}}{(\omega_{\alpha\nu}-\omega_{ln})[(\omega_{\alpha\nu}-\omega_{ln})^2 - \omega^2_\lambda]}$$

where $\omega_{\alpha\nu} = \hbar r_{\alpha\nu}^2/2MR_0^2$ and $r_{\alpha\nu}$ are the zeros of the spherical Bessel function of order α. The second term in $F_\lambda(\omega_\lambda)$ can be split into two parts, (α, ν) ranging over the occupied states in one of them and over the unoccupied states in the other. The first of these two parts changes sign under interchange of ω_{ln} and $\omega_{\alpha\nu}$ and therefore vanishes. So that we can write

$$F_\lambda(\omega_\lambda) = F_\lambda(0) - 4\omega_\lambda^2 \sum_{\substack{\text{occ. } (l,n) \\ \text{unocc. } (\alpha,\nu)}} (2l+1)\,(2\alpha+1)\,C_{l\lambda\alpha} \frac{\omega_{ln}\,\omega_{\alpha\nu}}{(\omega_{\alpha\nu}-\omega_{ln})\,[(\omega_{\alpha\nu}-\omega_{ln})+\omega_\lambda]\,[(\omega_{\alpha\nu}-\omega_{ln})-\omega_\lambda]}.$$

It is evident, on physical grounds, that $F_\lambda(0) = (4\pi/\hbar)\,C_\lambda(0) > 0$; this inequality is certainly verified in all the cases considered in section 4. On the other hand $\omega_{\alpha\nu} - \omega_{ln} > 0$, $(\omega_{\alpha\nu} - \omega_{ln}) + \omega_\lambda > 0$, $C_{l\lambda\alpha} \geqq 0$. If we denote by Ω the smallest difference $\omega_{\alpha\nu} - \omega_{ln}$ (α being such that $C_{l\lambda\alpha}$ does not vanish), it is clear that $F_\lambda(\omega) \to -\infty$ when $\omega \to \Omega$. Therefore the smallest zero of $F_\lambda(\omega)$ is contained in the interval $(0,\Omega)$. One should perhaps emphasise that Ω is not necessarily the difference corresponding to the last occupied level and the next (unoccupied) level; the two (occupied and unoccupied) levels must be "connected" by the deformation of order λ. Provided it is meaningful to speak of a deformation of order equal to the absolute value of the difference between the angular momenta of the last occupied level and the first unoccupied level, the first excited state of a closed-shell nucleus will rather be of the collective type than a one-particle excited state.

The expectation value of the nuclear angular momentum can be shown to reduce to

$$\langle \mathbf{M} \rangle = i \sum_{\lambda\omega_\lambda} B_\lambda(\omega_\lambda) \sum_{\mu\mu'} \alpha^*_{\lambda\mu\omega_\lambda}(t)\,\dot{\alpha}_{\lambda\mu'\omega_\lambda}(t)\,[\mathbf{m}_\lambda]_{\mu'\mu} \tag{46}$$

where $B_\lambda(\omega_\lambda)$ is given by (42) and $\mathbf{m}_\lambda$ denotes the three $(2\lambda+1)$-dimensional matrices associated with the representation of an angular momentum $\hbar\lambda$.

The results (40) and (46) for the expectation values of the energy and angular momentum resemble very closely the corresponding expressions for irrotational flow of a classical fluid.

4. Collective Frequencies; Results and Discussion

We shall now consider in some detail the solutions of the eigenfrequency equation (39), for the particular case $\lambda = 2$. It is con-

venient to use, as a unit for ω, the frequency $\omega_0(l = 0, n = 1)$ corresponding to the lowest energy level in an infinitely deep spherical well of radius R_0 (R_0 being a function of the atomic number).

We have considered nuclei with $N = Z$ and $A = 4$, 16, 36, 40,68, 80 and 116; these nuclei correspond to the successive complete filling of both the 1s, 2p, 3d, 2s, 4f, 3p and 5g proton and neutron shells. Table I gives, for these nuclei, the lowest frequency of quadrupole oscillations together with the frequencies of overtones with $\omega/\omega_0 < 3.42$. The lowest frequencies of quadrupole oscillations exhibit rather large fluctuations; the filling of s or p shells make the ratio ω/ω_0 rise while the filling of the d, f and g shells considered makes that ratio drop. This fact is more apparent if we compare the frequencies in the second column of table I with the collective frequencies of the liquid drop model (neglecting again Coulomb effects). One should not take the spherical well radius (R_w) exactly equal to the liquid drop (uniform mass distribution) radius ($R_0 = r_0 A^{1/3}$); one may, for instance, assume

TABLE I

Shells	ω/ω_0	$\omega_{min}/\omega_{L.D.}$ ($\beta = 0$)	$\omega_{min}/\omega_{L.D.}$ ($\beta \neq 0$)
1s	1.56	4.25	1.92
+ 2p	1.84 ; 2.50	3.98	2.33
+ 3d	0.296 ; 2.24 ; 3.07	0.56	0.37
+ 2s	2.21 ; 3.06	4.11	2.74
+ 4f	0.597 ; 2.66	1.02	0.72
+ 3p	2.59	4.28	3.09
+ 5g	1.005 ; 3.07	1.57	1.16

$R_w = R_0 + b = r_0(A^{1/3} + \beta)$ and take for β Swiatecki's estimate [16]) $\beta = (3\pi^2)^{1/3}/4 = 0.7733$. The ratio of the frequencies can then be written

$$\frac{\omega}{\omega_{L.D.}} = \frac{\omega}{\omega_0} \cdot \frac{A^{1/3}}{A^{1/3} + \beta} \cdot \frac{h\pi}{8r_0} \cdot \left[\frac{3}{2M\sigma}\right]^{1/2}$$

where $\sigma = 4\pi r_0^2 S = 15.4$ MeV; the values of this ratio for the nuclei considered are given (for $r_0 = 1.44 \times 10^{-13}$ cm), in the two last columns of table I, assuming both $\beta = 0$ and Swiatecki's estimate of β. The Coulomb effect, which we have ignored in our calculations and in the comparison with the liquid drop frequencies, is probably not equally important in both cases; still, at least for

reasonably light nuclei, the results would not change appreciably if Coulomb effects were included.

It is interesting to notice that the frequencies we have calculated, although showing large fluctuations, are of the same order of magnitude as the liquid drop frequencies. And, since the ratios $\omega/\omega_{\text{L. D.}}$ depend on r_0, this agreement in order of magnitude would cease to exist if nuclear dimensions were, for instance, 10 times larger or smaller.

The comparison between collective frequencies and frequencies of nucleon radial motion is also of interest; adopting for these Hill and Wheeler's estimate [17]), we have

$$\frac{\omega}{\omega_{Nl}^r} \sim \frac{\omega}{\omega_0} \cdot \frac{1}{2\beta_{l,n}} \cdot \left[1 - \frac{l(l+1)}{(\pi\beta_{l,n})^2}\right]^{1/2}$$

where $\pi\beta_{l,n}$ is the nth zero of the spherical Bessel function of order l. For example, one has, for $A = 36$, $\omega/\omega_{1s}^r \approx 0.15$, $\omega/\omega_{2p}^r \approx 0.10$, $\omega/\omega_{3d}^r \approx 0.07$; while, for $A = 40$, one has $\omega/\omega_{1s}^r \approx 1.10$, $\omega/\omega_{2p}^r \approx 0.73$, $\omega/\omega_{3d}^r \approx 0.54$, $\omega/\omega_{2s}^r \approx 0.55$. These examples seem to show that only in some cases the "adiabatic assumption" would be reasonably well justified.

Before commenting on the results in table I, we shall calculate the "static deformabilities" of the nuclei considered. It will turn out that these deformabilities also show the same sort of fluctuations as exhibited by the collective frequencies.

Equation (44) shows that one cannot speak of a surface tension in connection with the second order change in the energy; but we may write this as

$$\sum_{\lambda} S_\lambda \delta_\lambda \Sigma$$

where $\delta_\lambda \Sigma = \frac{1}{2} R_0^2 (\lambda - 1)(\lambda + 2) \sum_\mu |\alpha_{\lambda\mu}|^2$ and S_λ is an effective "static surface tension" for deformations of order λ.

For the case $\lambda = 2$ we may write equation (44) in the form

$$C_2(0) = \frac{\pi\hbar^2}{2MR_0^2} \overline{C}_2, \quad \overline{C}_2 = \sum_{\text{occ. } (N,l)} \overline{C}_2^{Nl}$$

where $\overline{C}_2$ is a sum of contributions of the occupied shells; considering the value of $\delta_2 \Sigma$ we have then

$$4\pi r_0^2 S_2(0) = \frac{\pi^2\hbar^2}{2Mr_0^2} \cdot A^{-4/3} \overline{C}_2.$$

Taking into account (37) and some recurrence relations for spherical Bessel functions we may derive

$$\overline{C}_2^{Ns} = \beta_{0n}^2 \left[\tfrac{1}{3}(\pi\beta_{0n})^2 - 1\right],$$

$$\overline{C}_2^{Np} = \tfrac{3}{5}\beta_{1n}^2 \left[\tfrac{3}{5}(\pi\beta_{1n})^2 - 1\right],$$

$$\overline{C}_2^{Nl} = \frac{(2l+1)}{(2l+3)^2\,(2l-1)^2}\beta_{ln}^2\{3\,(\pi\beta_{ln})^2 - (2l+3)\,(2l-1)\,[2l\,(l+1)-3]\},$$

the last equation corresponding to $l \geqq 2$.

In table II we have listed the contributions of the different shells ($\overline{C}_2^{Nl}$), their sum ($\overline{C}_2$) and the ratios $4\pi r_0^2 S_2(0)/15.4$ MeV, for the nuclei considered. The values in column 5 of the table were calculated using again $r_0 = 1.44 \times 10^{-13}$ cm and $\beta = 0$.

TABLE II

A	Shells	$\overline{C}_2^{Nl}$	$\frac{1}{4}\overline{C}_2$	$4\pi r_0^2 S_2(0)/15.4$ MeV
4	1s	+ 2.29	+ 2.29	9.24
16	2p	+ 13.64	+ 15.93	10.13
36	3d	− 3.41	+ 12.52	2.70
40	2s	+ 48.64	+ 61.16	11.46
68	4f	− 13.66	+ 47.50	4.38
80	3p	+ 126.28	+ 173.79	12.92
116	5g	− 27.27	+ 146.52	6.64

It is interesting to notice that, while some shells (s,p) give positive contributions to the effective surface tension, other shells give negative contributions. This means that such shells, by themselves, would prefer a non-spherical shape of the boundary. Still, as one would expect, $\overline{C}_2^{Nl}$ eventually becomes positive also for $l \geqq 2$, when n becomes large enough; that is when the corresponding wave function has a large enough number of radial nodes. Moreover, when one fills the levels in an infinitely deep well in the correct order, the sum $\overline{C}_2$ of the contributions from each shell remains positive. We have anticipated and used this result in section 3. One should emphasise that the effective "surface tensions" we have considered refer only to very small deformations of the spherically symmetric nuclei. For larger deformations level cross-overs will occur, and our results will not apply even if the second order approximation in the deformation parameters remains valid (Gallone and Salvetti [18]).

The effective surface tensions (for quadrupole deformations) listed in table II apart from showing the same sort of fluctuations as

the collective frequencies, are systematically larger than the surface tension taken from the semi-empirical mass formula. Certainly the effective surface tension depends on the well potential used; a finite well would give smaller values, while the potential energy term, which we have neglected, would tend to increase the effective surface tensions. Spin-orbit coupling would also affect the results probably mainly the places where sharp fluctuations occur. Still one may expect the general trend of the results to be the same as ours. Static deformations of the potential have been considered by several authors in connection with the nuclear quadrupole moments. In general the second order change in the energy has been taken to be the sum of the surface and Coulomb terms in the semi-empirical mass formula; and only the first order change has been calculated by quantum mechanics. Pfirsch [19]) has considered the second order change in the energy eigenvalues which he replaces by an average over all the initially degenerate levels. Still, even if he had not introduced this approximation, he would probably not get any marked fluctuations because of the additional degeneracy of several levels with different l in the isotropic harmonic oscillator potential used.

We shall now consider, in connection with the fluctuations we found, some experimental data and theoretical estimates of quadrupole moments of one-particle or one-hole nuclei. We shall refer to Bohr and Mottelson's [2]) estimate of quadrupole moments (based on a surface tension $4\pi r_0^2 S = 15.4$ MeV) and assume that the quadrupole deformabilities C_2 are the most significant for the quadrupole moments. We shall not consider Van Wageningen and de Boer's results [20]) because, as pointed out by Bohr and Mottelson, they have always used the strong-coupling limits for the projection factors.

The nucleus O_8^{17} has both the proton and neutron $s_{\frac{1}{2}}$, $p_{\frac{3}{2}}$ and $p_{\frac{1}{2}}$ shells completely filled and one extra neutron in the $d_{\frac{5}{2}}$ shell. We found that the 1s and 2p shells are very rigid (against quadrupole deformations); so that we should expect a much smaller quadrupole moment than the one calculated assuming the usual surface tension. In fact, Bohr's theoretical estimate is about 30 times larger than the experimental value: $Q_{\text{hydr.}} = -0.16$, $Q_{\text{obs.}} = -0.005$. In Al_{13}^{27} the $d_{\frac{5}{2}}$ neutron shell is now filled, as well as the $2s_{\frac{1}{2}}$ proton shell but for one particle. We have seen that the 3d shell gives a negative contribution to the effective surface tension: we would therefore expect a result closer to the hydrodynamical estimate.

And, in fact, $Q_{\text{hydr.}} \approx 2Q_{\text{obs.}}$; $Q_{\text{hydr.}} = +0.30$, $Q_{\text{obs.}} = +0.16$. In S_{16}^{33} the $d_{\frac{3}{2}}$ proton shell is now filled as well as the $2\,s_{\frac{1}{2}}$ shell; the $2\,s_{\frac{1}{2}}$ neutron shell is also filled and there is an extra neutron in the $d_{\frac{3}{2}}$ shell. We would expect the effective surface tension to rise (owing to the occupation of the $2\,s_{\frac{1}{2}}$ shells); and, in fact, $Q_{\text{hydr.}} \approx 3Q_{\text{obs.}}$; $Q_{\text{hydr.}} = -0.22$, $Q_{\text{obs.}} = -0.08$. For S_{16}^{35} we would expect the effective surface tension to drop owing to complete filling, but for one particle, of the $d_{\frac{3}{2}}$ neutron shell; but this does not seem to be the case: $Q_{\text{hydr.}} = +0.22$, $Q_{\text{obs.}} = +0.06$. Also Cl_{17}^{37}, where there is one proton in the $d_{\frac{3}{2}}$ shell and the same neutron shell is now completely filled, seems to contradict our results: $Q_{\text{hydr.}} = -0.26$, $Q_{\text{obs.}} = -0.066$. These discrepancies seem to disappear if one considers a finite well with spin-orbit coupling instead of the infinitely deep well (without spin-orbit coupling) which we have studied [21]).

The two isotopes of gallium provide a nice example; the difference in their configurations is that Ga_{31}^{71} has, when compared with Ga_{31}^{69}, an additional $p_{\frac{1}{2}}$ neutron shell filled. We would therefore expect a larger surface tension for Ga^{71} than for Ga^{69}. In fact, for Ga^{69} $Q_{\text{hydr.}} \approx 2.2\,Q_{\text{obs.}}$ ($Q_{\text{hydr.}} = +0.53$, $Q_{\text{obs.}} = +0.2$) while, for Ga^{71}, $Q_{\text{hydr.}} \approx 3.5\,Q_{\text{obs.}}$ ($Q_{\text{hydr.}} = +0.53$, $Q_{\text{obs.}} = +0.15$).

The nucleus Ge_{32}^{73} may also be a nice example; compared with Ga_{31}^{71} it has one additional $g_{\frac{9}{2}}$ neutron and, instead of one hole in the $p_{\frac{3}{2}}$ proton shell, a proton configuration $[p_{\frac{3}{2}}, f_{\frac{5}{2}}]^4$ (Bohr and Mottelson [2]). If the proton configuration is $(p_{\frac{3}{2}})^4$ one would understand the rather large value obtained by Bohr: $Q_{\text{hydr.}} \approx 6\,Q_{\text{obs.}}$ ($Q_{\text{hydr.}} = -1.2$, $Q_{\text{obs.}} = -0.2$).

The rather large value obtained by Bohr for the quadrupole moment of Bi_{83}^{209} ($Q_{\text{hydr.}} = -5.6$, $Q_{\text{obs.}} = -0.4$) can also be understood from our point of view since the $3s_{\frac{1}{2}}$ proton shell and the $4p_{\frac{3}{2}}$ and $4p_{\frac{1}{2}}$ neutron shells have been filled in reaching the proton and neutron magic numbers 82 and 126.

It must be stressed, however, that the previous considerations do not provide conclusive evidence for or against the fluctuations we find. Not only are the experimental quadrupole moments not precisely known but also our theoretical estimates are based on a very oversimplified model. Still, it is probably reasonable to conclude that the experimental results do give some indication of the existence of the fluctuations we have found.

In his paper on dynamics of nuclear deformations, Inglis [8]) used

a harmonic oscillator potential, initially isotropic; when an ellipsoidal deformation (the only type considered) takes place, it is assumed (as by Pfirsch [19]) that the "equipotential surfaces" become ellipsoids, enclosing the same volume as the corresponding undeformed spheres. It is further assumed that all those ellipsoidal surfaces have the same eccentricity. This is a very convenient assumption for the sake of simplicity of the calculations but, as Pfirsch himself emphasised, very probably overestimates the actual change in the potential. The time dependent problem associated with an ellipsoidal oscillation of the well potential is solved by Inglis using the adiabatic approximation; this turns out to be inadequate and the result that the collective frequency equals, for all closed-shell nuclei, twice the level spacing denies its own validity. One might consider solving the problem considered by Inglis without using the adiabatic approximation (as in method (ii) of section 2); one would probably get frequencies higher than those we obtained (due to overestimation of the change in potential). However the additional degeneracy of several levels with different values of l makes such problem a less interesting one to solve.

We have only considered, in this section, deformations and collective oscillations of the quadrupole type. For higher values of λ one would also get fluctuations but these would not follow the same trend. The possibility then arises, in contrast with Bohr and Mottelson's model, that, for some closed-shell nuclei, the first excited state is not $2+$ (we have seen that, for closed-shell nuclei, we expect the first excited state to be of the collective type). It would be interesting to check whether this possibility does occur and the places where one would expect it to occur. In fact it has been found that, for instance, the first excited state of Pb^{208} is $3-$. Our treatment does not allow one to consider $0+$ excited states of the collective type; only by making some assumption about nuclear interactions one might compare the excitation energies of those states with those of other states. As pointed out before, measurement of the lifetimes of the first excited states of closed-shell nuclei could provide valuable information on the nature of these states. A treatment, along the same lines, of the collective oscillations of closed-shell nuclei, for a finite square well with spin-orbit coupling, gives results which rather support our conclusions; furthermore, one gets only a limited number of "bound" collective modes instead of the infinite sequence of the infinitely deep well [21]). It is hoped that further work in

progress (by D. F. Taylor and the author) will be soon reported.

I wish to thank Professor L. Rosenfeld for suggesting the subject of collective motions in atomic nuclei and for his constant interest and advice. I would also like to thank D. F. Taylor for many friendly discussions; and the Instituto de Alta Cultura (Lisboa) for a grant which made this work possible. Finally I wish to thank Dr. Inglis for a preprint of his paper on dynamics of nuclear deformation.

References

1) A. Bohr, Dan. Mat. Fys. Medd. **26** (1952) no. 14
2) A. Bohr and B. R. Mottelson, Dan. Mat. Fys. Medd **27** (1953) no. 16
3) A. Bohr, Rotational states of atomic nuclei, Copenhagen (1954)
4) G. Süssman, Z. Physik **139** (1954) 543
5) H. A. Tolhoek, Physica **21** (1955) 1
6) F. Coester, Phys. Rev. **99** (1955) 170
7) D. R. Inglis, Phys. Rev **96** (1954) 1059
8) D. R. Inglis, Phys. Rev. **97** (1955) 701
9) L. Brillouin, C. R. **204** (1937) 1863
10) H. Feshbach, Phys. Rev. **65** (1944) 307
11) G. D. Wasserman, Phil. Mag. **37** (1946) 563; Proc. Camb. Phil. Soc. **44** (1947) 251
12) L. I. Schiff, Quantum Mechanics, New York (1949) p. 207
13) N. Cabrera, Cahiers Phys. **31** (1948) 24
14) E. U. Condon and G. H. Shortley, The Theory of atomic spectra, Cambridge (1935) p. 182
15) G. N. Watson, Theory of Bessel functions, New York (1945) p. 498
16) W. J. Swiatecki, Proc. Phys. Soc. **A64** (1951) 226
17) D. L. Hill and J. A. Wheeler, Phys. Rev. **89** (1953) 1102
18) S. Gallone and C. Salvetti, Nuovo Cimento **10** (1953) 145
19) D. Pfirsch, Z. Physik **132** (1952) 409
20) R. van Wageningen and J. de Boer, Physica **18** (1952) 369
21) D. F. Taylor, private communication

Nuclear Physics, North-Holland Publishing Co., Amsterdam, **1** (1956)

LIMITS TO SOME (n,np) CROSS-SECTIONS AT 14.5 MeV NEUTRON ENERGY

A. V. COHEN, S. B. HYDER and P. H. WHITE

Department of Physics, Imperial College, London

Received 17 October 1955

We have searched for activities due to (n,np) processes, using the apparatus described in a recent paper,[1]) by irradiating specimens with 14.5 MeV neutrons from the T(d,n) reaction. Only four reactions, Se^{80}(n,np), Pd^{108}(n,np), Ce^{142}(n,np) and W^{186}(n,np), could conveniently be investigated, since the resultant activity must be of suitable, unambiguously assignable half-life. In each case, an upper limit was placed on the reaction cross-section.

Specimens were placed close to the tritium target, at 90° to a beam of 0.5 MeV deuterons. The neutron flux, about 2×10^6n/cm^2/sec, was estimated from the counting-rate in an α-monitor. After irradiation, each specimen was placed under a Geiger counter, and the complex decay curve observed. In no case was any significant (n,np) yield found. The results, which are quoted in the table, show the estimated upper limit to the cross-sections at the 1 % level of significance; the expected error in absolute cross-sections is $\pm$ 30 %. As a check, a small copper specimen was irradiated; the measured (n,2n) cross-section was 700 mbn, in reasonable agreement with the accepted value[2]) of 480 mbn.

TABLE

Target nucleus	Se^{80}	Pd^{108}	Ce^{142}	W^{186}
Material	Element	Element	CeO_2	Element
Purity	99.7 %	99.97 %	99.9 %	99.9 %
Q, estimated, MeV	−11.5	−9.7	−8.8	−8.0
Upper limit to σ(n,np) at 1 % significance level	0.8 mbn	65 mbn	18 mbn	1.6 mbn

In order to interpret these results, we need to estimate Q-values for the reactions. The Q-value of Ce^{142}(n,np) was obtained from

Feather's work, [3]) while those of other reactions were estimated from the binding energy formula, using the compilations of Martin [4]).

The cross-sections expected on the basis of statistical theory may be calculated using a modification of the techniques described previously.[1]) Values for level densities in (p,α) reactions [5]) were used. These show less direct interaction effects than the (p,p') level-densities, [6]) and so give a better estimate of the purely statistical cross-section. One obtains estimates, which are rather sensitive to the assumed Q, of 8 μbn and 110 μbn for Se^{80} (n,np) and W^{186}(n,np) respectively.

To estimate direct interaction cross-sections, the methods of Austern *et al.* [7]) were extended. For the simplest case, one obtains for the knock-on process:

$$\sigma(\mathrm{n,np}) = \frac{(E_n + Q)}{\Delta N} \sum_{pt} \sigma_{pt}\,(\mathrm{n,np}),$$

$$\sigma_{pt}(\mathrm{n,np}) = \sigma_{np} \frac{2m^2}{8\pi^3 \hbar^3 p_n} \int\int\int \{j_0(Q' r_0)\}^2 \left[\int_{r_0}^{\infty} \{P(r)\}^{\frac{1}{2}} f_p(r) r^2 dr\right]^2 (E_r E_p)^{\frac{1}{2}} dw_r\, dw_p\, dE_p .$$

Here, the previous notation [1]) has been used, with the additional symbols:

E_n, p_n, $\mathbf{k}_n$ energy, momentum, and wave number of incident neutron,

E_p, $\mathbf{k}_p$, dw_p } energy, wave number, and element of solid angle of
E_r, $\mathbf{k}_r$, dw_r } emergent proton and neutron, respectively;

$\mathbf{Q}' = \mathbf{k}_n - \mathbf{k}_p - \mathbf{k}_r$, m = mass of proton, $P(r)$ = penetrability factor.

One predicts direct interaction cross-sections of 2μbn for Se^{80}(n,np) and 60 μbn for W^{186}(n,np) with a factor of uncertainty of about 5. For incident neutron energies of 20 MeV, either reaction mechanism predicts cross-sections of the order of millibarns.

Allan [8]) has observed the proton spectrum of Cu(n,p) reactions with E_n = 14 MeV, and suggests that the observed high yield of short-range protons might be due to (n,np) processes. This would require (n,np) cross-sections of about 20 mbn, but is not incompatible with the present theory because of the favourable Q-values in this case.

The present evidence, although negative, is therefore consistent with the presence of both statistical and knock-on mechanisms, but

more positive results would be provided by measurements at higher neutron energies.

We wish to express our sincere thanks to Professor S. Devons, for suggesting the problem and for helpful discussions. One of us (P.H.W.) is indebted to the Department of Scientific and Industrial Research for a Maintenance Grant.

References

1) A. V. Cohen and P. H. White, Nuc. Phys. **1** (1956) 73
2) E. P. Paul and R. L. Clarke, Can. J.Phys. **31** (1953) 267
3) N. Feather, Advances in Physics **2** (1953) 141
4) C. N. Martin, Numerical Tables of Nuclear Physics, Paris, Gauthier-Villars, 1954
5) P. C. Gugelot, Statistical Aspects of the Nucleus. Report of a Conference held at the Brookhaven National Laboratory, January 1955
6) P. C. Gugelot, Phys. Rev. **93** (1954) 425
7) N. Austern, S. T. Butler and H. McManus, Phys. Rev. **92** (1953) 350
8) D. L. Allan, Proc. Phys. Soc. A **68** (1955) 925

Nuclear Physics, North-Holland Publishing Co., Amsterdam, **1 (1956)**

ORBITAL MOMENTUM FORBIDDEN MAGNETIC DIPOLE TRANSITIONS IN SOME ODD PROTON NUCLEI

H. DE WAARD† and T. R. GERHOLM
Physics Department, University of Uppsala

Received 25 November 1955

Abstract: The half lives of the following excited nuclear states have been measured with delayed coincidence techniques:

145 keV level in Pr^{141}: $T_{1/2} = (19 \pm 2) \times 10^{-10}$ sec
163 keV level in La^{139}: $T_{1/2} = (15 \pm 1) \times 10^{-10}$ sec
160 keV level in I^{131}: $T_{1/2} = (9 \pm 1) \times 10^{-10}$ sec
279 keV level in Tl^{203}: $T_{1/2} = (1.2 \pm 0.3) \times 10^{-10}$ sec

Theoretical points of view about these l-forbidden ($\Delta l = 2$, $\Delta j = 1$) Ml transitions are briefly reviewed and it is shown that the matrix elements derived from the experimental half lives are in reasonable agreement with expectations based on the spin-orbit coupling encountered in the shell model.

1. Introduction

Measurements of the lifetimes of nuclear isomers should be of help in obtaining information about the structure of the nucleus. While certain general properties of isomeric transitions, e.g. the energy dependence of the lifetime for different multipole orders, follow from considerations that do not involve any particular model of the nucleus, quantitative estimates for the rate of transition in particular cases can only be made on the basis of some nuclear model.

Thus the *independent particle model* gives a reasonable estimate for the long lived M4-transitions [1,2]). These transitions were for some time considered as the only ones that showed the regularities to be expected if the extreme single particle version of the shell model was a good approximation of nuclear structure. Of the other isomeric species, especially those with short lifetimes, little could be understood quantitatively. There, the irregularities are so large that in particular cases the lifetimes of transitions of lower multipole

† On leave from Natuurkundig Laboratorium der Rijks-Universiteit te Groningen, Netherlands.

order are even considerably longer than those of a higher order. This is the case, for instance, for some peculiar very slow E1-transitions observed by Sunyar [3]) and by de Waard [4]) with lifetimes considerably longer than those of many E2-transitions of the same energy.

Certain fast E2-transitions can be understood within the framework of Bohr-Mottelson's [5,6]) collective nuclear model as taking place between rotational states of strongly deformed nuclei. But in general little information about multipole order can be derived from short isomeric lifetimes.

However, in another class of short lived isomeric transitions, that of the "*l*-forbidden" magnetic dipole transitions some marked regularities have been found by Graham and Bell [7]). Such transitions occur between shell model states differing by two units in orbital angular momentum. It turns out that these transitions give points in a logarithmic energy (E) versus lifetime (τ_γ) plot that are closely grouped along two straight lines: the line given by $\log \tau_\gamma = -11.0 - 3 \log E$ (E in MeV) closely matches transitions in odd proton nuclei, the one given by $\log \tau_\gamma = -11.7 - 3 \log E$ those in odd neutron nuclei.

In this paper measurements of lifetimes of *l*-forbidden M1-transitions in four more odd proton nuclei will be reported; in three cases the measured values give points in a $\log \tau_\gamma$ versus $\log E$ diagram close to the line given by $\log \tau_\gamma = -11.0 - 3 \log E$, in accordance with the results of Graham and Bell.

In the next section some theories will be reviewed that are of importance for the kind of isomerism observed here. In section 5 the experimental results will be discussed and compared with theory. It will be found that the rates of *l*-forbidden M1 transitions are in reasonable agreement with theoretical calculations based on spin-orbit coupling effects.

2. Theoretical Considerations

In order to calculate matrix elements

$$\mu = \langle \mathrm{i} \,|\, I \,|\, \mathrm{f} \rangle \qquad (1)$$

for transitions $\mathrm{i} \rightarrow \mathrm{f}$, it is necessary to know the form of the *interaction operator* I and the *wave functions* Ψ_i, Ψ_f of the states between which the transition occurs. When μ is known, the transition probability, $1/\tau_\gamma$, which is proportional to $|\mu|^2$ can be written down at once.

Possible forms of the interaction operator may be derived from rather general considerations, but the wave functions must be guessed at, resorting to some model of the nucleus.

There is a fundamental difference between the electric and magnetic multipole operators (I_{el}, I_{ml} respectively). As pointed out first by Siegert [8]) for the electric dipole case and later generally proved by Sachs and Austern [9]), the I_{el} are independent of interactions between nucleons; they only depend on the *charge distribution* in the nucleus. The correlation between charge distribution and electric multipole transition probability is clearly demonstrated, for instance, by the "fast" E2 transitions between rotational states. In the operators I_{ml}, on the other hand, which depend not only on the charge but also on the current distribution in the nucleus, apart from the "ordinary" magnetic multipole operator $I_{ml}^{(o)}$ that arises from the orbital and spin moments of the nucleons, each taken separately, "extraordinary" terms should be included, among others those that take into account the coupling between the magnetic moments of the nucleons.

Such coupling may be responsible for the deviations of the static magnetic moments from the Schmidt-lines, along which they should be grouped according to the independent particle model.

Another experimental observation that may be explained as an effect of coupling between nucleons is the occurrence of the so called l-forbidden magnetic dipole transitions between single particle states with different orbital quantum number l. For such transitions the matrix elements of the ordinary magnetic dipole operator vanish, since, apart from spin operators, they take the form

$$\mu = \langle \mathrm{i} \left| \frac{eh}{2Mc} \mathbf{n} \cdot \boldsymbol{\Sigma}_p \mathbf{l}_p \right| \mathrm{f} \rangle; \qquad (2)$$

$\mathbf{l}_p$ is the orbital momentum operator of the p-th proton and $\mathbf{n}$ an arbitrary unit vector. As soon as for one of the protons $\Delta l_{\mathrm{i}\to\mathrm{f}} \neq 0$, μ vanishes: of the matrix of which (2) gives the elements only the diagonal elements are $\neq 0$. The rate of l-forbidden M1 transitions between single particle states should therefore be determined by the strength of extraordinary terms of the magnetic dipole operator in as far as these do not also forbid $\Delta l_{\mathrm{i}\to\mathrm{f}} \neq 0$ transitions.

Since M1 transitions occur between states with the same parity that do not differ in nuclear spin by more than one unit, the l-forbidden M1 transitions between shell model states clearly must obey

the selection rules $\Delta l = 2$, $\Delta j = 1$. The regions where such transitions have been found are indeed in accordance with shell model expectations.

The mechanisms of coupling between nucleon moments that have been considered theoretically appear to fall in the three following categories:

1) the coupling resulting from charge and spin exchange interaction between pairs of nucleons,

2) spin-orbit coupling,

3) the coupling resulting from or represented by collective motion of nuclear matter.

A general formulation of the theory of exchange interactions has been given by Sachs and others [9,10,11]), who have derived possible forms of the exchange operators under certain general restricting conditions. According to Ross [12]), the velocity independent *spin exchange interaction* should contribute most to the extraordinary multipole moments†. Recent calculations of *charge exchange moments* by Russek [13]) show that the formalism of Sachs' theory accounts satisfactorily for the average trend of the deviations of the magnetic moments from the Schmidt-lines, if it is applied in conjunction with a modified shell model.

Russek's calculations also show, however, that the matrix elements of the charge exchange operator vanish between states with $\Delta l = 2$, even if configurational admixtures are allowed in these states.

In the general theory due to Sachs, the moment caused by *spin-orbit coupling*, that has been calculated separately by Jensen and Mayer [14]), results as a special case of a velocity dependent interaction [11]). Since, however, the general formulation does not lend itself readily to quantitative moment calculations, there appears to be some cause for considering the simple and more straightforward calculation by Jensen and Mayer separately. This will be done in some detail in section 5. Since the regions where the l-forbidden M1 transitions occur are all near closed shells, collective effects, in Bohr and Mottelson's sense, probably do not greatly influence the transition rates.

Hitherto, attention has been focused mostly on the form of the interaction operator I_{ml}. In order to calculate matrix elements, assumptions must be made about the nuclear wave functions Ψ_i and Ψ_f. For the eigenfunctions of the single particle states of a

† See also the remarks in section 5.

spherical nucleus, matrix elements can be evaluated. We know, however, from the experimental data of nuclear spectroscopy, that even near closed shells noticeable admixtures to single particle functions occur. It may be thought, therefore, that the very uncertainty of these wave functions would make it impossible to obtain any detailed information about interaction moments from lifetime measurements. Also, one might ask whether departures from single particle functions would not destroy the l-forbiddenness of the M1 transitions considered here. This latter possibility has been expounded by Volkov [15]), who goes to the extreme of calculating matrix elements of the *ordinary* magnetic dipole moment operator between states with $\Delta l = 2$, using wavefunctions that consist of equally weighted mixtures of all possible odd particle configurations belonging to the odd particle open shell. On this assumption $|\mu|^2$-values are found that even considerably *exceed* the experimental values for odd proton nuclei. Volkov remarks that any modification of the wave functions that emphasizes even-particle states or orthodox shell model states will of course reduce the estimate for $|\mu|^2$ and therefore improve the agreement between theory and experiment.

A rather strong argument against this explanation lies in the experimentally observed constancy of the matrix elements, discussed in section 5. In Volkov's model the transition rates would depend critically on the extent to which the single particle wave function is admixed. It can hardly be expected that this admixture varies so little for the nuclei investigated here.

3. Instrument and Methods

The delayed coincidence technique offers the most generally applicable method for the determination of short lifetimes of excited nuclear energy levels. When the nuclear decay is not very simple, it is necessary to use some sort of energy selection of the nuclear radiation. The best way to do this is to use magnetic spectrometers in one or both channels. With an electron-electron coincidence spectrometer it is also possible to get rid of certain systematic errors, discussed below, and to reach the ultimate limit of measurable lifetime, set by the scintillators (photoelectron production statistics) and the photomultipliers (transit time spread).

However, the small solid angles of the magnetic electron-electron coincidence spectrometers result in a low coincidence counting rate,

which makes the measurements time consuming. It therefore becomes necessary to use strong (and thin) sources and one is often restricted to not too short lived isotopes that can be produced with high specific activity.

If these limitations cannot be overcome, one may have to resort to absorption methods, in order to get at least a rough energy discrimination. In principle it is necessary, and under favourable conditions even sufficient, that the absorber prevents either the preceding or the delayed radiation from being detected in both counters. Sometimes the energy of the nuclear transition in question can be found from delayed coincidence absorption measurements (cf. I^{131} below).

The measurements discussed in this paper were all made with the absorption method. Details of absorber thickness and geometrical arrangement will be given in each particular case.

The sources and the absorbers were sandwiched between $10 \times 10 \times 4$ mm^3 stilbene crystals, fastened to 1P21 photomultiplier tubes†. The crystal surfaces were ground. 200 μg/cm^2 Al-foils were used as light reflectors. Perspex lightguides, machined in different ways to collect the light onto the photocathode, were tried but generally not used since little improvement was obtained in this way.

A block diagram of the instrument is shown in fig. 1. The two photomultipliers, selected out of six, were normally operated at 2000 volt. Pulses are taken from the multiplier anodes and fed via equalizers into both ends of a helical delay line. The 100 ohm output impedance of the equalizers matches the characteristic impedance of the helical delay line and the RG7U-connecting cables. The coincidence arrangement is identical with that described by Bell *et al.* [16]). The resolving time†† of this fast coincidence unit is a few millimicroseconds.

A very rough energy discrimination may be provided by the use of pulse height selection in the side channels. Signals to the pulse height selectors are taken out from one of the last dynodes. The slow

† Though this type of photomultiplier has a poor light collection, it is probably still the most suitable tube available for measurements of very short lifetimes, chiefly because of its small cathode to first dynode transit time spread.

†† The resolving time is defined here as the width at half maximum of a prompt coincidence rate versus delay curve. It therefore depends somewhat on the adjustment of the equipment and the source used for recording the prompt coincidence curve.

triple coincidence unit (resolving time $\sim 5\ \mu$sec) selects only those coincidences from the fast unit that correspond to pulses in the side channels lying within the pulse height selector channels. In this way the performance of the instrument may be considerably improved.

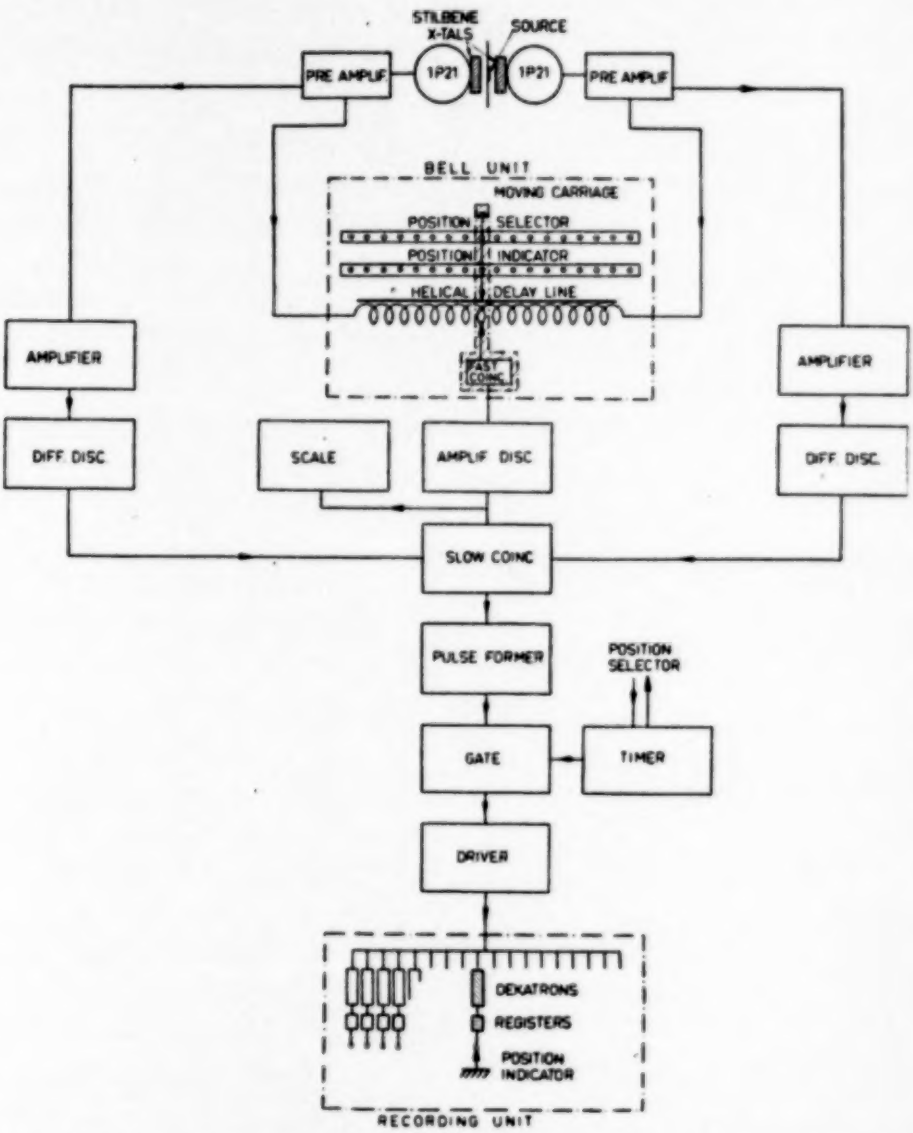

Figure 1. Block diagram of the automatized fast coincidence equipment

The remaining blocks of the diagram shown in fig. 1 refer to the automatic recording features of the equipment. The coincidence counting rates for a number of different delays are automatically recorded on a number of registers. The fast coincidence unit is attached to a carriage moving along the delay line. At certain points,

chosen by position selection switches, the carriage stops and counts coincidences for a time predetermined by the timer setting. After a count is finished, the carriage moves to the next position because each time the timer stops a relay is closed that actuates the carriage motor. As shown in fig. 1 the counts are recorded on simple scales of 10, consisting of dekatrons and mechanical registers. In the present design counting rates corresponding to 32 different time delays can be automatically recorded, but provision is made for an extension to 53 different positions. The direction of motion is automatically reversed in the extreme positions. The instrument will therefore continue to scan the delay interval, collecting coincidences, until it is shut down.

When the lifetime of the excited nuclear level is of the same order as (or longer than) the resolving time of the coincidence circuit, the plot of coincidences versus time delay differs markedly from a prompt coincidence curve. In this case the half life may simply and accurately be determined from the exponentially decaying slope of the curve (cf fig. 2 below).

For lifetimes considerably shorter than the resolving time the shape of the whole curve must be taken into account. Methods for analyzing such delayed coincidence curves have been developed by Newton [17]) and Bay [18]), making use of the differences between prompt and delayed coincidence curves. Alternatively, as was first suggested by Graham and Bell [1]), one can compare 2 plots of the delayed coincidences, one obtained before and one after interchanging the functions of the two detectors in such a way that the delayed pulses occur first in one and then in the other channel, everything else remaining unchanged. When the absorption method is used this simply means that the source and absorber assembly should be turned round between the two crystals.

A few words of caution are necessary here. The shape of the delayed coincidence curve may be distorted by other causes than the presence of delayed radiation. A systematic error is then introduced. For instance, a high background of random coincidences will broaden the base part of the curve and make the measured half life too large. This effect may be corrected for by subtracting the random coincidence background, measured separately with a large time delay inserted in one channel.

Another effect, tending to reduce the apparent lifetime, is caused by an admixture of prompt coincidences. These may be caused, for

instance, by electrons scattered back from one crystal through source and absorber into the other.

Particular care should be taken when Bell's selfcomparison method is used in combination with the absorption method. When electron-gamma coincidences are studied, the fundamental difference between the absorption of an electron and of a gamma-quantum in the scintillation crystal may introduce a spurious time delay. Such unwanted delays may also occur if the energy difference between the two electrons in an electron-electron coincidence pair is large. In such cases "comparison-selfcomparison" measurements may help to eliminate systematic errors (cf Tl^{203} below).

4. Measurements

4.1. PERFORMANCE OF THE INSTRUMENT. HALF LIFE THE 84 keV LEVEL OF Yb^{170}

The 84 keV excited state of Yb^{170} offers a suitable case for checking the performance of the fast coincidence equipment. The half life of this level, excited in the beta-decay of Tm^{170} (129 day), has been measured by Graham, Wolfson and Bell [19]) who give $T_{\frac{1}{2}} = (15.7 \pm 0.5) \times 10^{-10}$ sec. This is a typical case of a fast E2 transition enhanced over Weisskopf's estimate by a factor of 140. This enhancement is due to the large electric quadrupole moment that is characteristic for the much deformed nuclei in the rare earth region.

Thulium oxide was bombarded with 20 MeV deuterons. The activities produced in the target were chemically separated using an ion exchange column. A part of the thulium-fraction was taken out, deposited on a 30 mg/cm^2 aluminium foil and placed between the two stilbene crystals.

The maximum energy of the beta-rays leading to the 84 keV level is 884 keV. Thus, the aluminium backing is transparent to most of the beta-rays. The conversion electrons, however, are completely absorbed.

From the exponential slope of the delayed coincidence plot (fig. 2) a half life $T_{\frac{1}{2}} = (16 \pm 1) \times 10^{-10}$ sec was obtained, in agreement with the value given by Graham, Wolfson and Bell. This checks the calibration of the helical delay line.

4.2. THE HALF LIFE OF THE 147 keV EXCITED STATE IN I^{131}

The well known 180 keV isomeric state in Te^{131} (30 hours) is de-excited by an M4 transition to the ground state of Te^{131} (25 min),

which decays by beta-emission to I^{131} (8.2 day). The beta-ray spectrum shows a complex form indicating that several excited states in I^{131} are involved. From a recent investigation by Hebb [20]) it appears that there are also beta-branches from the isomeric level of Te^{131} to higher excited states in I^{131}.

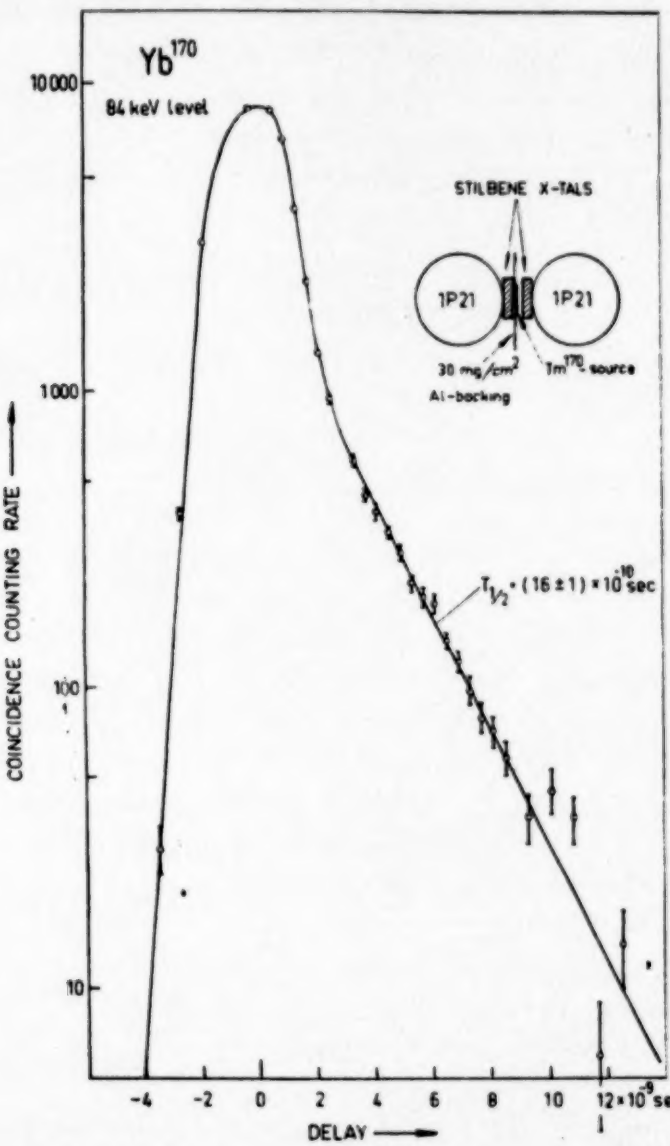

Figure 2. Delayed coincidence plot of the 84 keV level in Yb^{170}

The activity was produced by bombarding tellurium oxide with 20 MeV deuterons. Te^{131m} was chemically separated, adding iodate and iodide carriers to hold back the active iodine fraction.

The isomeric Te^{131m} activity was identified by observing the 180 keV gamma-ray transition to the ground state in the scintilla-

tion spectrum. A single channel pulse height analyzer, stabilized with counting rate feedback [21]) was adjusted to select pulses corresponding to the 180 keV transition. The decay was followed for several half lives. The half life of the isomeric state thus found is (34.5 ± 1) hours, which is slightly higher than the value of 30 hours given by Abelson [22]) and by Seaborg *et al.* [23]). Combining this new value with the observation of Hebb [20]) that about 70 percent of the beta decay starts from the isomeric level, the discrepancy that existed for Te^{131m} in the empirical lifetime versus energy relation for M4 transitions [24]) is removed.

The sources used for the fast coincidence measurements were deposited on 270 mg/cm² aluminium foils and covered with a 0.6 mg/cm² mylar sheet. The aluminium backing is transparent only to beta-rays with energy well above 1 MeV. The lower energy beta-transitions from the isomeric Te^{131m} (maximum 0.98 MeV, according to Hebb [20])) cannot contribute to the coincidence counting rate. Neither can $\beta - e^-$ coincidences from the 8.2 day I^{131} activity that grows from Te^{131m} contribute, since the maximum energy of I^{131} beta-ray is also less than 1 MeV. The delayed coincidence curve was found to be strongly distorted by a prompt coincidence admixture mostly caused by backscattered beta-rays. The delayed coincidence run was therefore repeated with the source covered with a 24 mg/cm² aluminium absorber. It is assumed that this will not affect the intensity of the backscattered beta-rays. The conversion electrons, however, are almost completely absorbed. The difference of these two curves, normalized to the same height should yield the contribution of delayed coincidences only (fig. 3).

The half life determined from the exponential slope of this delayed coincidence difference plot is $T_{\frac{1}{2}} = (9 \pm 1) \times 10^{-10}$ sec.

In the decay scheme given by Hebb [20]), the existence of a 99 or 51 keV level is suggested in addition to the more intensive 147 keV level. The question therefore arises to which level the measured half life should actually be referred.

To settle this point a delayed coincidence absorption measurement was made with Te^{131m}, making use of the 84 keV delayed transition in Tm^{170} and the 145 keV delayed transition in Pr^{141} (cf. below) for energy calibration. In each case a fixed time delay of 3.2×10^{-9} sec was introduced, just sufficient to make the contribution of prompt coincidences negligible with a considerable contribution of delayed coincidences still present. The coincidence

counting rates were measured for aluminium absorbers of different thickness, inserted between the source and the delayed counter.

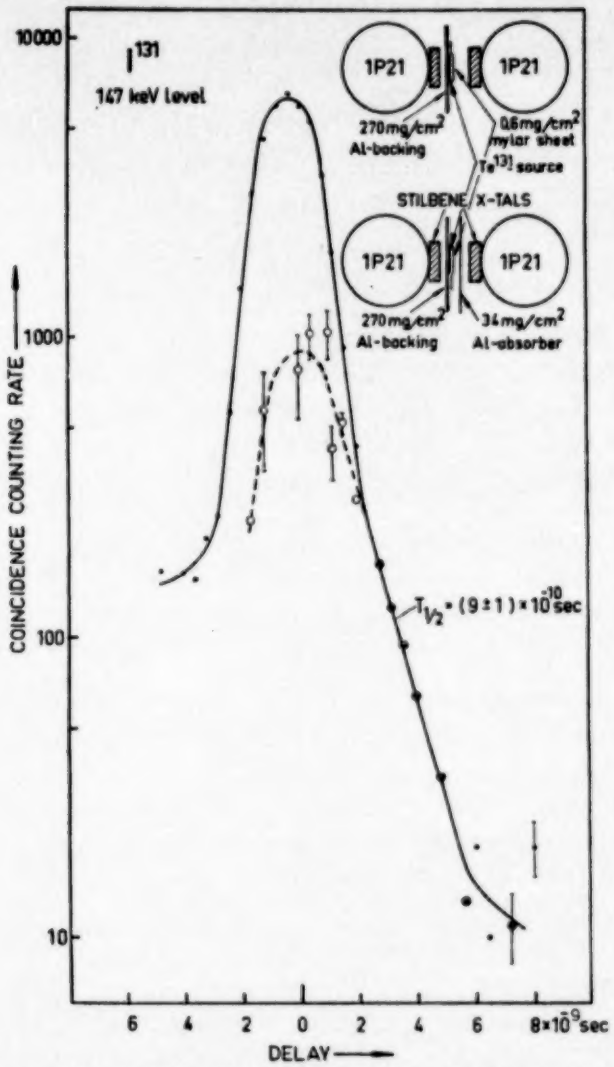

Figure 3. Delayed coincidence plot of the 147 keV level in I^{131}
Dotted curve: prompt coincidence admixture subtracted

The result (fig. 4) clearly excludes the 99 (or 51) keV levels and the measured $(9 \pm 1) \times 10^{-10}$ sec half life is therefore uniquely assigned to the 147 keV level.

4.3. THE HALF LIFE OF THE 163 keV EXCITED STATE IN La^{139} †

The 84 min beta decay of Ba^{139} has been studied by several investigators. According to a decay scheme recently put forward by Mitchell and Hebb [28]) there is a 65 % beta-branch to the 163 keV

† The result of this work has already been published, see ref. [28]).

excited state in La^{139}. The maximum energy of the beta rays leading to this level is 2.227 MeV.

The activity was produced by bombarding barium oxide with

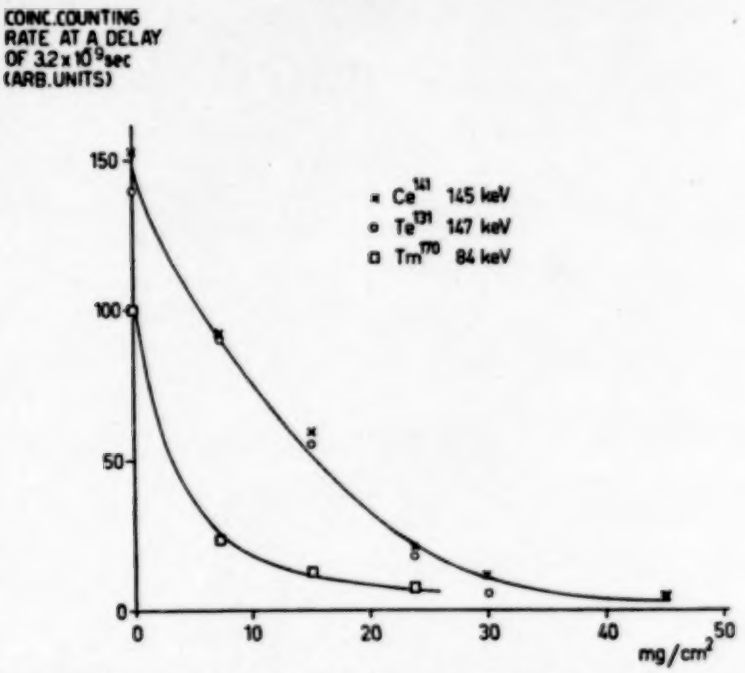

Figure 4. Delayed coincidence absorption measurements used to establish the delayed radiation in I^{131} at 147 keV

20 MeV deuterons. Chemically separated sources were deposited as bariumsulfide on a 100 mg/cm² aluminium foil and covered with a 0.6 mg/cm² mylar sheet. The aluminium backing is transparent to most beta-rays leading to the 163 keV level, while the conversion electrons de-exciting it are completely absorbed. The sources were placed between the two stilbene counters.

The delayed coincidence plot was taken as the sum of eight different runs, corrected for decay, with two different sources. The half life, determined from the exponential slope, is $T_{\frac{1}{2}} = (15 \pm 1) \times 10^{-10}$ sec.

4.4. THE HALF LIFE OF THE 145 keV EXCITED STATE IN Pr^{141} †

About 70 percent of the beta-decay (33.1 day) of Ce^{141} leads to the 145 keV excited state in Pr^{141}. The maximum energy of the beta-rays exciting this level is 440 keV.

† The result of this work has already been published, see ref. [27]). The half life given here has been determined from new measurements with somewhat improved accuracy.

Cerium oxide was irradiated at Harwell and deposited on a 16 mg/cm² aluminium foil. This backing is transparent to most of the beta-rays. The conversion electrons de-exciting the 145 keV level are, however, completely absorbed. The source was placed between the two stilbene crystals.

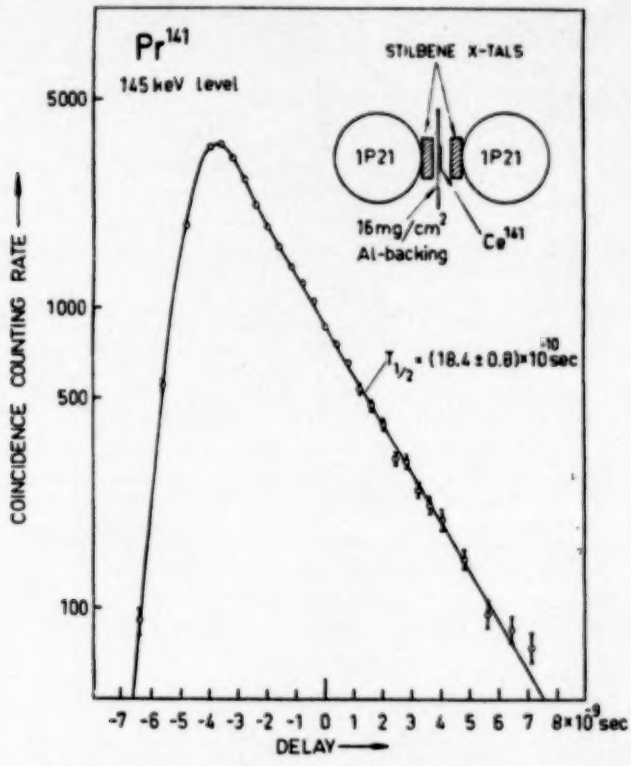

Figure 5. Delayed coincidence plot of the 145 keV level of Pr^{141}

By a suitable adjustment of the discriminators in the side channels, it was possible to get rid almost completely of prompt coincidences caused by back scattered beta-rays. To achieve this, the discriminator level in the beta-channel was set high, while in the other channel a differential discriminator with a rather narrow channel width was used. Its level was adjusted to the maximum of the conversion electron pulse height distribution. The new delayed coincidence plot obtained in this way (fig. 5) is almost undistorted and the half life, determined from the exponential slope is $T_{\frac{1}{2}} = (18.4 \pm 0.8) \times 10^{-10}$ sec, which is somewhat more accurate than the value reported earlier (see footnote).

4.5. HALF LIFE OF THE 279 keV EXCITED STATE IN Tl^{203}

A value $T_{\frac{1}{2}} = (1.2 \pm 0.3) \times 10^{-10}$ sec was found for the half life of this level. Mercury sources, obtained from Harwell, were deposit-

ed on 5 mg/cm² mylar sheets as the nitrate. These sheets were mounted on 300 mg/cm² aluminium absorbers and covered by thin mylar foils (0.6 mg/cm²). They were then sandwiched between the two stilbene crystals. The crystal at the absorber side detects the 279 keV gamma in coincidence with the betas of maximum energy

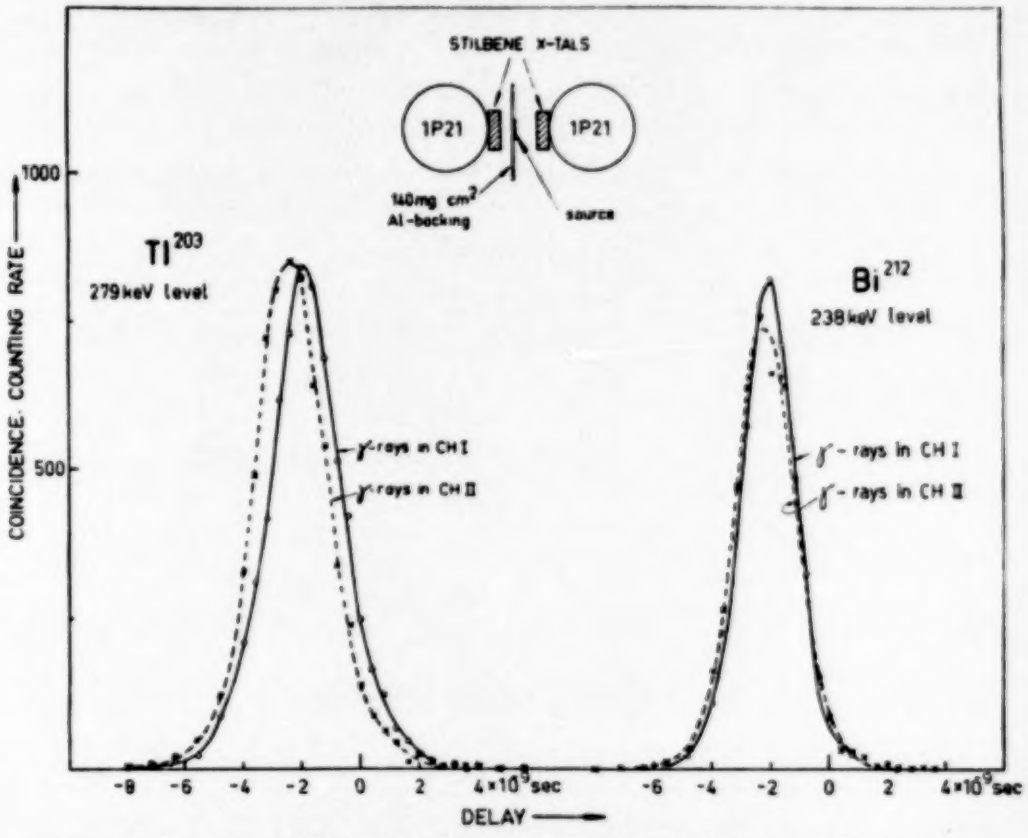

Figure 6. Representative "selfcomparison-comparison" plots. In order to reduce instrumental errors centroid shifts of self comparison pairs of delayed coincidence plots obtained with Hg^{203} (left) have been compared with such pairs ot ThB (right), which is suitable as a reference source because the energies of its strongest coincident beta and gamma radiations are not much different from those in mercury and because the lifetime of the level involved in ThB is known to be very short ($<2\times10^{-11}$ sec; see ref. [7]). Self comparison pairs were obtained by recording first one run and then, after turning round the source plus absorber assembly, another. The half life of the 279 keV level of Tl^{203} has been obtained as the average of 6 runs similar to the one given in the figure. $T_{\frac{1}{2}}$ is given as 0.346 times the difference of the centroid shifts of self comparison pairs obtained with sources of Hg and ThB (From fig. 6 only follows, for instance, $T_{\frac{1}{2}} = 0.346\ (3.94 - 0.83)\times10^{-10}$ sec $= 1.08\times10^{-10}$ sec)

220 keV accepted by the other crystal. Pulse height selectors in both channels are adjusted to transmit pulses corresponding to energies roughly between 75 and 150 keV. An account of the "self comparison-comparison" method used to determine the half life in this

particular case has recently been given by one of the authors [28]). The method is illustrated by fig. 6 and briefly explained in the subscript of this figure.

5. Discussion of Results

To derive from the experimental half lives ($T_{\frac{1}{2}}$) the lifetimes (τ_γ) for deexcitation by gamma emission of magnetic dipole character, the total conversion coefficient α_{tot} and the E2/M1 mixing ratio must be ascertained. Except for the 147 keV level of I^{131} which was assumed to be pure M1, these data could be obtained from published nuclear spectroscopic data of these states combined with the theoretical conversion coefficients of Rose's tables [29]).

Rose's calculations have been carried out in the "point nucleus" approximation. No attempt has been made here to correct for the effects of the finite size of the nucleus on M1-conversion coefficients that were predicted by Sliv [30]) and recently also found experimentally [31,32]). Such effects do not sensitively influence the τ_γ-values to be reported here.

The lifetimes are given by

$$\tau_\gamma^{(M1)} = 1.44(1 + \alpha_{tot.})(1 + \text{E2/M1})T_{\frac{1}{2}}.$$

TABLE I

Conversion and lifetime results for *l*-forbidden Ml transitions in odd proton nuclei

Nucleus	Energy (keV)	Half life (10^{-10} sec)	K/L ratio			E2/M1 ratio	α_{tot}	τ_γ for M1 (10^{-10} sec)	$\lvert\mu\rvert^2_{exp}$	reference ††
			Exp	M1†	E2†					
$_{53}I^{131}$	147	8 ±1	—	7.6	3.6	0 ?	0.25	15±2	0.032	
$_{55}Cs^{133}$	81	60 ±4	7.5	7.5	1.7	0	2.05	260±20	0.014	7)
$_{55}Cs^{135}$	248	2.8±0.8	7.0	7.7	5.3	0.4	0.1	6.2±1.5	0.02	7)
$_{57}La^{139}$	163	15 ±1	7.9	7.5	3.7	0	0.25	27±2	0.016	
$_{59}Pr^{141}$	145	18.4±0.8	7.3	7.25	3.2	0	0.43	39±4	0.012	
$_{61}Pm^{147}$	91.5	24.4±0.8	7.3	7.1	1.9	0	2.2	113±5	0.022	7)
$_{81}Tl^{203}$	279	1.2±0.3	3.3	5.7	1.6	2.3	0.20	7.2±1.3	0.012	

† According to Rose [30]).

†† Further references may be obtained from the paper referred to here.

Table I summarizes all the relevant data from which the lifetimes (given in column 9) have been derived. The transitions measured by Graham and Bell [7]) in the odd proton nuclei Cs^{133}, Cs^{135} and Pm^{147} have also been included.

Fig. 7 shows a logarithmic lifetime versus gamma energy plot

for the seven nuclei investigated. Only the point for I^{131} deviates considerably from a line $\log(\tau_\gamma E^3) = -11.0$ drawn through the points. If there would be an E2 admixture in the transition in I^{131}, the point would move closer to the line; a ratio E2/M1 ≈ 1 should be needed to bring it on the line. More spectroscopical data must be awaited to decide about this lifetime.

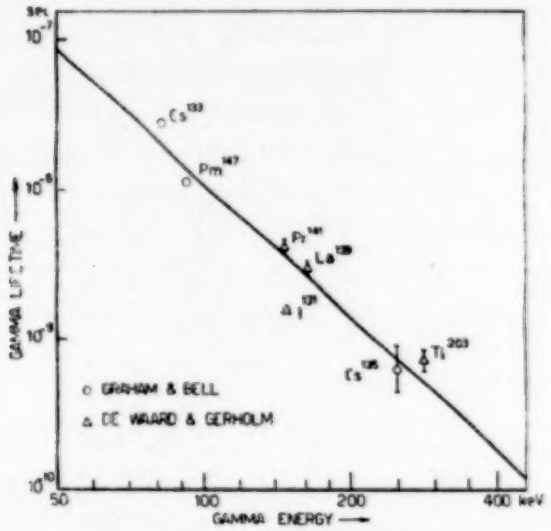

Figure 7. Lifetime versus energy plot of l-forbidden Ml isomers in odd proton nuclei

Disregarding the point for I^{131}, the scatter of the other points round the line given in fig. 7 amounts to a relative standard deviation of the absolute square of matrix element μ

$$\Delta |\mu|^2/|\mu|^2 = 25 \text{ percent.}$$

This scatter is of the same magnitude as that found for the $|\mu|^2$ values of M4 transitions.

As pointed out in section 2, the small scatter indicates that the precise form of the wave functions does not greatly influence the transition probability. It must be expected that the amount of configurational admixture increases on going from Cs^{133} ($Z = 55$) to Pm^{147} ($Z = 61$), but no effect of this is visible in the measured points. This suggests that the transition is not caused by a breakdown of the l-forbiddenness due to the terms of the wave function that represent the configurational admixtures. It must then be caused by extra-ordinary terms of the magnetic dipole moment operator with non-vanishing matrix elements between particle states differing by 2 units in orbital angular momentum. As noted in section 2, spin-orbit coupling and spin exchange have been shown

to give rise to such terms. The magnitude of these effects may be estimated if the strength of the coupling is known. From the available theories it appears that this strength is not very sensitive to details of nuclear structure, in accordance with the small scatter of the experimental values of $|\mu|^2_{exp}$. These values, given in column 10 of Table I, were found by comparing the experimental gamma lifetimes with those calculated from Moszkowski's formula [2]) for allowed M1 transitions in odd proton nuclei. (In this formula $|\mu|^2 = (\mu_p - \frac{1}{2})^2 S = 5.25S$, S being a statistical factor of order 1.)

Jensen and Mayer [14]) have calculated the extraordinary moment contribution due to spin-orbit coupling. They state that the transition probability of a $d_{3/2} - s_{1/2}$ transition should correspond to the radiation of an oscillating magnetic dipole with an amplitude of 0.25 n.m., assuming a spin-orbit splitting energy $E_s^{(l)} = 2$ MeV for $l = 4$ and at $A = 100$. It appears from their paper that

$$|\mu| \simeq E_s^{(l)}/(2l+1) \tag{3}$$

Their value of $E_s^{(l)}$ is an estimate based on shell model statistics.

In some of the cases under discussion here, however, the spin-orbit splitting energy of the d-shell is accurately known from spectroscopic measurements. In the decay of Pb^{203}, for instance, the $d_{5/2}$ and $d_{3/2}$ levels of Tl^{203} have been identified [33]) at 679 keV and 279 keV respectively. Further, Thulin [34]) assigned the $d_{5/2}$ and $d_{3/2}$ levels of Cs^{135} in the decay of Xe^{135} at 248 and 620 keV, respectively. In the decay of Ba^{133}, apart from the 81 keV $d_{5/2}$ level an excited state at 401 keV has been observed [35]), the intensity of which is in accordance with a $d_{3/2}$ assignment.

In the other cases more detailed spectroscopical investigations might reveal $d_{3/2}$ levels in I^{131} and La^{139}, resulting from the decay of Te^{131} and Ba^{139} or Ce^{139}, but there is little chance to excite them in Pr^{141} and Pm^{147} from beta decay, since the ground states of the parent nuclei ($f_{7/2}$) here only allow second order forbidden beta transitions to $d_{3/2}$ states.

However, the available data already show that the $d_{3/2} - d_{5/2}$ energy difference $E_s^{(2)}$ does not vary greatly for three of the investigated nuclei, one of which is remote in Z from the other two. There is, therefore, little reason to suspect otherwise for the other nuclei. This then would imply that the matrix elements should be rather constant, which agrees with experiment.

Furthermore, if Jensen and Mayer's result for $|\mu|$ is adapted to

the observed spin orbit splitting energy $E_s^{(2)}$, using (3), a fair quantitative agreement results between the experimental and theoretical values of $|\mu|^2$, as is illustrated by Table II, the theoretical values being somewhat too small.

TABLE II

Nucleus	$E_s^{(2)}$ (keV)	$\|\mu\|^2_{exp}$	$l-s$ coupling	
			$\|\mu\|^2_{theor}$	$\|\mu\|^2_{theor} S_{rel}$
Cs^{133}	320	0.014	0.005	0.0085
Cs^{135}	370	0.02	0.007	0.012
Tl^{203}	400	0.012	0.008	0.008

It must be noted that Mayer and Jensen's calculations, performed for a $d_{3/2} - s_{1/2}$ transition, should have been repeated with wave functions appropriate to the $d_{5/2}$ and $g_{7/2}$ states encountered in the ceasium isotopes. This calculation has not been carried through but if it is assumed that the different angular dependence of these latter wavefunctions can be accounted for by introducing the same statistical factor $S(j_1, l, j_1)$ in the absolute square of matrix element as was calculated by Moszkowski [2]), this would mean that the $|\mu|^2$ values for the ceasium isotopes must be multiplied by a factor $S_{rel} = S(5/2, 1, 7/2) : S(3/2, 1, 1/2) = (12/7) : 1 = 1.7$. Column 5 of Table II shows that this improves the agreement between theory and experiment somewhat.

The foregoing discussion must be taken "cum grano salis" in so far as any result on matrix element calculations is uncertain because the radial dependence of the wave functions is not accurately known. Calculations by Moszkowski [2]) show, however, that this uncertainty hardly exceeds a factor two.

A few words should be said also about Ross' calculations [12]) of *spin exchange moments*. For quantitative calculations of these, an assumption must be made about the strength of the spin interaction coupling. In contrast to spin-orbit coupling, there appears to be no direct way to derive independent information about this strength from the properties of heavy nuclei. Sachs [36]) has observed that if the strength of the spin exchange moment is adjusted so as to yield the right magnitude of the magnetic moment anomaly between H^3 and He^3, it also gives about the right order of magnitude for the lifetimes of the *l*-forbidden M1 transitions. It must be assumed then, that the spin exchange moment does not change very much on going from $A = 3$ to $A \approx 150$.

A serious objection against ascribing the observed transition rates entirely to the extraordinary moment operator resulting from spin-orbit coupling is the fact that this operator contributes only for odd proton nuclei, whereas Graham and Bell [7]) have observed that *l*-forbidden M1 transitions in odd neutron nuclei are actually faster by a factor of about 5.

Ross [37]) † has pointed out to us that, when the matrix elements of the spin exchange moment operator $\mu(2)$ (see Ross [12])) are calculated correctly, it turns out that these are non vanishing only because of fluctuations of the nuclear density especially near the nuclear surface. Now there are theoretical as well as some experimental arguments for assuming that protons are confined to a somewhat smaller region in the nucleus than neutrons, which would mean that neutron wave functions may be appreciable where the proton density is changing rapidly, but, on the other hand that the neutron density changes much less where proton wave functions are appreciable. Since $\mu(2)$ operates between opposite kinds of nucleons, this would result in larger matrix elements for odd neutron nuclei than for odd proton nuclei, in accordance with experiment.

As a consequence of these arguments it must be emphasized that, while spin-orbit coupling (a velocity dependent interaction) goes a long way in accounting for the observed lifetimes of *l*-forbidden M1 transitions in odd proton nuclei, velocity *in*dependent spin exchange currents probably also contribute. The relative contributions of the two effects are at the moment hard to assess, but it does not seem impossible that relevant calculations of spin exchange moments may be made in the light of the new experimental data of the nucleon density distribution that have been provided especially by electron and alpha scattering.

The authors are much indebted to Professor Kai Siegbahn for his unfailing support and stimulating interest in this work. Thanks are further due to Dr R. E. Bell, who has constructed the delayed coincidence unit for us and to Dr H. Atterling and the members of the cyclotron group at the Nobel Institute for several irradiations. The authors also wish to thank Mr Y. Jonsson, who has assisted us in the measurements. The first author gratefully acknowledges the financial help of the Netherlands Organization for Pure Research (Z.W.O.).

† We are thankful to Dr Ross for his remarks, quoted here.

References

1) V. F. Weisskopf, Phys. Rev. **83** (1951) 1073
2) S. A. Moszkowski, Phys. Rev. **89** (1953) 474
3) M. Goldhaber and A. W. Sunyar, Beta and Gamma Ray Spectroscopy Ch. XVI (II) p. 463, ed. Kai Siegbahn, North-Holland Publ. Company, Amsterdam 1955
4) H. de Waard, Phil. Mag. **46** (1955) 445
5) A. Bohr and B. R. Mottelson, Dan. Mat. Fys. Medd. **27** (1953) no 16
6) A. Bohr and B. R. Mottelson, Beta and Gamma Ray Spectroscopy Ch. XVII ed. Kai Siegbahn, North-Holland Publ. Company, Amsterdam 1955
7) R. L. Graham and R. E. Bell, Can. J. Phys. **31** (1953) 377
8) A. J. F. Siegert, Phys. Rev. **52** (1937) 787
9) R. G. Sachs and N. Austern, Phys. Rev. **81** (1951) 705
   N. Austern and R. G. Sachs, Phys. Rev. **81** (1951) 710
10) R. G. Sachs and M. Ross, Phys. Rev. **84** (1951) 379
11) C. H. Blanchard, R. Avery and R. G. Sachs, Phys. Rev. **78** (1950) 292
12) M. Ross, Phys. Rev. **88** (1952) 935
13) A. Russek, Phys. Rev. **99** (1955) 834
14) J. H. D. Jensen and M. G. Mayer, Phys. Rev. **85** (1952) 1040
15) A. B. Volkov, Phys. Rev. **94** (1954) 1664
16) R. E. Bell, R. L. Graham and H. E. Petch, Can. J. Phys. **30** (1952) 35
17) T. D. Newton, Phys. Rev. **78** (1950) 490
18) Z. Bay, Phys. Rev. **77** (1950) 419
19) R. L. Graham, J. L. Wolfson and R. E. Bell, Can. J. Phys. **30** (1952) 459
20) E. Hebb, Phys. Rev. **97** (1955) 987
21) H. de Waard, Nucleonics **13** (July 1955) 36
22) P. Abelson, Phys. Rev. **56** (1939) 1
23) G. T. Seaborg, J. J. Livingood and J. W. Kennedy, Phys. Rev. **57** (1940) 363
24) M. Goldhaber and A. W. Sunyar, Phys. Rev. **83** (1951) 906
25) T. R. Gerholm and H. de Waard, Physica **21** (1955) 601
26) A. Mitchell and E. Hebb, Phys. Rev. **95** (1954) 727
27) H. de Waard and T. R. Gerholm, Physica **21** (1955) 599
28) H. de Waard, Phys. Rev. **99** (1955) 1045
29) M. E. Rose, Beta- and Gamma-Kay Spectroscopy Ch. XIV, ed. Kai Siegbahn, North-Holland Publ. Company, Amsterdam 1955
30) C. A. Sliv, Zh. Eksp. Teor. Fiz. **21** (1950) 770; J. de Phys. **16** (1955) 523
31) E. Sokolowski, K. Edvarson and K. Siegbahn, Nuc. Phys. **1** (1956) 160
32) A. H. Wapstra and G. J. Nijgh, Nuc. Phys. **1** (1956) 245
33) J. R. Prescott, Proc. Phys. Soc. **67A** (1954) 254
34) S. Thulin, Phys. Rev. **94** (1954) 734
35) R. D. Hill, G. Scharff-Goldhaber and M. McKeown, Phys. Rev. **84**, (1951) 382
36) R. G. Sachs, Nuclear Theory p. 276, Cambridge, Mass. 1953
37) M. Ross, private communication, Oct. 1955

Nuclear Physics, North-Holland Publishing Co., Amsterdam, **1 (1956)**

REMARQUES SUR UNE FORMULATION MATHÉMATIQUE DU MODÈLE DE GELL-MANN

GIULIO RACAH

The Hebrew University, Jerusalem

Received 18 January 1956

Dans un travail [1]) publié dans le premier numéro de ce journal B. d'Espagnat et J. Prentki ont réussi à donner une formulation mathématique assez élégante du modèle de Gell-Mann [2,3]), et ont obtenu en même temps une restriction fort intéressante du nombre des types de champs que l'on peut introduire dans la théorie. Puisque ce travail est couvert d'une couche assez épaisse de notations et de symbolismes compliqués, nous pensons qu'il y a quelque intérêt à examiner ses hypothèses et ses résultats d'un point de vue tout-à-fait élémentaire.

L'idée essentielle de ce travail est d'introduire non seulement un spin isobarique mais aussi une parité dans l'espace isobarique, et de postuler l'invariance du Lagrangien des interactions fortes par rapport non seulement aux rotations mais aussi aux réflexions dans cet espace. Une tentative dans la même direction, qui avait été faite par Pais [4]), avait rencontré des difficultés; mais tandis que Pais avait considéré seulement des particules paires ou impaires, ces auteurs assignent aux particules à spin isobarique $\frac{1}{2}$ une „parité généralisée" $+i$ ou $-i$.

Si l'on fait aussi l'hypothèse que toutes les particules à spin isobarique entier sont paires, et que l'on assigne à chaque particule une „charge isofermionique" U correspondant à la puissance de i qui caractérise sa parité, il est évident que toute interaction trilinéaire (entre deux champs à spin isobarique $\frac{1}{2}$ et un champ à spin isobarique entier) qui est invariante par rapport aux réflexions, conserve aussi la charge isofermionique totale. Le fait que tant I_3 que U sont conservés par les interactions fortes permet de définir

$$Q = I_3 + \tfrac{1}{2}U$$

comme charge électrique. En assignant à chaque particule une valeur de U en accord avec le modèle de Gell-Mann en même temps qu'une "parité" i^U, on assure automatiquement les règles de sélection de ce modèle.

L'introduction de particules impaires donne lieu à des difficultés, parce que

$$-1 = i^2 = i^{-2},$$

et il n'y a plus de correspondance biunivoque entre parité et U. Il y a en effet des interactions qui sont invariantes par rapport aux réflexions et qui conservent la charge totale seulement si l'on assigne à ces particules $U=2$; et il y a aussi des interactions également invariantes qui conservent la charge totale seulement si l'on assigne à ces particules $U=-2$.

Comme on ne peut pas renoncer à la conservation de la charge, on est conduit à choisir entre la suppression de certains termes d'interaction et la suppression des particules qui donnent lieu à difficultés de ce genre. Il est maintenant évident que le deuxième choix est *exactement équivalent* à la limitation $|U| \leqq 1$.

Références

1) B. d'Espagnat et J. Prentki, Nuc. Phys. **1** (1955) 33
2) M. Gell-Mann, Phys. Rev. **92** (1953) 833
3) M. Gell-Mann and A. Pais, Proceedings of the Glasgow Conference (1954)342
4) A. Pais, Physica **19** (1953) 833

Nuclear Physics, North-Holland Publishing Co., Amsterdam, **1 (1956)**

CURVATURE CORRECTION TO THE SAGITTA DISTRIBUTION OF IONIZATION TRACKS

H. WERGELAND and H. ÖVERAAS

Fysisk Institutt, Norges Tekniske Högskole, Trondheim

Received 26 September 1955

A convenient measure for the multiple scattering of a charged particle is the ordinate or "sagitta" from chords to arcs of the ionization track. From measurements of the sagitta one obtains the mean square deflection per unit length for example by the formula [1,2])

$$\overline{\vartheta^2} = 96\frac{\overline{Y^2}}{L^3}, \tag{1}$$

where L is the length of the chord, and Y the ordinate of the middle point.

Searching for a possible explanation to the fact that some careful measurements of multiple scattering [3]) appear to give a much smaller scattering than theoretically expected, we tried to refine Scott's formula (1) by taking into account the curvature of the track.

Consider an ionization track,

$$y = y(x);\ y(0) = y(L) = 0, \tag{2}$$

and the probability $P(\Delta\vartheta,\Delta s)$ for a deflection $\Delta\vartheta$ on the element of path Δs. $\vartheta(s)$ is certainly a Markow process and under certain conditions P can be approximated in the Gaussian form:

$$P_{12} = [2\pi(s_2 - s_1)\overline{\vartheta^2}]^{-\frac{1}{2}} e^{-(\vartheta_2-\vartheta_1)^2/2(s_2-s_1)\overline{\vartheta^2}}. \tag{3}$$

The probability $w(Y(X))$ of finding the ordinate Y at the point X on the chord is then

$$W(Y(X)) = \int d\vartheta_0 P(\vartheta_0|\vartheta_1) d\vartheta_1 P(\vartheta_1|\vartheta_2) \ldots d\vartheta_{N-1}|P(\vartheta_{N-1}|\vartheta_N) d\vartheta_N, \tag{4}$$

where the Markow chain connects a subdivision $s_1, s_2, s_3, \ldots s_N$ of the track which can be made infinitesimal, and the ϑ's shall assume all values compatible with (2). Strictly speaking (4) is not quite correct as (2) constrain the ϑ's to the intersection of four

surfaces in the N-dimensional space, but we omit the appropriate change of probability measure since it does not affect the leading term of the distribution we want.

If the path s is replaced by the abscissa x, and sine and tangent replaced by angle, one obtains for w a purely Gaussian distribution leading to eq. (1), as shown by Scott *et al.*

In order to remove the limitation to small angles we shall utilize the saddle point method in a version devised by Onsager and Machlup [4]): Because of the properties of Gauss integrals

$$W(Y(X)) \approx e^{-\mathrm{Min}(J)} \tag{5}$$

where

$$J[\vartheta] = \sum_{i=0}^{N-1} (\vartheta_{i+1} - \vartheta_i)^2 / 2\overline{\vartheta^2}\Delta s \to (1/2\overline{\vartheta^2}) \int_0^T \dot{\vartheta}^2 ds,$$

and the minimum is to be sought under the conditions

$$\begin{aligned} &y(0) = x(0) = 0, \\ &y(S) = Y,\ x(S) = X, \\ &y(T) = 0,\ x(T) = L. \end{aligned} \tag{6}$$

In so far as the subsidiary conditions (6) are linear or quadratic in ϑ eq. (5) is even an exact equation. It should therefore in general give a correction at least including the second order in small angles.

In order to determine w, we have thus to solve the variational problem

$$J = \min\ ;\ \delta L = \delta X = \delta Y = 0, \tag{7}$$

whereby the variation $\delta\vartheta$ has to be free at the end points according to the form of the problem (4). This latter imposes "natural boundary conditions" $\dot{\vartheta}(0) = \dot{\vartheta}(T) = 0$, on the extremals.

After some calculation one obtains

$$\begin{aligned} x(s) &= \frac{2k}{\alpha} Z(\alpha s - K), \\ y(s) &= \frac{2}{\alpha} \mathrm{cn}(\alpha s - K) + \frac{\alpha L}{2K} s, \end{aligned} \tag{8}$$

as the equations for "the Most Probable Path" in natural coordinates. Here

cn = cosinus amplitudinis,
Z = Jacobian zeta function,
K, E = the complete elliptic integrals of first and second kind,
k = modulus.

The constants of integration (Lagrangian multipliers) are determined by

$$X = \frac{2}{\alpha} Z(\alpha S - K) + \frac{\alpha L}{2K} S,$$

$$Y = \frac{2k}{\alpha} \mathrm{cn}(\alpha S - K), \tag{9}$$

$$L = \frac{2}{\alpha} Z(\alpha T - K) + \frac{\alpha L}{2K} \cdot T = \frac{2}{\alpha} (2E - K).$$

For the functional itself one finds

$$J_{\min} = \frac{4\alpha}{\overline{\vartheta^2}} [E - (1 - k^2)K], \tag{10}$$

which is now to be expressed in terms of X, Y and L.

When $X = L/2$ the elimination is greatly simplified. The argument of the elliptic functions is then zero and the arc corresponds just to a half period of cn. One has then exactly

$$Y = \frac{2k}{\alpha}. \tag{11}$$

But the last elimination of the modulus k is not possible in closed form. In first approximation,

$$k = \frac{\pi}{2} \cdot \frac{Y}{L} \tag{12}$$

with an error of order $(Y/L)^3$. In this approximation

$$J = \frac{\pi^4}{2L^3 \overline{\vartheta^2}} \cdot Y^2. \tag{13}$$

Hence the relation between the measured value $\overline{Y^2}$ and the theoretical quantity $\overline{\vartheta^2}$ will be

$$\overline{\vartheta^2} = \pi^4 \frac{\overline{Y^2}}{L^3} \tag{14}$$

instead of (1).

The error implied by the small angle approximation appears therefore to be minute indeed, meaning only a change of the factor 96 in (1) to $\pi^4 = 97{,}4\ldots$.

References

1) W. Scott, Phys. Rev. **76** (1949) 215
2) B. Rossi, High Energy Particles p. 72, New York 1952
3) E. Hisdal, Phil. Mag. **43** (1952) 790
4) L. Onsager and Machlup, Phys. Rev. **91** (1953) 1509

Nuclear Physics, North-Holland Publishing Co., Amsterdam, **1 (1956)**

ALEXANDRE PROCA

1897—1955

Alexandre Proca est mort à Paris, le 13 décembre 1955, après une longue et cruelle maladie.

Né en Roumanie, A. Proca fut élève puis Assistant à l'Ecole Polytechnique de Bucarest. Arrivé à Paris, il entreprend d'abord des recherches expérimentales dans le laboratoire de Madame Curie, puis, orienté vers une carrière de théoricien, il entre au Centre National de la Recherche Scientifique. Celui-ci formait alors la „Caisse des Sciences" que venait de fonder Jean Perrin. Proca devait y poursuivre toute sa carrière: Maître de Recherches en 1939, il devient, en 1944 membre de la Mission Française à Londres. Revenu à Paris il est Directeur de Recherches depuis 1946 et dirige un Séminaire de Physique théorique qui groupe un ensemble remarquable de jeunes Chercheurs.

Les travaux d'Alexandre Proca ont été tout d'abord axés sur la théorie de Dirac. Sa thèse „Sur la théorie relativiste de l'électron de Dirac" (Masson-1933) complète la symétrie relativiste de la théorie en introduisant le temps propre comme variable conjuguée du moment m_0c. Il s'attache aussi à donner une interprétation des 16 covariants de la théorie. Enfin, il développe ce formalisme en utilisant les quaternions et en définissant des „moments d'ordre supérieur".

Au cours de cette étude, A. Proca est frappé par les différences profondes qui séparent la théorie de l'électron (particule de masse non nulle et d'énergie positive ou négative) de la théorie du photon où intervient une énergie positive et, dans les conceptions usuelles, une masse nulle. Il cherche à obtenir des équations relativistes susceptibles de décrire le comportement d'une particule de masse non nulle, d'énergie positive et de spin entier.

A cette époque, on connaissait des équations relativistes satisfaisant à cette condition. Les équations de Maxwell, complétées par

un terme de masse décrivent en effet le comportement d'une particule de spin 1. Louis de Broglie avait obtenu ces équations en 1934 à partir de la théorie de Dirac et les utilisait pour édifier la théorie d'un photon doué d'une masse propre non nulle.

Parti de la théorie non relativiste de Gordon, Proca retrouve ces équations en utilisant un lagrangien approprié. Il suppose que des équations de ce type — c'est-à-dire des équations de Maxwell complétées par un terme de masse — peuvent décrire un autre type d',,électron''. Il étend ce formalisme au cas où se manifeste un champ extérieur. En fait, ces équations devaient se trouver remarquablement adaptées à la description du méson que Yukawa mettait à l'origine du champ nucléaire. Les équations relativistes de la particule de spin 1 — généralement appelées équations de Proca — devaient remplacer avec succès l'équation de Gordon dans toutes les applications au champ mésonique.

A. Proca effectue ensuite une série de recherches sur la théorie du méson. En collaboration avec S. Goudsmit, il détermine par une voie théorique la masse du méson. D'autre part, il cherche à appliquer de façon plus complète les principes de la Relativité Restreinte à la théorie des particules à Spin: Ainsi décompose-t-il l'espace-temps habituel en deux sous-espaces imaginaires spinoriels sous-jacents. Il veut profiter de cette hypothèse pour accroître les possibilités de ce genre de théorie.

Enfin, il propose une équation de Dirac complétée par des termes en $\lambda\gamma^{\mu}\gamma^{\nu}(x_{\mu}\partial_{\nu}-x_{\nu}\partial_{\mu})$; λ est alors une constante ayant les dimensions de l'inverse d'une longueur. L'équation de Dirac ainsi modifiée décrit le comportement d'une nouvelle particule dont la charge et le moment électrique total sont constants, mais qui possède une énergie variable croissante ou décroissante, suivant le signe de λ. Il est donc possible d'attaquer de cette manière le problème des corpuscules non conservatifs et d'éviter l'introduction de neutrinos.

Les derniers travaux de Proca cherchent à établir les lois du mouvement d'un corpuscule unique dont les états-correspondant à des masses et à des spins différents — seraient susceptibles de représenter les diverses particules. A cet effet, il étudie en particulier les changements de spins et leurs répercussions dans les équations d'ondes corpusculaires.

Il a travaillé jusqu'à la fin. Sa dernière sortie a été pour accueillir le Professeur Heitler à son Séminaire. Le courage et la sérénité dont il a fait preuve pendant ces derniers mois, supportant sans une plainte

l'évolution d'une maladie qui le privait de tout usage de la parole, restant affable et dévoué en dépit de changements dont il n'ignorait pas l'issue, ont fait l'admiration de tous.

Marie-Antoinette Tonnelat

Principales Publications

Sur la théorie relativiste de l'électron de Dirac, Annales de Physique **5** (1933) 347

Ondes et photons, Journ. Phys. **5** (1934) 6, 121 et 157

Sur les particules qu'on peut associer à une onde de lumière, C. R. Ac. Sc. **198** (1934) 643

Sur la théorie ondulatoire des électrons positifs et négatifs, Journ. Phys. **8** (1936) 347

Théorie non relativiste des particules à spin entier, Journ. Phys. **9** (1938) 61

Sur les masses des particules élémentaires, Journ. Phys. **10** (1939) 209

Sur un nouveau type d'électron, Portugaliae Physica **1** (1943) 59

Non conservative fundamental particles, Nature **154** (1944) 674

Transmutation des particules fondamentales: Changement de spin, Journ. Phys. **12** (1951) 123

Sur l'espace-temps des particules fondamentales et les espaces spinoriels sous-jacents, Bull. scient. Roumain **1** (1952) 18

BOOK REVIEWS

IRVING KAPLAN, *Nuclear Physics*. (Addison-Wesley Publishing Co., Cambridge, Mass. 1955. xi-609 pages. $ 10).

This book is designed as an introduction to nuclear physics for engineers and physicists and no previous knowledge of atomic or nuclear physics is assumed. The presentation is largely descriptive and gives a well integrated account of experimental results and their general interpretation, whilst avoiding both the detail of mathematical theory and the intricacy of experimental techniques. This has resulted in an extremely readable book which covers a wide range of material. Each chapter has a useful list of references to other books and to original papers and has a set of examples based on the material presented in the book.

The first part (144 pages) of the book is an account of the background of nuclear physics. It introduces the main phenomena utilised in studying the nucleus including alpha, beta and gamma rays and indicates their importance in relation to the historical development of nuclear physics. The general characteristics of atomic structure are described and an outline is given of the basic concepts of quantum theory and special relativity.

The second part (296 pages) of the book describes the physics of the nucleus. The main properties of the nucleus are described first and then a more detailed treatment is given of natural and artificial radioactivity. Three chapters devoted to alpha, beta, and gamma rays discuss both their relation to radioactivity and their use in experiments. Nuclear reactions are treated in two chapters one dealing with nuclear disintegration and the other with their use in investigating nuclear structure. There is a very brief account of the nature of nuclear forces and their relation to nuclear saturation, and of nuclear models.

The third part (150 pages) describes a variety of special topics which will be of particular interest to nuclear engineers. These include neutron physics and nuclear fission and their relation to nuclear energy, and there are also chapters on charged particle accelerators and on isotope separation.

The book is very readable and seems eminently suitable for providing the kind of general knowledge of nuclear physics which will be required by an engineer or scientist working in a related field. It would also be of value to an honours physics student but would need to be supplemented by a more specialised account of nuclear theory.

R. J. Eden

V. CHARLES, *Problèmes élémentaires de physique atomique et de chimie nucléaire* (avec tableaux et solutions), Gauthier-Villars, Paris 1955. 145 pages. 900 fr. frçs.

Ce livre d'un niveau très élémentaire, contient un certain nombre de problèmes relatifs à la physique classique et à la microphysique. L'auteur insiste surtout sur les différents systèmes d'unités (d'une façon abusive même), mais ne dégage rien des analogies et différences des mécaniques classique et quantique: par exemple l'effet Compton n'est traité que relativement aux lois de conservation de l'énergie et de la quantité de mouvement; on aurait pu y ajouter sans entrer dans le détail du calcul, que l'expérience donne beaucoup plus, la section efficace de diffusion etc. Tel qu'il est, malgré son titre prometteur, le livre de M. Charles ne comble pas une des lacunes de la littérature scientifique de langue française: l'absence de cours de mécanique quantique destiné aux expérimentateurs ou ingénieurs, avec de nombreux problèmes se rapportant à la physique atomique ou nucléaire et à l'électrodynamique sous son aspect élémentaire.

C. Marty

A. E. S. GREEN, *Nuclear Physics* (McGraw-Hill Book Co., New York, Toronto, London 1955. xv-535 pages. 64s.6d.)

This book treats the physics of nuclei with excitation energies from zero up to a few tens of MeV. It is written for students who have taken a course on modern extra-nuclear physics, and have had either little or no introduction to quantum mechanics.

The book falls into two parts. The first (316 pages) deals mainly with experimental facts and techniques. The second (219 pages) treats theory and the nuclear forces. At the end of each chapter there is a useful list of examples and an extensive bibliography.

Chapter 1 is a review of parts of modern physics. Chapter 2 deals with nuclear masses, charges, sizes and moments. There follow three chapters (3, 4, 5) on the production, analysis and detection of energetic particles and γ-rays. This account of experimental techniques is a useful and comprehensive introduction, although parts are rather superficial (e.g. the comparative discussion on p. 156 of the uses of the cloud chamber and nuclear emulsions). Chapters 6 and 7 treat the empirical facts of radioactivity and nuclear reactions. The first part of the book is then completed by Chapters 8 and 9 on the nuclear mass surface and the Bohr-Wheeler theory of fission.

The rest of the book is mainly theoretical. It is introduced by Chapter 10 on basic quantum mechanics. The material here has been selected so as to help the beginner over his first shock when presented with the new theory, rather than with a view to completeness. Topics which might have been included here are the probability current and the concept of parity, both of which are used in other places. Chapter 11 then deals with nuclear models. Chapters 12 and 13 give a brief account of the theory of radioactivity and of nuclear reactions. The closing Chapter 14 deals with nuclear forces.

The theoretical treatment is very condensed, and many formulae are stated without proof. There is also some lack of definitions (e.g. no definition is given of the multipole operators appearing in the formulae for the electromagnetic transition probabilities). More could have been done to clarify some of the physical ideas (e.g. a discussion of the mean free path of a nucleon in nuclear matter would have been helpful in the chapter on nuclear models). Altogether one feels that a more thorough treatment would have been possible in a book of this size without appreciably raising the level of difficulty.

In this connection, one is naturally led to compare this book with Fermi's Chicago lecture notes, which cover much the same ground and are addressed to the same audience. The comparison shows that, where the subject matter overlaps, Fermi conveyed considerably more information in about three-quarters of the number of words.

There is an unhappily large number of statements which are either incorrect (e.g. on p. 13, that momenta in standing waves are restricted to discrete values) or misleading (e.g. on p. 350, that the conservation of energy is a consequence of time dependent perturbation theory).

A. Herzenberg

FOR PROSPECTIVE CONTRIBUTORS

Since the nomenclature in the field of Nuclear Physics is not yet quite unified and a number of illogical expressions are unfortunately still widely used, it is advisable to give the following indications about the terminology adopted in this journal.

(1) The word 'electron' applies to particles with an elementary charge of either sign. When it is desirable to emphasize the sign of the charge, the words 'positon' and 'negaton' are used. Thus the illogical phrase 'electron-positron pair' is replaced by 'electron pair', or, if required, by 'positon-negaton pair'.

(2) Nuclei (or nucleids, *not* 'nuclids') are conveniently divided according to the parity of the proton and neutron numbers Z, N, into four families as follows:

even mass nuclei	{ even nuclei (Z even, N even) odd nuclei (Z odd, N odd)
odd mass nuclei	{ odd proton nuclei (Z odd, N even) odd neutron nuclei (Z even, N odd).

(3) The expressions 'isotopic spin', 'isotopic quantum number' are replaced by 'isobaric spin', 'isobaric quantum number'.

(4) For the elementary particles use is made of the latest nomenclature adopted by international agreement.

Editors and publishers have taken steps to secure prompt publication of accepted contributions; to achieve this end they count on the co-operation of authors, who are expected, as a matter of course, to submit neatly prepared typescripts of well-written papers and to return carefully corrected proofs without delay.

APPLICATIONS OF SPINOR INVARIANTS IN ATOMIC PHYSICS

By H. C. BRINKMAN

Central Laboratory T. N. O. Delft, Netherlands

A survey of the method of spinor invariants, in 1930 introduced by H. A. Kramers. The author summarizes the development of this technique and consequently this book is mainly mathematical. An exception is the introduction of the electron-spin, which has been discussed rather fully. Indeed the introduction of spinors in physics originates from Pauli's incorporation of the electron spin in wave-mechanics. Moreover, the treatment of the electron spin by various authors shows formal differences, some of which the author has pointed out explicitly.

Contents: 1. Rotations and Unitary Transformations. 2. Wave-functions and Spinor Invariants. 3. Application of Spinor Invariants to detailed Calculations.

1956 - 6 × 9 - 96 PAGES

PRICE GUILDERS 11.00 - (22s.)

Obtainable through your bookseller

Sole Agency for U.S.A.:

INTERSCIENCE PUBLISHERS, INC. 250 Fifth Avenue, New York 1, N. Y.

NORTH-HOLLAND PUBLISHING COMPANY

Just out

COLLECTED SCIENTIFIC PAPERS

OF H. A. KRAMERS

Late Professor of Theoretical Physics in the University of Leyden

Born in Rotterdam, Hendrik Anthony Kramers studied at the University of Leyden from 1912 to 1916, when he went to Copenhagen to work with Niels Bohr. There he worked out his famous formula for the scattering of light by atoms.
In 1926 Kramers was appointed to the chair of Theoretical Physics at Utrecht. In 1933 he succeeded Ehrenfest at Leyden. Kramers' publications had a great influence on the modern development of theoretical physics.
After his premature death in 1952 his many friends and pupils wished to commemorate him by an edition of his collected scientific papers.

1956 — 7.2×10.8 — 982 pages — one plate f 45,— $ 12.00 £ 4.10.0

NORTH-HOLLAND PUBLISHING COMPANY
NIEUWE ZIJDS VOORBURGWAL 46-50 AMSTERDAM-C HOLLAND

INTERSCIENCE TRACTS ON PHYSICS AND ASTRONOMY

Editor: R. E. MARSHAK, *Harris Professor of Physics, University of Rochester, N.Y.*

1. PHYSICS OF FULLY IONIZED GASES

By LYMAN SPITZER, JR., *Princeton University Observatory, Princeton, N.J. 1956. 116 pages, 9 illus., 6 tables. $1.75 Paperbound. $ 3.50 Clothbound.*

2. MAGNETOHYDRODYNAMICS

By T. G. COWLING, *Department of Mathematics, The University, Leeds, Yorkshire, England. In preparation. $1.75 Paperbound. $ 3.50 Clothbound.*

ELECTROMAGNETIC WAVES

By G. TORALDO DI FRANCIA, *Istituto Nazionale di Ottica, Florence, Italy. 1956. 6×9. Approx. 330 pages, 64 illus. Approx. $ 5.50*

INTERSCIENCE PUBLISHERS

250 Fifth Avenue
NEW YORK 1, N.Y.

88/90 Chancery Lane
LONDON, W.C. 2, ENGLAND